European Journal of Soil Science

Effects of altitude on soil properties in coastal fog ecosystems in Morro Moreno National Park, Antofagasta, Chile

Journal:	*European Journal of Soil Science*
Manuscript ID	EJSS-294-21.R2
Manuscript Type:	Original Article
Date Submitted by the Author:	06-Jan-2022
Complete List of Authors:	Fuentes, Bárbara; Universidad Catolica del Norte Gómez, Francisco; Universidad Catolica del Norte Valdez, Catalina; Universidad Catolica del Norte Videla, Anael; Universidad Catolica del Norte Castro-Severyn, Juan; Universidad Catolica del Norte Barahona, Sergio; Universidad Catolica del Norte Riquelme, Rodrigo; Universidad Catolica del Norte Quispe, Javier; Universidad Catolica del Norte Bol, Roland; Forschungszentrum Juelich, IBG3 Remonsellez, Francisco; Universidad Catolica del Norte
Keywords:	Atacama Desert, Camanchaca, Chilean coastal desert, climate change, soil microbial diversity, Pacific coast, soil physicochemical properties

Effects of altitude on soil properties in coastal fog ecosystems in Morro Moreno National Park, Antofagasta, Chile

Bárbara Fuentes[1], Francisco Gómez[1], Catalina Valdez[1], Anael Videla[1], Juan Castro-Severyn[1], Sergio Barahona[1], Roland Bol[2,3], Rodrigo Riquelme[4], Javier Quispe[1], Francisco Remonsellez[1,5,*]

[1] Departamento de Ingeniería Química, Universidad Católica del Norte, Antofagasta, Chile.

[2] Agrosphere (IBG-3), Institute of Bio- and Geosciences, Forschungszentrum Jülich GmbH, Germany.

[3] School of Natural Sciences, Environment Centre Wales, Bangor University, Bangor, LL57 2UW, UK.

[4] Departamento de Ciencias Geológicas, Universidad Católica del Norte, Antofagasta, Chile.

[5] Centro de Investigación Tecnológica del Agua en el Desierto-CEITSAZA, Universidad Católica del Norte, Antofagasta, Chile.

***Corresponding author:** Francisco Remonsellez, E-mail: fremonse@ucn.cl

ORCID ID:

Francisco Remonsellez https://orcid.org/0000-0002-3930-2116

Bárbara Fuentes https://orcid.org/0000-0003-3183-094X

Juan Castro-Severyn https://orcid.org/0000-0002-4301-2226

Roland Bol https://orcid.org/0000-0003-3015-7706

RUNNING TITLE: Altitudinal effects on coastal fog ecosystem soils

ACKNOWLEDGMENTS

The authors thank the professional staff of the Antofagasta office of the Corporación Nacional Forestal (CONAF): Felipe González Soza, Juan Ignacio Olguín, and Diego Sepulveda Martinez.

FUNDING SOURCES AND AUTHORISATION

This work was supported by the Chilean projects CONICYT Acción Regional ARIII70001 (FIC-R GORE Antofagsta) and CONICYT MEC80180018 as well as a Collaborative Research Center project (CRC1211: 'Earth-Evolution at the Dry Limit) funded by the German Research Foundation (DFG). JC-S was supported by Universidad Católica del Norte 2020 Postdoctoral Fellowship and ANID 2021 postdoctoral FONDECYT 3210156. SB was supported by project CORFO ING2030 16EN12–71940 (Assistant Investigator). This research activities in the National System of Protected Wild Areas of Chile related to this project were authorised by the Chilean Government through the Corporación Nacional Forestal (CONAF; Authorization #921361).

DATA AVAILABILITY STATEMENT

The raw sequencing data presented in this study have been deposited in the DDBJ/ENA/GenBank SRA database under the BioProject PRJNA687011.

CONFLICT OF INTEREST DISCLOSURE

There are no conflicts of interest to declare.

Effects of altitude on soil properties in coastal fog ecosystems in Morro Moreno National Park, Antofagasta, Chile

RUNNING TITLE: Altitudinal effects on coastal fog ecosystem soils

ABSTRACT

The rare Pacific coast fog ecosystems are under threat by climate change and local factors. Although coastal fog is known to affect soil properties and microbial diversity, few studies on the Pacific coast have examined the specific microbiomes associated with these ecosystems. We evaluated the effects of coastal fog on the physicochemical, mineralogical, and microbiological properties of bare and bulk soils from different altitudes in the Morro Moreno National Park (MMNP) in the Antofagasta region, Chile. We found that the temperature and relative humidity of the soil varied temporally (daily) and spatially (with altitude). We detected that soil organic matter and organic phosphorus content tended to increase with altitude, whereas the pH, electrical conductivity and total phosphorous decreased. Our results did show that coastal fog could induces physical weathering below 300 masl and chemical weathering at the intermediate altitudes of ~400–600 masl. The biodiversity of bacteria and fungi increased considerably above 400 masl. Actinobacteria and Bacteroidetes dominate the bacteria in bare soil, and Bacteroidetes dominate the bulk soil communities at all altitudes. Ascomycota and Basidiomycota dominate the fungal community in both soil types. Moreover, the conductivity and CaO content appear to be more closely associated with microbial communities from lower altitudes. In addition, the organic C content, humidity, and Weathering Index 2 (WI2) isolate some communities at 500 and 600 masl. The microbiological diversity reported in this work reflects the variable and different microbial niches comprising the MMNP environment. Linkages between soil property and microbial variations with altitude within this Northern Chilean coastal fog ecosystem were elucidated. This novel scientific knowledge contributes to global network strategies for fog ecosystem conservation which aim to preserve the microbial niches and diversity in such soils.

Keywords: Atacama Desert, Camanchaca, Chilean coastal desert, climate change, soil microbial diversity, Pacific coast, soil physicochemical properties

1. INTRODUCTION

Globally, fog ecosystems are scarce because they require special climatic and geographic conditions. Their formation depends on unique local characteristics, including temperature, aridity index, latitude, terrain elevation, distance from the coastline, and slope angle (Moat et al. 2021). According to Weathers et al. (2020), fog is a medium, vector, and connector because it links the atmosphere, biosphere, and hydrosphere and connects atmospheric, terrestrial, and marine ecosystems. Fog also plays a key role in controlling ecosystem processes because it modulates environmental conditions such as heat, water, and radiative interactions between the atmosphere and terrestrial systems (Sotomayor and Drezner 2019; Weathers et al. 2020). It supplies and regulates the flow of water, nutrients, and light to ecosystems and determines the strength and type of coupling between the atmosphere, vegetation, and soil processes driving ecosystem functions (Weathers et al. 2020). In addition, fog ecosystems support diverse plant species dependent on fog as the only water source. However, the soil-water-plant relationships in fog ecosystems are poorly understood.

Fog ecosystems are vulnerable and constantly threatened by global and local factors. Global factors include climate change and a lack of understanding of these ecosystems and the biodiversity they support. At the local scale, threats include lack of protection, urban development, atmospheric contamination, industrial and mining activities, overgrazing, invasive species, and irresponsible tourism practices (Moat et al. 2021).

Fog ecosystems occur mainly in coastal areas, such as California in the US, the coast of desert in Chile and Perú, South Africa, and other Mediterranean areas with dry summers, which remain unclear (Torregrosa et al. 2014). The arid and hyper-arid Pacific coast, including parts of Peru and Chile (the Sechura Desert and the Atacama Desert), extends for 3,000 km and harbours localised fog ecosystems isolated from each other (Moat et al. 2021). On the Pacific coast, the atmospheric conditions are affected by a stable, subtropical anticyclone that generates a uniform coastal climate, nearly devoid of rainfall but characterised by the regular formation of thick stratus clouds below 1,000 m (Rundel et al. 1991; Cereceda et al. 1992, 2008; Garreaud et al. 2008, 2010). Fog ecosystems vary widely with latitude, aspect, substrate, and elevation, ranging from hilltop woody plant refugia to wider expanses of vegetation and productive crusts. The vegetation patterns in the fog ecosystems

of Chile and Perú have received some attention (Rundel et al. 1991; Muñoz-Schick et al. 2001; Muenchow et al. 2013). However, the soil physicochemical and mineralogical characteristics and their effects on the microbial composition in fog ecosystems have been little studied, although they are fundamental to the dynamics of these ecosystems. It remains unknown how climate change might affect coastal fog ecosystems on the southern Pacific coast in the short, medium, and long term. The occurrence of coastal fog, named 'Camanchaca', along the northern Chile coast is strongly affected by the topography. Sectors known for their coastal fogs include higher reliefs such as the Fray Jorge National Park in the Coquimbo region, Paposo and Morro Moreno National Park (MMNP) in the Antofagasta region, and Alto Patache in the Tarapacá region. These coastal cloud banks are usually less than 250 m thick and form at altitudes ranging from 400 to 800 m (Rundel et al. 1991; Cereceda et al. 1992).

Specifically, the MMNP is a fog ecosystem with great importance for Chile's natural heritage. It is located on the hyperarid coast of the Atacama Desert, where the 'Camanchaca' supports a rich fog ecosystem with high biodiversity (Oltremari et al. 1987; Guerra et al. 2010; DS 5/2010).

The geographic conditions of the MMNP, plus formal protection from the Chilean government, make the MMNP ideal for studies on the impact of the fog and elevation on vegetation variations, soil parameters, and microbial communities. Such studies could generate invaluable information about the Pacific Coast's fog ecosystems and the potential effects of global climate change upon them. To understand these unique ecosystems and design and implement appropriate conservation strategies, it is necessary to create a soil property baseline and an inventory of bacterial and fungal variations with altitude. Therefore, this study aimed to evaluate the effects of coastal fog on the physicochemical, mineralogical, and microbiological properties of soils relative to the altitude and proximity to plants. The resulting data will constitute the first inventory of variations in soil properties, bacteria, and fungi in relation to altitude in fog ecosystems.

2. MATERIALS AND METHODS

2.1. Site description and soil sampling

The study area was the MMNP (UTM coordinates (0340496; 7397723), officially declared a protected area in 2010 (DS 5/2010) by the Chilean Government. It covers 7,313 ha on the southern Mejillones Peninsula in the Antofagasta region (northern Chile; see Figure 1). Coastal fog in the MMNP is due to water-saturated air masses from the ocean pushed by prevailing southwestern winds. These humid air masses are transported to MMNP which is up to 950 m high and extends over ~10 km on the south side of the Mejillones Peninsula (Figure 1). The MMNP's location and its unique relief create a fog oasis with a verdant core of around 100 km^2. Factors favouring the oasis include elevations ≤750 m; distance from the coastline ≤5 km, strong slope angle ≤ 16.5 °, slope direction SE, high fog duration > 3 months, and great isolation > 50 km (Moat et al. 2021). In MMNP a total of 90 plant species have been reported, among which 57 are endemic to Chile, 29 are native, and 4 have been introduced; moreover, 13 species in the Antofagasta region are endemic (Oltremari et al. 1987; Guerra et al. 2010; DS 5/2010).

Soil samples were collected at different altitudes (100, 200, 300, 400, 500, 600, and 700 metres above sea level, masl) along a transect on the southern, fog-exposed Morro Moreno hillslope. The altitudinal transect including the central sampling points and geographical coordinates are shown in Figure 1. The vegetation was visually identified by the team. We defined a radius of 15 m around each sampling point for soil sample collection. At each altitude, topsoil samples were collected in random geographical directions at fixed distances, 5, 10, and 15 m between the individual sampling points. The samples ranged from almost unweathered materials to poorly regolitized diorites to metadiorites (mainly plagioclase, quartz, amphibole, and biotite as well as minor apatite, sphene, and opaque minerals; Cortés et al. 2007). The soil layers are thin, and bedrock outcrops are common; therefore, topsoil samples were collected from a depth ranging from 0 to 3 cm. This sampling strategy was helpful for the lowest sampling point, characterised by poorly regolitized colluvium built up by pebble–boulder clasts of diorite to metadiorite. Six samples were collected within a 15 m radius of each sampling point: including three bare soils (vegetation-free) and three bulk soils (surrounding the plant roots). Note that plants in the MMNP have different conservation statuses based on Chilean

regulations (DS 29/ 2012). Consequently, the rhizospheric soil underneath plants was inaccessible, and we did not disturb the ecosystem.

Furthermore, bare soil samples without lithic elements or vegetation cover were selected, and each sampling point was at least 1.5 m away from the nearest plant. Bulk soil samples were collected underneath the foliage, near plants, or around cacti. In both cases, sampling points for replicates were separated by at least 5 m. Approximately 200 g of soil was collected and stored in polyethylene bags. Subsamples for microbiological analysis were stored in sterile tubes.

2.2. Soil temperature and relative humidity monitoring

The soil surface temperature (T) and relative humidity (RH) at different altitudes (300, 500, 600, 700 masl) were monitored every hour daily for two months (June and July 2019, winter) using THERMO-S-KIT-H Hygrochron temperature and humidity data loggers (iButtonLink LLC, Whitewater, WI, USA). The temperature and RH measurement accuracies were ± 0.5 °C and ± 3.5%, respectively. The loggers were installed at the central soil sampling point at each altitude. The temperature and RH data at 400 masl were calculated as the mean of the data recorded at 300 and 500 masl.

2.3. Soil physicochemical properties

The electrical conductivity (EC) and pH were measured in a soil–distilled water suspension with a solution ratio of 1:2.5 using a conductivity meter (HANNA HI98192) and pH meter (HANNA HI991001). The organic matter (OM) content was determined using dichromate oxidation. The total P (TP), inorganic P (IP), and organic P (OP) contents of the soils were determined using the extraction method proposed by Saunders and Williams (1955). The P concentration was measured with the method reported by Murphy and Riley (1962). Base saturation (exchangeable bases Ca^{2+}, Mg^{2+}, Na^{+}, and K^{+}) and cation exchange capacity (CEC) were calculated.

2.4. Fog water sampling and characterisation

Fog water samples were obtained with a handmade fog collector installed on a hilltop. The fog collector was constructed using a standard raschel mesh with a fog-collecting area of 1.0 m^2. Plastic

pipes formed the mesh support. Fog water was collected in a glass bottle and stored until measurement. The fog water was filtered through a 0.45 µm membrane and analysed using inductively coupled plasma optical emission spectrometry (ICP-OES) with a Perkin Elmer Optima 7,000 DV.

2.5. Mineralogical characterisation

The soil sample mineralogy was determined with X-ray diffraction (XRD) analysis. The XRD analysis was carried out using a Siemens D5000 diffractometer (Cu Kα1 radiation). The X-ray generator was operated at a power of 40 kV and 30 mA. The goniometer was equipped with a graphite monochromator. Powder patterns were analysed using DiffracPlus and total pattern analysis software (TOPAS). Crystalline phases were identified using the International Centre for Diffraction Data (ICDD) database. The X-ray fluorescence (XRF; Siemens SRS-3000) was used to quantify the total oxides.

2.6. Weathering index calculations

In this study, the most frequently used weathering indices (WIs) were calculated using the total oxides, quantified by XRF, and expressed in moles. The WIs include the Weathering Index of Parker (WIP), Vogt's Residual Index (V), Chemical Index of Alteration (CIA), Chemical Index of Weathering (CIW), Plagioclase Index of Alteration (PIA), weathering index 1 (WI1), and weathering index 2 (WI2) (see the index formulation in Supplementary material Table S1; Vogt 1927; Ruxton 1968; Parker 1970; Nesbitt and Young 1982; Harnois 1988; Fedo et al. 1995; Price and Velbel 2003).

2.7. Metabarcoding and microbial community analysis

The total DNA was extracted from the bare and bulk soil samples collected at the seven different altitudes using the DNeasy PowerSoil Kit ® (Qiagen) according to the manufacturer's instructions. The bacterial 16S rRNA gene V4 region (~250 bp) amplification (515F and 806R primers: Caporaso et al. 2012), the fungal rRNA internal transcribed spacer (ITS) gene region (ITS1F and ITS2 primers: White et al. 1990; Gardes and Bruns 1993), 250 bp paired-end library construction, and sequencing on a MiSeq (Illumina) platform were performed at the Environmental Sample Preparation and

Sequencing Facility at the Argonne National Laboratory (Illinois, USA). Subsequently, analyses were conducted using R v3.5.2 (R Core Team, 2018) and RStudio v1.1.463 (RStudio Team, 2016). The R package DADA2 v1.16.0 pipeline (Callahan et al., 2016) was used to infer each sample's amplicon sequence variants (ASVs). Briefly, the reads were evaluated for quality control and subsequently trimmed (Ns = 0, length ≥ 150 bp, expected errors ≤ 2), followed by dereplication, denoising, and merging of paired reads. After the ASV table was built by 97% clustering, the chimeras were removed, and the taxonomic assignment was carried out using the Silva v138 (for bacteria; Quast et al. 2012) and UNITE v8.2 (for fungi; Abarenkov et al. 2020) databases and the DADA2 Ribosomal Database Project's (RDP) naive Bayesian classifier (Wang et al. 2007). The data were normalised by variance-stabilising transformation using the R package DESeq2 v1.28.1 (Love et al. 2014). Using the R package DECIPHER v2.16.1 (Wright 2016), a multi-sequence alignment was performed to infer the phylogeny using FastTree v2.1.10 (Price et al. 2009). Furthermore, a phyloseq object (containing the ASVs, taxonomy assignation, phylogenetic tree, and meta-data) was created using the R package Phyloseq v1.32.0 (McMurdie and Holmes 2013) and used to calculate the alpha diversity indexes (Shannon, Simpson, and Chao1). The beta diversity (Principal Coordinates Analysis PCA–Bray Curtis distance with environmental variables fit) was calculated using the R package ampvis2 v2.4.5 (Andersen et al. 2018). Finally, taxonomy composition plots were generated using the R package ggplot2 v3.3.2 (Wickham 2016).

2.8. Statistical analysis

The normal distribution of the data obtained from the bare and bulk soil analyses (pH, CE, OM, TP, IP, and OP) was tested using the Shapiro–Wilk test ($n < 50$). Because the distribution was normal, a parametric statistic was used ($\alpha = 0.05$, considered significant). The Levene test was used to verify the homogeneity of the variances ($\alpha = 0.05$). Analysis of variance (ANOVA) between groups (bare and bulk soil) and the altitude was used, and comparisons were made for each pair using Tukey's test. Differences were considered significant at $p \leq 0.05$. All statistical analyses were performed using IBM SPSS statistical software v22.

3. RESULTS

3.1. Vegetation associated with the MMNP

A vegetation gradient was observed along the studied altitude transect across the MMNP. The study area's lower section (100 masl) is vegetation-free, but *Nolana* spp. is sporadically present at ~200 masl (Supplementary material, Figure S1). At 300 masl, *Tetragonia angustifolia* shrubs and *Copiapoa boliviensis* appeared (Supplementary material, Figure S1). Between 400 and 500 masl and above, lichens were observed in addition to the above-mentioned species (Supplementary material, Figure S1). Above 600 masl, *Copiapoa boliviensis* and *Eulychnia morromorenoensis* (endemic species) were prevalent (Supplementary material, Figure S1). *Copiapoa boliviensis*, known as the 'Atacameño cactus', occurs as a solitary body or in the form of cushions, whereas *Eulychnia morromorenoensis* is a branched columnar cactus, reaching 2 to 7 m in height. In addition, *Eriosyce recondita* (common name: 'Quisquito') was also observed at this altitude (Supplementary material, Figure S1). This small cactus stands alone at ground level in the sand, and identification with the naked eye is difficult. It should be noted that *Eriosyce recondita* and *Eulychnia morromorenoensis* are classified as 'Endangered' and 'Vulnerable', respectively, in the Chilean National Species Inventory (DS 29/2012).

3.2. Variations in temperature and relative humidity

The daily T and RH patterns at different altitudes are shown in Figure 2. Both parameters varied temporally and spatially. A temperature increase was recorded between 8:45 am and 6:45 pm at all altitudes (Figure 2A). The RH decreased within this time frame at all altitudes (Figure 2B). These variations were expected because T and RH are related, and temperature changes cause variations in the evaporation and humidity ratios (Figure 2). The minimal RH was observed at ~12:45 pm and 1:45 pm. The temperature maxima at altitudes of 700 and 300 masl were 29.7 and 23.5 °C, respectively. At intermediate altitudes, lower maximum temperatures of 21.0 °C (400 masl), 18.6 °C (500 masl), and 15.6 °C (600 masl) were recorded. At noon, it was hotter at 700 masl than at the low altitudes. In the evening and night, the temperatures were lower at all altitudes. Lower temperatures were recorded during the night and early morning (Figure 2A).

Regarding the RH, minima of 32.6% and 54.0% were detected at 700 and 300 masl, respectively (Figure 2B). At intermediate altitudes, RH minima were recorded at 59.5% (400 masl), 64.9% (500 masl), and 72.8% (600 masl). Therefore, the soil surface temperature decreased with increasing RH. On the other hand, higher temperatures and lower RH values were recorded at the extreme altitudes of 300 and 700 masl. These findings indicated that the RH from fog buffered the soil surface temperature at intermediate altitudes. As the fog decreased at noon, temperatures increased at all altitudes. Thus, the RH increase due to fog leads to a decrease in the soil surface temperature and affects the soil moisture. The tempering effect of fog is most apparent at 500–600 masl, where it creates suitable conditions for plant establishment and survival.

3.3. Impact of fog on soil properties

The analysed fog water from MMNP had a pH value of 5.54 ± 0.11 and a low EC of 204.66 ± 3.79 µS cm^{-1}. The main cations in the fog water were: Na^{+} (20.28 ± 1.31 mg L^{-1}); Ca^{2+} (7.76 ± 0.16 mg L^{-1}); Mg^{2+} (3.94 ± 0.07 mg L^{-1}); and K^{+} (1.47 ± 0.15 mg L^{-1}). The main anions were: Cl^{-} (99.01 ± 3.85 mg L^{-1}), SO_4^{2-} (45.80 ± 2.62 mg L^{-1}), and HCO_3^{-} (27.33 ± 3.06 mg L^{-1}).

The soil pH variations along the altitudinal transect are shown in Table 1. The pH values of all samples (bare and bulk soils) ranged between 6.4 and 8.7. With increasing altitude, the pH decreased. The observed differences were significant ($p < 0.05$). High alkaline pH values were recorded at elevations of 100, 200, and 300 masl. However, above 400 masl, the pH values began to decrease and tended to be around 7.5 above this altitude. In addition, the pH differences between the bulk and bare soil samples at each altitude were insignificant ($p < 0.05$).

Variations in the EC along the altitudinal transect are shown in Table 1. The EC decreased with increasing altitude, and the differences were significant ($p < 0.05$). However, the differences between the EC values of bare and bulk soils were insignificant. The highest EC values were recorded at 100 masl (6.86 and 10.96 mS cm^{-1} for bare and bulk soil, respectively). The lowest ECs were detected from 500 masl, with an average value of 1.95 ± 0.06 mS cm^{-1}.

On the other hand, the base saturation percentage of bare and bulk soils was high (>90%) along the altitudinal transect. However, the CEC was low at all sample points, with an average of 5.5 ± 0.67

meq 100 g^{-1}, consistent with the CEC of sandy soils (Tan 1993). Notably, samples collected at 400 and 500 masl exhibited slightly higher CEC values (6.5 ± 0.24 meq 100 g^{-1}) than those from other altitudes (5.1 ± 0.3 meq 100 g^{-1}).

The OM concentration significantly increased ($p < 0.05$) along the altitudinal transect (Table 1). In general, we detected a higher OM content in the bulk soil than in the bare soil, and the difference was significant ($p < 0.05$). The bulk soil OM concentration ranges from 0.41% to 2.56%. Higher values were detected at 500 and 600 masl. Regarding bare soil, the OM content varied between 0.07% and 1.61%, and the highest value was detected at 600 masl. Above 400 masl, the OM concentration increased, possibly because the moisture from fog promotes vegetation growth at these altitudes.

On the other hand, Table 1 shows the TP, IP, and OP concentrations of bare and bulk soil along the altitudinal gradient. The TP and IP concentrations of bare soil decreased with the increase in the altitude from 100 to 600 masl and significantly differed ($p < 0.05$). In two subgroups, a higher TP content was identified at altitudes of 100, 200, 400, and 700 masl. A lower TP was obtained at 300, 500, and 600 masl. In contrast, the variation in the OP content of bare soil with the altitude was insignificant ($p < 0.05$; Table 1). The IP content of bare soil varied between 61% and 99% along the altitudinal transect, with an average of 80%. Significantly low TP and IP values were obtained for bulk soil at 300, 400, 500, and 600 masl ($p < 0.05$). The highest TP and IP values were recorded at 100–200 and 700 masl (Table 1). In general, higher TP contents were detected in bare soil samples (average of 669 ± 306 mg kg^{-1}; n = 21) than in bulk soils (average of 576 ± 439 mg kg^{-1}; n = 21). The OP percentage was slightly higher in bulk soil, accounting for 26% of TP on average, than in bare soil (19% of TP). The TP and IP concentrations of bare and bulk soils varied with altitude (significant difference, $p < 0.05$). However, significant differences between bare soil and bulk soil were not observed.

3.4. Mineralogical characterization

The XRD analyses revealed a variety of minerals along the altitudinal gradient (Table 2). The main minerals in the bare and bulk soils from all altitudes were magnesiohornblende, calcium albite, quartz, and chlorite. Anorthite, pyrophyllite, kaolinite, anhydrite, and sanidine mainly occurred in the bare soil

292 samples. Hematite, jarosite, and orthoclase were detected in the bulk soil samples collected above
293 400 masl. Secondary minerals, such as kaolinite and haematite, produced by primary mineral
294 weathering, were also detected (Table 2).
295 The major oxide compositions of the bare and bulk soils from different altitudes were determined by
296 XRF analysis (Table 3). Similar values were obtained for the bare and bulk soils. The major element
297 analyses showed that SiO_2 ranged from 45.35% to 53.17% in both soils. On the other hand, the Al_2O_3
298 values of bare and bulk soil ranged between 14.39% and 22.25% and 15.14% and 19.05%,
299 respectively. The MgO and CaO contents of all samples varied between 4.83% and 8.30%, and
300 5.46% and 9.29%, respectively. The Na_2O and K_2O concentrations ranged from 1.80% to 3.58% and
301 0.42% to 1.47%, respectively.
302 Long-term exposure of rocks to atmospheric conditions causes physical and chemical weathering,
303 and visual signs of physical weathering occur in the MMNP. For example, the occurrence of tafone
304 rocks below 300 masl (Supplementary Material, Figures S2) indicates salt weathering in the coastal
305 area. Table 4 lists the WIs calculated for the bare and bulk soils at different altitudes (WIP, V, CIA,
306 CIW, PIA, WI1, and WI2). The WIP obtained in this study ranged from 53.15 to 79.30. High WIP
307 values were determined for lower altitudes of 100-200 masl and at 700 masl. The V ratio obtained in
308 our study varied between 0.41 and 0.84. The highest values occurred above 300 masl until 600 masl
309 in bare soils. In bulk soils, highest V values were detected at 400 and 500 masl. The CIA index in this
310 study ranged between 40.95 and 58.97, where the highest values were detected at intermediate
311 altitudes. The CIW index obtained in this study for both bare and bulk soils ranged from 42.04 to
312 59.90. Higher CIW values were detected for bare soils at 300, 400, and 500 masl, with values of
313 59.90, 55.45, and 53.63, respectively. Meanwhile high CIW values of bulk soils were 57.85 (400 masl)
314 and 51.20 (500 masl).
315 The PIA index determined in this study ranges from 38.34 to 57.42. The WI1 ranges between 3.46
316 and 5.89, and the WI2 varies from 12.37 to 14.81 for both bare and bulk soils. The WI1 values of bare
317 soils were lower at 300 and 400 masl (3.46 and 4.26) than those of bulk soils (5.02 and 4.05) at the
318 same altitude. The WI2 does not show an altitude-dependent trend.
319

3.5. Diversity and variability of soil microbiomes

Our results indicate that the environmental parameters (T and RH) vary significantly (Figure 2), which is reflected in the substantial variation in microbial communities and soil characteristics at different altitudes. The Actinobacteria and Bacteroidetes phyla are clear dominants in the bare soil, while only Bacteroidetes are the most abundant in the bulk soil communities at all altitudes (Figure 3). The Proteobacteria abundance was roughly homogeneous in all communities in both soil types (Figure 3A). However, Halobacterota, Planctomycetota, and Firmicutes phyla distribution and abundance were highly heterogeneous, and they were only detected in communities exhibiting contrasting abundances (Figure 3A). On the other hand, the abundance and composition of fungi in these communities, were more stable than the bacteria in MMNP; showing a clear dominance of Ascomycota members in both soil types, followed by the Basidiomycota phylum (Figure 3B). Variations in this pattern only occur in some bare soil communities. In addition, there were not many differences between the bare and bulk soil fungal communities, despite the substantial differences in their bacterial compositions (Figure 3).

Regarding the alpha diversity measures, the Chao1, Shannon, and Simpson indexes showed that the greatest bacterial and fungal biodiversity occurred in samples collected between 500 and 700 masl, showing that these indexes increase considerably with the altitude (Figure 4A). Also, the effects of all environmental variables and soil properties on the microbial community composition and structure were tested and we observed that many of those (conductivity, mean/max T, mean RH, organic C, altitude) were significant and could affect the communities' structure, distribution, and grouping (by similitudes) (Figure 4B). In addition, some structure or grouping by altitude was evident among communities. In most cases, bare and bulk soil communities from the same altitude were similar and distinct from those of other altitudes. Furthermore, the conductivity and CaO content seem more associated with microbial communities from lower altitudes (100, 200, and 300 masl). At the same time, the organic C content, humidity, and WI2 weathering index isolated some communities (bulk soils from the 500 masl and both soil types from the 600 masl) from the main groups, which were under different levels of pressure from other variables.

4. DISCUSSION

4.1. Vegetation associated to MMNP

Our observations of the altitude-dependent plant variation were similar to previous reports on the flora in foggy ecosystems in Northern Chile (Supplementary material, Figure S1). For example, Oltremari et al. (1987) showed that the vegetation in the Morro Moreno sector exhibits a clearly defined altitudinal stratification including four strips: coastal desert strip (150–350 masl) in the east, middle desert strip (350–750 masl), fertile strip (750–900 masl), and desert over 900 masl. On the other hand, there is a sector with abundant coastal fog in the Antofagasta region close to Tocopilla (22°S, Chile), which is characterised by desert scrub consisting of *Nolana peruviana* on the ravines and slopes below 500 masl, and *Eulychnia iquiquensis* and *Ephedra breana* on slopes above 500 masl (Luebert et al. 2007). Oltremari et al. (1897) reported mainly *Nolana aplocaryoides*, *Cristaria oxyptera*, and *Philippiamra pachyphilla* for the Morro Moreno sector (150–350 masl). Lichens have also been reported on granitoid particles in foggy ecosystems of the Pan de Azúcar National Park (Jung et al. 2020a). In the Alto Patache Chilean fog oasis, 77 lichen species have been identified (Vargas Castillo et al. 2017). Oltremari et al. (1987) reported *Heliotropium picnophyllum*, *Polyachyrus fuscus*, and *Copiapoa boliviana* at altitudes ranging from 350 and 750 masl. The authors also reported *Heliotropium chenopodiaceum*, *Lycium fragosum*, and *Eulychnia morromorenoensis* above 500 masl. Our observations are consistent with those previously described in MMNP, and several of the species have also been found in other 'Camanchaca' areas in Chile (Oltremari et al. 1987; Luebert et al. 2007; Guerra et al. 2010; Pliscoff et al. 2017).

4.2 Variations in temperature and relative humidity

Temperature (T) and Relative Humidity (RH) varied temporally and spatially. Distinctives curves for both were observed during the day at all studied altitudes (Figure 2). As expected, like Cáceres et al. (2007), we registered large T daily oscillations, with maximum T values at noon. In addition, minima values of RH were at noon meanwhile the maximum RH values which are reached at night. During the day the lowest temperatures and highest RH were reached at intermediate altitudes, which indicated the greatest presence of fog. The variation of the T and the RH data demonstrate the

amelioration of extreme temperature conditions by fog at intermediate altitudes of 400, 500, and 600 masl. Marzol-Jaén et al. (2011) showed the effect of fog on the microclimatic conditions on Tenerife. They observed lower temperatures and wind speeds and increased humidity during fog. Gultepe et al. (2009) reported a similar relationship between the T and RH. They showed that fog reduces extreme weather conditions, and at fog-affected sites, the temperature and moisture generally fluctuate less. Fog improves local conditions by reducing longwave radiation and creating fewer extreme temperatures. Together with fog, the plant canopy ameliorates high temperatures. On the other hand, in foggy ecosystems, plant species act as condensation surfaces. They are integral parts of the ecosystem, improving the storage of water, which can be used by other species (Sotomayor and Drezner 2019). Li et al. (2018) studied the effects of potential changes in fog distribution on the soil moisture dynamics in the Namib Desert and demonstrated that fog affects the soil moisture dynamics during rainless periods, which has critical implications for the biogeochemical soil processes.

4.3 Effect of fog on soil properties

Soil stores water and provides nutrients and specific niches for microbial life, supporting the fog ecosystem flora and fauna. In fog ecosystems, the soil is exposed to constant wetting and drying such that the soil moisture is related to the arrival rate of the fog and soil depth (Li et al. 2018). In our study pH and EC decreased with the altitude in both bare and bulk soils (Table 1). The soil pH decrease is a consequence of multiple simultaneous processes such as the release of H^+ by the weathering of the soil minerals, production of carbonic acid by atmospheric CO_2 dissolution, organic acid release by the soil microorganisms and plant roots, decomposition of organic matter, and ion uptake by biota. Water is also a source of H^+ ions, and the H^+ from fog water is absorbed by the clay complex in an exchangeable form, leading to a reduction in soil pH (Tan 1993). On the other hand, the higher EC values observed at the lower altitudes are related to the higher salt content, which could be reflected in the higher CaO and Na_2O contents (Table 3).

The coastal fog also contains ions that interact with the soil. Is the case of Mg^{2+}, Na^+, and Cl^- ions in the fog water originate from sea salts, and SO_4^{2-}, K^+, and HCO_3^- are derived from soil dust (Schemenauera and Cerecedab, 1992). Similar results were reported for fog water samples by

Beiderwieden et al. (2005), with median pH and EC values of 4.58 and 23 μS cm^{-1}, respectively. Nieberding et al. (2018) reported that the pH values of fog events in a subtropical mountain cloud forest varied from acidic (pH < 5.0) to very acidic (pH < 4.0). Both Beiderwieden et al. (2005) and Nieberding et al. (2018) reported varying concentrations of ions such as Ca^{2+}, Mg^{2+}, Na^{+}, SO_4^{2-}, and NO_3^{-}. The fog deposition and continuous wetting and drying cycles contribute nutrients, salts, and contaminants to the soil. The effects of these external inputs on the soil properties should be investigated further.

The OM increased with the altitude showing significantly higher values in bulk soils, which could be attributed to the vegetation (Table 1). Vegetation adds OM to the soil, as shown by the higher OM concentrations in bulk soil (associated with plants). Therefore, we infer that the highest OM content is related to the high RH generated by fog and the amelioration of the temperature. For example, in the southern Iquique coastal area (in North Chile), the vegetation cover is associated with constant coastal fog events, leading to vegetation development between 300 and 800 masl (Muñoz-Schick et al. 2001).

Phosphorus is an essential nutrient for plants, it is uptake as a phosphate ion and once inside the biomass it can form part of organic P compounds, which are returned to the soil through the incorporation of plant remains and detritus. In general, higher TP contents were detected in bare soil samples than in bulk soils (Table 1). This can be attributed to the fact that the P remains in the soil and has not been immobilized in the plant biomass. Additionally, significantly low TP and IP values were obtained for bulk soil at intermediate altitudes, with OP percentage were slightly higher in bulk soils (Table 1). These findings would indicate that P was uptake and extracted by the vegetation. Additionally, the highest organic P values in bulk soil would come from plant debris or microbial biomass.

4.4 Mineralogical and weathering analysis

The XRD analyses revealed a variety of primary minerals as well as secondary minerals produced by primary mineral weathering (Table 2). Based on the Jackson–Sherman soil weathering stages, an abundance of primary minerals (inherited from parent materials, particularly igneous rocks), such as magnesiohornblende and calcium albite, indicates an early stage of weathering (Sposito 2008). In

arid regions, the early weathering stage is mainly associated with low water content, low humus content, and limited leaching (Sposito 2008). The presence of chlorite is related to low-degree metamorphism deep below the surface. Feldspars weathering (e.g. albite and anorthite) generates clay minerals and releases Ca, Na, and K ions, whereas amphiboles weathering (e.g. hornblende) releases Fe and Mg into the solution (Wani et al. 2016). The detection of kaolinite and iron oxides originating from chemical weathering in the soil indicates hydrolysis, removal of cations and silica, and oxidation of Fe^{2+}. Muenchow et al. (2013), who studied soils from different altitudes in a Peruvian Desert fog oasis, showed that the altitude reflected the water availability and soil properties and identified a humid bromeliad vegetation belt (at ~700 masl), which harboured the largest number of species). In addition, the same authors indicate that signs of humification and a brownish colour due to iron oxide release from primary minerals, the elevated clay, soil OM, and cation concentrations indicated advanced soil development.

Long-term exposure of rocks to atmospheric conditions causes weathering, and the observation of tafone rocks indicated the presence of this phenomenon in the MMNP (Supplementary Material, Figure S2). Physical weathering causes rock disintegration, generating smaller grains without changing their chemical or mineralogical composition (Wani et al. 2016). For example, salt bursts occur in coastal deserts and are promoted by frequent alternating drying and wetting cycles. Dissolved substances are not eluted; instead, they accumulate in the soil and on the rocks' outer surfaces due to evaporation (Blume et al. 2016). To quantify chemical weathering, we calculated the weathering indices (Table 4) that are used to approximate the degree of weathering of the rocks. Most indices are based on the molar ratio between mobile and immobile major oxides. Feldspars are the most abundant reactive (labile) minerals. Consequently, the dominant process during chemical weathering of the upper crust is the degradation of feldspars and the concomitant formation of clay minerals (Nesbitt and Young 1982). The WIP considers the susceptibility of Na^{+}, K^{+}, Ca^{2+}, and Mg^{2+} to be mobilised during weathering (Parker 1970). The WIP values are commonly between 0 and 100, with the least weathered rocks having the highest values. In our study, high WIP values were determined for lower altitudes of 100 and 200 masl, indicating a lower degree of weathering compared to higher altitudes. Vogt's Ratio (V) is defined by the ratio of the number of oxides of immobile cations

460 (mainly Al) to that of mobile cations (magnesium, calcium, and sodium) based on the assumption that
461 the potassium content remains constant during weathering (Price and Velbel 2003). The optimum
462 Vogt's ratio (V) of fresh and weathered rocks is 0 and 1, respectively. A larger value indicates higher
463 weathering intensity (Price and Velbel 2003). Our results showed that the highest V ratio values
464 occurred above 300 masl. The CIA index measures the weathering intensity on a scale from 1 to 100,
465 where a higher value represents more intense chemical weathering (Fedo et al. 1995). In general,
466 the CIA index in this study indicated a low weathering. However, it was possible to detect highest
467 values at intermediate altitudes. Low values of CIA suggest the lack of chemical alterations and cool
468 and/or arid climate conditions (Fedo et al. 1995). Unweathered rocks and minerals ranging from
469 gabbro through K-feldspar have a similar CIA value of ~50 (Fedo et al. 1995).
470 The CIW index is similar to the CIA but eliminates K_2O from the equation. The CIW measures the
471 weathering intensity on a scale from 1 to 100, where a higher value represents more intense chemical
472 weathering (Fedo et al. 1995). In our case, CIW index showed highest values at intermediate
473 altitudes. The PIA value of non-weathered rocks is 50, and that of clay minerals, such as kaolinite,
474 illite, and gibbsite, is close to 100 based on the CIA formula (Fedo et al. 1995). The PIA index
475 determined in this study were close to 50 indicating a low degree of weathering. Silica-based WIs,
476 such as WI1 and WI2, show the ratio between the mobile/immobile index (Ruxton 1968). The WI1
477 (also known as Ruxton Ratio R) is expressed by the SiO_2/Al_2O_3 ratio and assumes that Al_2O_3 remains
478 immobile during weathering. Meanwhile, silica is lost from total element content (Ruxton 1968), where
479 0 indicates the optimum weathering value and >10 indicates the optimum fresh value. The values of
480 WIs calculated for the bare and bulk soils at different altitudes (Table 4) showed values close 5,
481 indicating some weathering level. The lesser values of WI1 were detected at intermediate altitude
482 (400 masl), indicating some level of weathering, possibly related to the fog at this altitude. In spite of,
483 it was observed that in arid coastal environments the low weathering of the soil predominates, it was
484 confirmed that the components of the coastal fog such as water and salts could influence the physical
485 and chemical weathering of the soil at different altitudes. However, additional studies are required to
486 clarify the processes.
487

488

489 **4.5 Diversity and variability of soil microbiomes**

490 The Atacama array of ecological niches is a microbial diversity reservoir, rich in organisms adapted
491 to challenging conditions (Azua-Bustos et al. 2012; Bull et al. 2016) and highly niche-specific. In this
492 context, a vastly different microbial diversity can occur in geographical and altitudinal proximity.
493 Although research on these systems is sparse, it is known that fog affects the species diversity in
494 coastal deserts (Rundel and Mahu 1976). The dominance of Actinobacteria and Bacteroidetes phyla
495 among the samples suggests different adaptations for each niche associated with the particular
496 abiotic conditions, namely moisture, temperature and other physicochemical parameters with
497 significant variance (Figure 3). Particularly, the dominance of Actinobacteria was expected since this
498 phylum is especially prevalent in soils and has been detected in extreme and foggy environments;
499 while Proteobacteria, Firmicutes, Bacteroidetes, and Chloroflexi (although they are also prevalent,
500 mainly due to their stress tolerance and metabolic versatility) were less abundant (Dueker et al. 2011;
501 Nielson et al. 2017; Evans et al. 2019; Warren-Rhodes et al. 2019). Despite the vital roles
502 Cyanobacteria taxa play in bio-weathering and lithomatrix transformation processes (Jung et al.
503 2020b), they were absent in both soil types (Figure 3A). This may be due to a lack of the liquid water
504 these microorganisms require. Therefore, microalgae, which are more efficient at obtaining water
505 from fog or air humidity, may dominate these communities. Moreover, it is known that Cyanobacteria
506 members are associated with superficial biocrusts, where they are exposed to sunlight (Samolov et
507 al. 2020), explaining why we did not detect them. Nonetheless, it has been reported that other
508 heterotrophic microorganisms, such as basidiomycete fungi (Kirtzel et al. 2020) and bacteria
509 (Matlakowska et al. 2012), can carry out bio-weathering, fulfilling the role of the absent Cyanobacteria.
510 The great abundance of Ascomycota followed by the Basidiomycota in most of the samples from both
511 soil types is the same pattern reported for coastal Maine (USA), the Namib Desert (Namibia), and
512 Salar Grande (Chile) (Evans et al. 2019; Gómez-Silva et al. 2019). The patterns of fungal
513 communities (regarding bacterial one) may be due to plants' ability to select and shape the soil
514 microbiology, a process in which fungal communities tend to remain more stable, as their members
515 a less diverse (Fonseca-García et al. 2016; Yan et al. 2017). On the other hand, it has been reported

516 that plant-growth-promoting microorganisms increase plant organic acid exudation, degrade
517 minerals, and intensify the weathering (Lopez-Bacillio et al. 2020), dynamics that might occur in the
518 MMNP. Also, hypolithic microbial communities thriving on the seaward face of the coastal range can
519 survive by using fog as their primary moisture source (Azúa-Bustos et al. 2011). However, the fog
520 biotic input to the communities (ocean–terrestrial cells transfer) must also be considered, as the
521 presence of aerosol microorganisms has been verified (Dueker et al. 2011; Evans et al. 2019). The
522 results of studies in the Namib Desert showed that different wetting events and soil environmental
523 conditions affect the microbial community structures of the desert (Evans et al. 2019).
524 As we stated that microbial diversity increases considerably with altitude, specially from 400 masl
525 (Figure 4A) this can be explained by the variation of several of the previously studied physicochemical
526 and environmental factors. At these altitudes, the humidity (Figure 2), the OM concentration (Table
527 1), the degree of soil weathering (Table 4), and the plant coverage/diversity (Supplementary Material,
528 Figure S1) are all higher, suggesting that these parameters could influence diversity. Particularly,
529 many of our tested environmental variables and soil properties could significantly affect the
530 communities' structure and distribution (Figure 4B). This confirms previous reports describing the
531 considerable impact of polyextreme environments on organisms, resulting in heterogeneous
532 taxonomic patterns (Vásquez-Dean et al. 2020). Our finding supports previous reports in which the
533 soil RH and T are correlated with microbial diversity richness and diversity, and a combination of
534 these variables with altitude and EC best explains community composition variations for several
535 Atacama areas (Nielson et al. 2017: Warren-Rhodes et al. 2019). However, the interplay among the
536 variables has not been determined.
537 Furthermore, as mentioned before, microorganisms can be transported over varying distances by air
538 or moving animals, but efficient dispersal depends on the species resistance to unfavourable
539 conditions during transport (Samolov et al. 2020). However, fungal and bacterial communities can
540 adapt to long-term drought regimes (Frossard et al. 2015). A study by Evans et al. (2019) reported
541 that local sources strongly control fog microbial communities, resulting in more marine species in fog
542 near the coast; in addition, fog deposits show a higher microbial diversity than air. Also, Jung et al.
543 (2020b) discovered a ground cover or biocrust named grit–crust biocenosis, dominated by lichens,

544 fungi, and algae attached to grit-sized (~6 mm) quartz and granitic particles in fog soils on the coast
545 of the Atacama Desert (comparable to biocenosis forming a layer on top of the soil and rock surfaces,
546 i.e. cryptogamic ground cover). The authors stated that every fog event in the Atacama Desert led to
547 photosynthetic activity by the soil communities. This enabled the unique biocenosis to fulfil various
548 ecosystem services, preventing erosion, contributing to C, N, and P accumulation, and assisting soil
549 formation through bioweathering. These effects could significantly contribute to biogeochemical
550 cycles in low-OM desert environments. In accordance with these studies, our results also show a
551 correlation between water availability and high microbial diversity.
552 On the other hand, Lopez and Bacilio (2020) proposed that cacti could act as rock-weathering and
553 soil formation pioneers. They could fulfil this function due to their long-life cycles and association with
554 beneficial microbial communities in the rhizosphere, rhizoplane, or endosphere, which enable them
555 to participate in the early development of soil. The microbial biomass associated with cacti improves
556 growth by increasing photosynthesis and the exudation of organic acids that degrade minerals and
557 increase nutrient uptake. Together, plants and microbes intensify the weathering and cover a broader
558 spectrum of mineralisation. This is relevant because, as we previously described, the coverage by
559 cactus species in the MMNP is substantial, and the species differ along the altitude gradient. Hence,
560 the changes in vegetation correlate with the changes in microbiological composition.
561 Notably, our results highlight the variability of conditions in this 'small' altitudinal range, evidenced by
562 the number of environmental and physicochemical variables significantly influencing the composition
563 and structure of microbial communities. Also, the considerable microbiological diversity reported in
564 this work reflects the different niches comprising the MMNP environment.
565 Finally, using our study results, we constructed a diagram of the fog effect on soil formation, including
566 the essential aspects of soil weathering (Figure 5). Single processes of biogeophysical and
567 biogeochemical weathering by bacteria (phototrophs), green algae, lichens, and fungi have been
568 reported. Such processes include the biological transformation of clay minerals, for example, by the
569 K depletion of interlayers of mica/illite and the oxidation of structural Fe (II) in less weathering-
570 resistant silicates such as biotite, as well as the dissolution of phosphate salts such as apatite. Many
571 studies have investigated the weathering of quartz, one of the commonest minerals. The atoms are

linked in a SiO4 framework in quartz, making it one of the most weathering-resistant minerals. It has been demonstrated that various microorganisms mediate biochemical weathering processes of rock-forming minerals such as the excretion of pH-shifting substances that interfere with the lithomatrix (acidolysis or alkalinolysis) and the production of chelating compounds, such as siderophores, for the manipulation of the redox potential via extracellular enzymes (Jung et al. 2020b).

5. CONCLUSIONS

This is the first report showing the variations of soil properties and microbial communities with altitude on the Pacific coast. Significant changes in the soil parameters and microbial communities (bacteria and fungi) along an altitudinal gradient (100–700 masl) were detected at Morro Moreno National Park (MMNP). Fog increased the relative humidity and reduced the daily temperature ranges affecting the vegetation and the soil and microbial community. We also found signals of soil weathering at intermediate altitudes. Changes in soil parameters and microbial community composition were more closely related to altitude than to soil type (bulk or bare). Bacteria differed at each altitude, while fungi tend to be more stable, suggesting specialisations related to other conditions (amount and type of vegetation and the water availability). Linkages between soil property and microbial variations with altitude within these Northern Chilean coastal fog ecosystems were elucidated. This novel scientific knowledge contributes to global network strategies for fog ecosystem conservation which aim to retain microbial niches and diversity. The study data on the characteristics, particularly the biodiversity, of these unique environments can be used to create a baseline of soil properties and a first inventory of the microbial community in fog ecosystems on the Pacific coast. This information will be invaluable for creating a global study network to evaluate fog ecosystems on the Pacific coast and elsewhere.

6. REFERENCES

1. Abarenkov, K., Zirk, A., Piirmann, T., Pöhönen, R., Ivanov, F., Nilsson, H., & Kõljalg, U. (2020). UNITE general FASTA release for Fungi. Version 04.02.2020. UNITE Community.
2. Andersen, K. S., Kirkegaard, R. H., Karst, S. M., & Albertsen, M. (2018). ampvis2: an R package to analyse and visualise 16S rRNA amplicon data. *BioRxiv*, 299537. https://doi.org/10.1101/299537
3. Azúa-Bustos, A., González-Silva, C., Mancilla, R. A., Salas, L., Gómez-Silva, B., McKay, C. P., & Vicuña, R. (2011). Hypolithic cyanobacteria supported mainly by fog in the coastal range of the Atacama Desert. *Microbial Ecology, 61(3)*, 568–581. https://doi.org/10.1007/s00248-010-9784-5
4. Azua-Bustos, A., Urrejola, C., & Vicuña, R. (2012). Life at the dry edge: microorganisms of the Atacama Desert. *FEBS Letters, 586(18),* 2939–2945. https://doi.org/10.1016/j.febslet.2012.07.025
5. Beiderwieden, E., Wrzesinsky, T., & Klemm. O. (2005). Chemical characterization of fog and rainwater collected at the eastern *Andes cordillera*. *Hydrology and Earth System Sciences Discussions, 2 (3)*, 863-885. https://doi.org/10.5194/hess-9-185-2005
6. Blume, H.P., Brümmer, G. W., Fleige, H., Horn, R., Kandeler, E., & Kögel-Knabner, I. (2016). Inorganic soil components – minerals and rocks. In: Scheffer/Schachtschabel Soil Science. Sringer, Berlin Heidelberg. pp. 7–53. https://doi-org.ezproxy2.ucn.cl/10.1007/978-3-642-30942-7_2
7. Bull, A. T., Asenjo, J. A., Goodfellow, M., & Gómez-Silva, B. (2016). The Atacama Desert: technical resources and the growing importance of novel microbial diversity. *Annual Review of Microbiology, 70,* 215–234. https://doi.org/10.1146/annurev-micro-102215-095236
8. Cáceres, L., Gómez-Silva, B., Garró, X., Rodríguez, V., Monardes, V., & McKay, C. P. (2007). Relative humidity patterns and fog water precipitation in the Atacama Desert and biological implications. *Journal of Geophysical Research, 112,* G04S14. https://doi.org/10.1029/2006JG000344

9. Callahan B., McMurdie P., Rosen M., Han A., Johnson A., & Holmes S. (2016). DADA2: High-resolution sample inference from Illumina amplicon data. *Nature Methods, 13(7),* 581–583. https://doi.org/10.1038/nmeth.3869
10. Caporaso, J. G., Lauber, C.L., Walters, W. A., Berg-Lyons, D., Huntley, J., Fierer, N., Owens, S. M., Betley, J., Fraser, L., Bauer, M., & Gormley, N. (2012). Ultra-high-throughput microbial community analysis on the Illumina HiSeq and MiSeq platforms. *The ISME Journal 6(8),* 1621-1624. https://doi.org/10.1038/ismej.2012.8
11. Cereceda, P., Larrain, H., Osses. P., Farías, M., & Egaña, I. (2008). The spatial and temporal variability of fog and its relation to fog oases in the Atacama Desert, Chile. *Atmospheric Research, 87(3-4),* 312-323. https://doi.org/10.1016/j.atmosres.2007.11.012
12. Cereceda, P., Schemenauer, R. S., & Valencia, R. (1992). Posibilidades de abastecimiento de agua de niebla en la Región de Antofagasta, Chile. *Revista de Geografía Norte Grande, 19*, 3–14.
13. Cortés, J., Marquardt, C., González, G., Wilke, H.-G., Marinovic, N. (2007). Cartas Mejillones y Península de Mejillones, Región de Antofagasta. Servicio Nacional de Geología y Minería, Carta Geológica de Chile, Serie Geología Básica, Nos. 103 y 104, 58 p., 1 mapa escala 1:100.000. Santiago.
14. DS 5. (2010). Crea Parque Nacional "Morro Moreno", en la Región de Antofagasta. Ministerio de Bienes Nacionales. Chile.
15. DS 29. (2012). Aprueba reglamento para la clasificación de especies silvestres según estado de conservación. Ministerio del Medio Ambiente. Chile.
16. Dueker, M. E., O'Mullan, G. D., Weathers, K. C., Juhl, A. R., & Uriarte, M. (2011). Coupling of fog and marine microbial content in the near-shore coastal environment. *Biogeosciences Discussions, 8(5), 9609-9637*. doi:10.5194/bgd-8-9609-2011
17. Evans, S. E., Dueker, M. E., Logan, J. R., & Weathers, K. C. (2019). The biology of fog: results from coastal Maine and Namib Desert reveal common drivers of fog microbial composition. *Science of the Total Environment, 647,* 1547–1556. https://doi.org/10.1016/j.scitotenv.2018.08.045

18. Fedo, C. M., Eriksson, K. A., Krogstad, E. J. (1995). Geochemistry of shales from the Archean (~3.0 Ga) Buhwa Greenstone Belt, Zimbabwe: implications for provenance and source-area weathering. *Geochimica et Cosmochimica Acta, 60(10),* 1751–1763. https://doi.org/10.1016/0016-7037(96)00058-0
19. Fonseca-García, C., Coleman-Derr, D., Garrido, E., Visel, A., Tringe, S. G., & Partida-Martínez, L. P. (2016). The cacti microbiome: interplay between habitat-filtering and host-specificity. *Frontiers in Microbiology, 7,* 150. https://doi.org/10.3389/fmicb.2016.00150
20. Frossard, A., Ramond, J. B., Seely, M., & Cowan, D. A. (2015). Water regime history drives responses of soil Namib Desert microbial communities to wetting events. *Scientific Reports, 5,* 12263. https://doi.org/10.1038/srep12263
21. Gardes, M., & Bruns, T. D. (1993). ITS primers with enhanced specificity for basidiomycetes-application to the identification of mycorrhizae and rusts. *Molecular Ecology, 2(2),* 113–118. https://doi.org/10.1111/j.1365-294X.1993.tb00005.x
22. Garreaud, R., Barichivich, J., Christie, D. A., & Maldonado, A. (2008). Interannual variability of the coastal fog at Fray Jorge relict forests in semiarid Chile. *Journal of Geophysical Research: Biogeosciences, 113*(G04). https://doi.org/10.1029/2008JG000709
23. Garreaud, R. D., Molina, A. Y., & Farias, M. (2010). Andean uplift, ocean cooling and Atacama hyperaridity: A climate modeling perspective. *Earth and Planetary Science Letters, 292(1-2),* 39–50. https//doi:10.1016 /j.epsl.2010.01.017
24. Gómez-Silva, B., Vilo-Muñoz, C., Galetović, A., Dong, Q., Castelán-Sánchez, H. G., Pérez-Llano, Y., Sánchez-Carbente, M. D. R., Dávila-Ramos, S., Cortés-López, N. G., Martínez-Ávila, L., Dobson, A. D. W., & Batista-García, R. A. (2019). Metagenomics of Atacama lithobiontic extremophile life unveils highlights on fungal communities, biogeochemical cycles and carbohydrate-active enzymes. *Microorganisms, 7(12),* 619. https://doi.org/10.3390/microorganisms7120619
25. Guerra C., Guerra, C., & Silva, A. (2010). Guía de la Biodiversidad en la Península de Mejillones Morro Moreno, Parque Nacional. Gobierno de Chile, Ministerio del Medio Ambiente. Tercera edición. Gráfhika Impresores.

26. Gultepe, I., Pearson, G., Milbrandt, J., Hansen, B., Platnick, S., Taylor, P., Gordon, M., Oakley, J. P., & Cober, S. G. (2009). The fog remote sensing and modeling field project. *Bulletin of the American Meteorological Society, 90(3),* 341–359. http://www.jstor.org/stable/26220960

27. Harnois, L. (1988). The CIW index: a new chemical index of weathering. *Sedimentary Geology, 55,* 319–322. 10.1016/0037-0738(88)90137-6

28. Jung, P., Baumann, K., Emrich, D., Springer, A., Felde, V. J. M. N. L., Dultz, S., Baum, C., Frank, M., Büdel, B., & Leinweber. P. (2020a). Lichens bite the dust – A bioweathering scenario in the Atacama Desert, *iScience, 23(11)*, 101647. https://doi.org/10.1016/j.isci.2020.101647

29. Jung, P., Baumann, K., Lehnert, L. W., Samolov, E., Achilles, S., Schermer, M., Wraase, L. M., Eckhardt, K., Bader, M. Y., Leinweber, P., Karsten, U., Bendix, J., & Büdel, B. (2020b). Desert breath—How fog promotes a novel type of soil biocenosis, forming the coastal Atacama Desert's living skin. *Geobiology. 18,* 113–124. https://doi.org/10.1111/gbi.12368

30. Kirtzel, J., Ueberschaar, N., Deckert-Gaudig, T., Krause, K., Deckert, V., Gadd, G. M., & Kothe, E. (2020). Organic acids, siderophores, enzymes and mechanical pressure for black slate bioweathering with the basidiomycete Schizophyllum commune. *Environmental Microbiology, 22(4),* 1535–1546. https://doi.org/10.1111/1462-2920.14749

31. Li, B., Wang, Li., Kaseke, K.F., Vogt, R., Li, L., & Seely, M. K. (2018). The impact of fog on soil moisture dynamics in the Namib Desert. *Advances in Water Resources, 113,* 23–29. https://doi.org/10.1016/j.advwatres.2018.01.004

32. Lopez, B.R., & Bacilio, M. (2020). Weathering and soil formation in hot, dry environments mediated by plant–microbe interactions. *Biology and Fertility of Soils, 56(4),* 447–459. https://doi.org/10.1007/s00374-020-01456-x

33. Love, M., Huber W. & Anders S. (2014). Moderated estimation of fold change and' ' dispersion for RNA-seq data with DESeq2. *Genome Biology, 15(12)*, 550. https://doi.org/10.1186/s13059-014-0550-8

34. Luebert, F., García, N., & Schulz, N. (2007). Observaciones sobre la flora y vegetación de los alrededores de tocopilla (22°S, chile). *Boletín del Museo Nacional de Historia Natural, Chile, 56*, 27–52.

35. Marzol-Jaén, M., Sànchez-Megía, J., & García-Santos, G. (2011). Effects of fog on climatic conditions at a sub-tropical montane cloud forest site in northern Tenerife (Canary Islands, Spain). In L. A. Bruijnzeel, F. N Scatena, & L. S. Hamilton (Eds.), Tropical Montane Cloud Forests: Science for Conservation and Management (International Hydrology Series, pp. 359–364). Cambridge: Cambridge University Press. doi:10.1017/CBO9780511778384.040

36. Matlakowska, R., Skłodowska, A., & Nejbert, K. (2012). Bioweathering of Kupferschiefer black shale (Fore-Sudetic Monocline, SW Poland) by indigenous bacteria: implication for dissolution and precipitation of minerals in deep underground mine. *FEMS Microbiology Ecology. 81(1),* 99–110. https://doi.org/10.1111/j.1574-6941.2012.01326.x

37. McMurdie, P. J., & Holmes, S. (2013). phyloseq: An R package for reproducible interactive analysis and graphics of microbiome census data. *PloS One, 8(4),* e61217. https://doi.org/10.1371/journal.pone.0061217

38. Moat, J., Orellana-Garcia, A., Tovar, C., Arakaki, M., Arana, C., Cano, A., Faundez, L., Gardner, M., Hechenleitner, P., Hepp, J., Lewis, G., Mamani, J.- M., Miyasiro, M., & Whaley,O. Q. (2021). Seeing through the clouds – Mapping desert fog oasis ecosystems using 20 years of MODIS imagery over Peru and Chile. *International Journal of Applied Earth Observation and Geoinformation, 103,* 102468. https://doi.org/10.1016/j.jag.2021.102468.

39. Muenchow, J., Hauenstein, S., Bräuning, A., Bäumler, R., Rodríguez, E. F., & von Wehrden, H. (2013). Soil texture and altitude, respectively, largely determine the floristic gradient of the most diverse fog oasis in the Peruvian Desert. *Journal of Tropical Ecology, 19(5), 427-438*. https://doi.org/10.1017/S0266467413000436

40. Muñoz-Schick, M., Pinto, R., Mesa, A., & Moreira-Muñoz, A. (2001). “Oasis de neblina”, en los cerros costeros de sur de Iquique, Región de Tarapacá, Chile, durante el evento, El Niño 1997-1998. *Revista Chilena de Historia Natural, 74(2),* 389–405. http://dx.doi.org/10.4067/S0716-078X2001000200014

41. Murphy, J., & Riley, J.P. (1962). A modified single solution method for the determination of phosphate in natural waters. *Analytica Chimica Acta, 27,* 31–36. https://doi.org/10.1016/S0003-2670(00)88444-5

42. Neilson, J. W., Califf, K., Cardona, C., Copeland, A., Van Treuren, W., Josephson, K. L., Knight, R., Gilbert, J. A., Quade, J., Caporaso, J. G., & Maier, R. M. (2017). Significant impacts of increasing aridity on the arid soil microbiome. *MSystems, 2(3),* e00195–16. https://doi.org/10.1128/mSystems.00195-16

43. Nesbitt, H. W., & Young, G. M. (1982). Early Proterozoic climates and plate motions inferred from major element chemistry of lutites. *Nature, 299(5885),* 715–717. https://doi.org/10.1038/299715a0

44. Nieberding, F., Breuer, B., Braeckevelt, E., Klemm, O., Song, Q. & Zhang, Y. (2018). Fog water chemical composition on Ailaoshan Mountain, Yunnan Province, SW China. *Aerosol Air Quality. Research. 18(1)*, 37–48. https://doi.org/10.4209/aaqr.2017.01.0060

45. Oltremari, J., Schlegel, F., & Schlatter, R. (1987). Perspectiva de Morro Moreno como área silvestre protegida. *Bosque, 8(1),* 21–30.

46. Parker, A. 1970. An index of weathering for silicate rocks. Geological Magazine 107(6): 501–504. https://doi.org/10.1017/S0016756800058581

47. Pliscoff, P., Zanetta, N., Hepp, J., & Machuca, J. (2017). Efectos sobre la flora y vegetación del evento de precipitación extremo de agosto 2015 en Alto Patache, Desierto de Atacama, Chile. *Revista de geografía Norte Grande, (68),* 91–103. https://dx.doi.org/10.4067/S0718-34022017000300091

48. Price, J., & Velbel, M. (2003). Chemical weathering indices applied to weathering profiles developed on heterogeneous felsic metamorphic parent rocks. *Chemical Geology, 202(3-4), 397–416*. https://doi.org/10.1016/j.chemgeo.2002.11.001

49. Price, M. N., Dehal, P. S., & Arkin, A. P. (2009). FastTree: computing large minimum evolution trees with profiles instead of a distance matrix. *Molecular Biology and Evolution, 26(7),* 1641–1650. https://doi.org/10.1093/molbev/msp077

50. Quast, C., Pruesse, E., Yilmaz, P., Gerken, J., Schweer, T., Yarza, P., Peplies, J. & Glöckner, F. O. (2012). The SILVA ribosomal RNA gene database project: improved data processing and web-based tools. *Nucleic Acids Research, 41(D1),* D590–D596. https://doi.org/10.1093/nar/gks1219

764 51. R Core Team. (2018). R: A language and environment for statistical computing. R Foundation
765 for Statistical Computing, Vienna, Austria. URL https://www.R-project.org/.
766 52. RStudio Team. (2016). RStudio: Integrated development for R. Boston, MA: RStudio Inc.
767 Retrieved from http://www.rstudio.com/
768 53. Rundel, P. W., & Mahu, M. (1976). Community structure and diversity in a coastal fog desert in
769 northern Chile. *Flora, 165(6),* 493–505. https://doi.org/10.1016/S0367-2530(17)31888-1
770 54. Rundel, P. W., Dillon, M. O., Palma, B., Mooney, H.A., Gulmon, S. L., & Ehleringer, J. R. (1991).
771 The phytogeography and ecology of the coastal Atacama and Periuvan Deserts. *Aliso: A Journal*
772 *of Systematic and Evolutionary Botany, 13(1),* 1–49. DOI 10.5642/aliso.19911301.02
773 55. Ruxton, B. (1968). Measures of the degree of chemical weathering of rocks. *The Journal of*
774 *Geology, 76(5),* 518-527. https://doi.org/10.1086/627357
775 56. Samolov, E., Baumann, K., Büdel, B., Jung, P., Leinweber, P., Mikhailyuk, T., Karsten, U., &
776 Glaser, K. (2020). Biodiversity of algae and cyanobacteria in biological soil crusts collected along
777 a climatic gradient in chile using an integrative approach. *Microorganisms, 8(7),* 1047.
778 https://doi.org/10.3390/microorganisms8071047
779 57. Saunders, W. M. H., & Williams, E. G. (1955). Observations on the determination of total organic
780 phosphorus in soil. *European Journal of Soil Science, 6(2),* 254–267.
781 https://doi.org/10.1111/j.1365-2389.1955.tb00849.x
782 58. Schemenauer, R., & Cereceda, P. (1992). The quality of fog water collected for domestic and
783 agricultural use in Chile. *Journal of Applied Meteorology and Climatology, 31(3),* 275-290.
784 https://doi.org/10.1175/1520-0450(1992)031<0275:TQOFWC>2.0.CO;2
785 59. Sotomayor, D. A., & Drezner, T. D. (2019). Dominant plants alter the microclimate along a fog
786 gradient in the Atacama Desert. *Plant Ecology, 220(4),* 417–432.
787 https://doi.org/10.1007/s11258-019-00924-1
788 60. Sposito, G. 2008. The chemistry of soils. Second Edition. Ed. Oxford University Press
789 61. Tan, K. H. (1993). Principles of soil chemistry. Second edition. Ed. Dekker Inc., USA.

62. Torregrosa, A., O'Brien, T., & Faloona, I. (2014). Coastal fog, climate change, and the environment. *Eos, Transactions American Geophysical Union, 95(50),* 473–474. https://doi.org/10.1002/2014EO500001

63. Vargas Castillo, R., Stanton, D., & Nelson, P. R. (2017). Aportes al conocimiento de la biota liquénica del oasis de neblina de Alto Patache, Desierto de Atacama. *Revista de geografía Norte Grande, (68),* 49–64. https://dx.doi.org/10.4067/S0718-34022017000300049

64. Vásquez-Dean, J., Maza, F., Morel, I., Pulgar, R., & González, M. 2020. Microbial communities from arid environments on a global scale. A systematic review. *Biological Research, 53(1),* 1–12. https://doi.org/10.1186/s40659-020-00296-1

65. Vogt, T. 1927. Sulitjelmafeltets geologi og petrografi. *Norges Geologiske Undersokelse, 121,* 1–560 (in Norwegian, with English abstract).

66. Wang, Q., Garrity, G. M., Tiedje, J. M., & Cole, J. R. (2007). Naive Bayesian classifier for rapid assignment of rRNA sequences into the new bacterial taxonomy. *Applied and Environmental Microbiology, 73(16),* 5261–5267. https://doi.org/10.1128/AEM.00062-07

67. Wani S. A., Najar G. R., Wani J. A. A., Ramzan M., & Hakeem K. R. (2016). Weathering and approaches to evaluation of weathering indices for soil profile studies – An Overview. In: K. Hakeem, J. Akhtar, M. Sabir (Eds.), Soil Science: Agricultural and Environmental Prospectives. Springer, Cham DOI https://doi-org.ezproxy2.ucn.cl/10.1007/978-3-319-34451-5_8

68. Warren-Rhodes, K. A., Lee, K. C., Archer, S. D., Cabrol, N., Ng-Boyle, L., Wettergreen, D., Zacny, K., Pointing, S. B., & the NASA Life in the Atacama Project Team (2019). Subsurface microbial habitats in an extreme desert Mars-analog environment. *Frontiers in Microbiology, 10,* 69. https://doi.org/10.3389/fmicb.2019.00069

69. Weathers, K. C., Ponette-González, A. G., & Dawson, T. E. (2020). Medium, vector, and connector: Fog and the maintenance of ecosystems. *Ecosystems, 23(1),* 217–229. https://doi.org/10.1007/s10021-019-00388-4

816 70. White, T. J., Bruns, T., Lee, S. J. W. T., & Taylor, J. (1990). Amplification and direct sequencing
817 of fungal ribosomal RNA genes for phylogenetics. *PCR Protocols: A Guide to Methods and*
818 *Applications, 18(1),* 315–322.
819 71. Wickham, H. (2016). ggplot2: elegant graphics for data analysis. Springer.
820 72. Wright, E. S. (2016). Using DECIPHER v2. 0 to analyse big biological sequence data in R. *R*
821 *Journal, 8(1).*
822 73. Yan, Y., Kuramae, E. E., de Hollander, M., Klinkhamer, P. G., & van Veen, J. A. (2017).
823 Functional traits dominate the diversity-related selection of bacterial communities in the
824 rhizosphere. *The ISME Journal, 11(1),* 56–66. https://doi.org/10.1038/ismej.2016.108

825 **FIGURES**

826

827

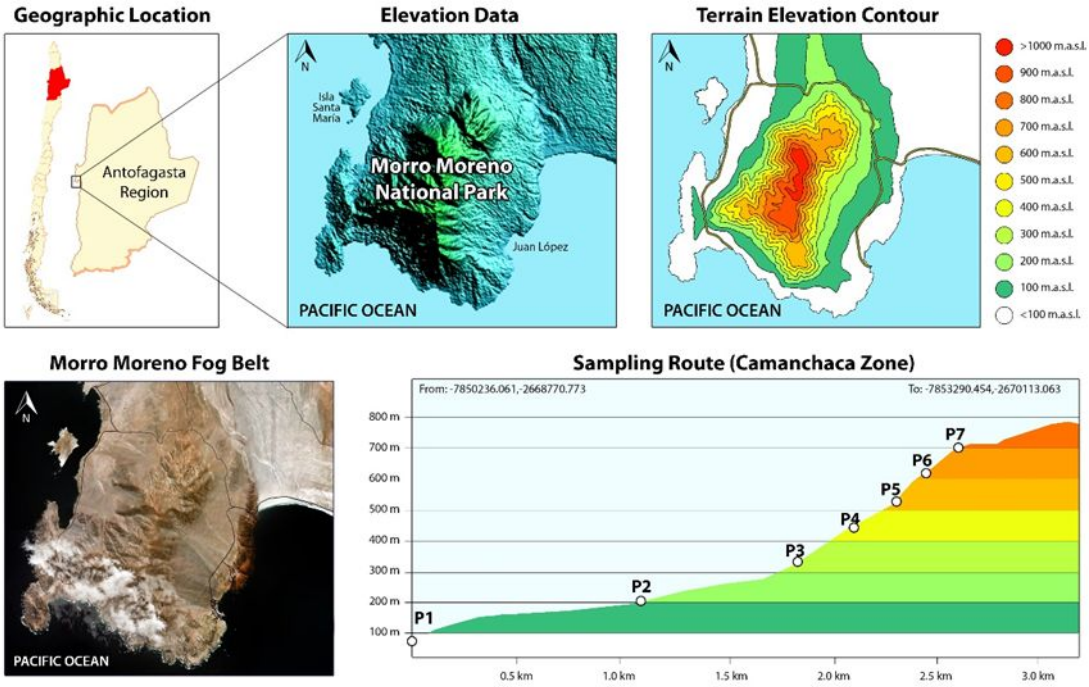

828

829 **Figure 1**. Location of Morro Moreno National Park and sampling points at different altitudes.
830 Geographical Universal Transverse Mercator UTM coordinates: 100 masl (0340496; 7397723), 200
831 masl (0340338; 7398100), 300 masl (0340519; 7398122), 400 masl (0340507; 739828), 500 masl
832 (0340478; 7398482), 600 masl (0340523; 7398628), and 700 masl (0340542; 7398713).

833

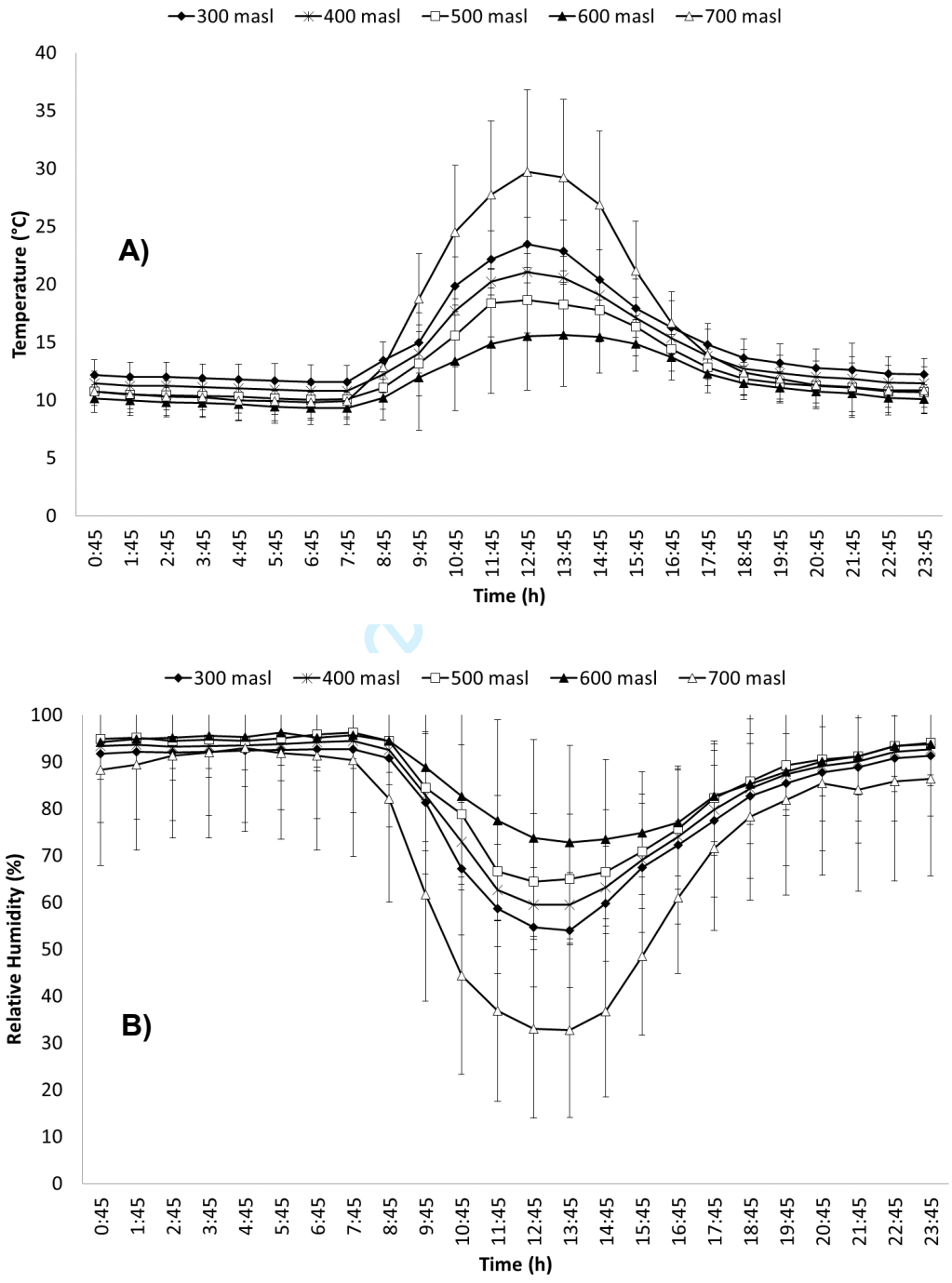

834

835

836 **Figure 2.** Temperature (A) and relative humidity (B) at different altitudes in the Morro Moreno National
837 Park. The data in both graphs represent averages of 69 measures. The vertical bar indicates the
838 standard deviation.

839

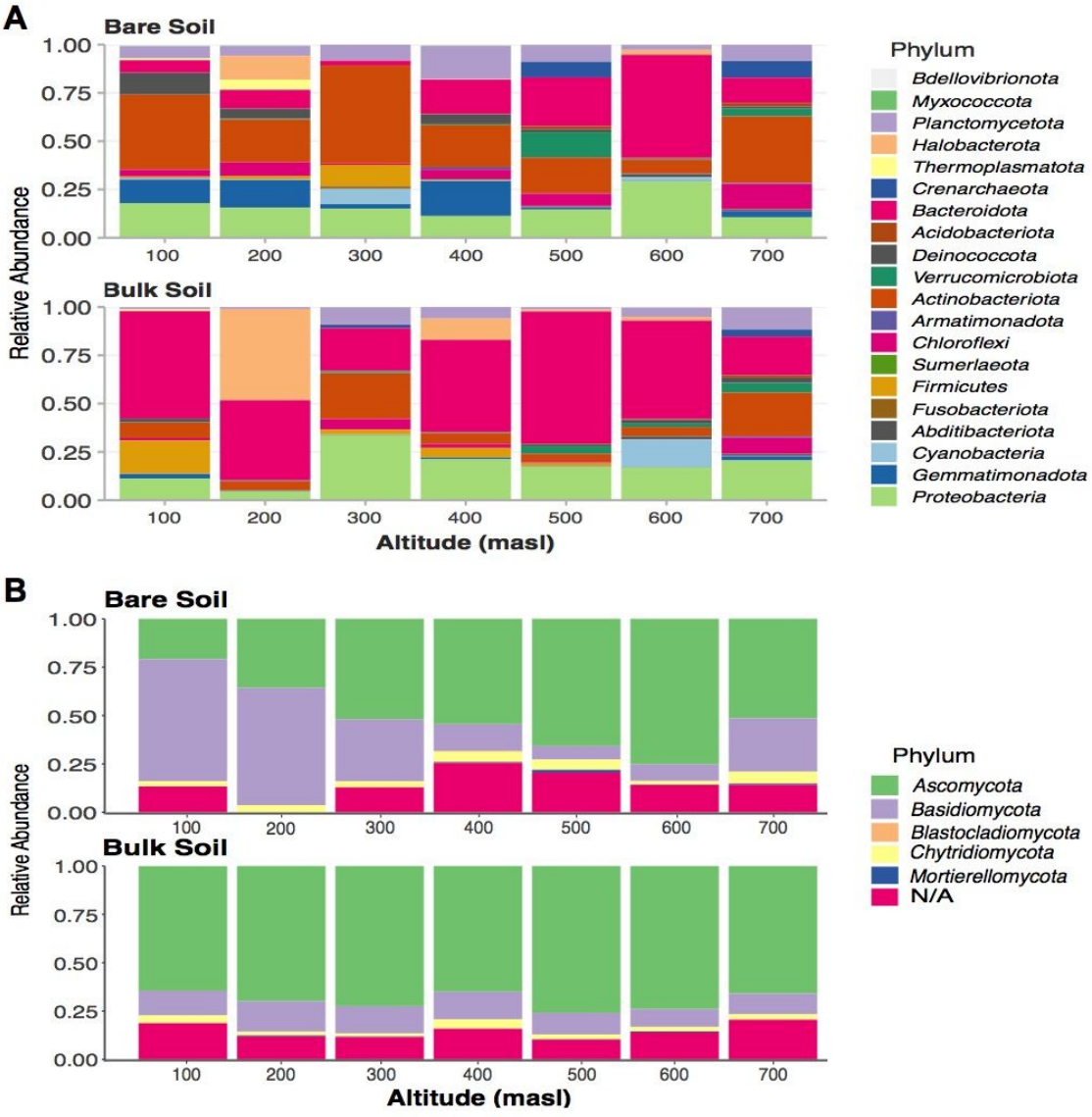

840

841 **Figure 3.** Taxonomic composition and relative abundance of microbial communities in bare and bulk

842 soil samples from different altitudes in the MMNP. Stacked bars show **(A)** the top 20 most abundant

843 bacteria and the **(B)** identified fungi at the phylum taxonomic level.

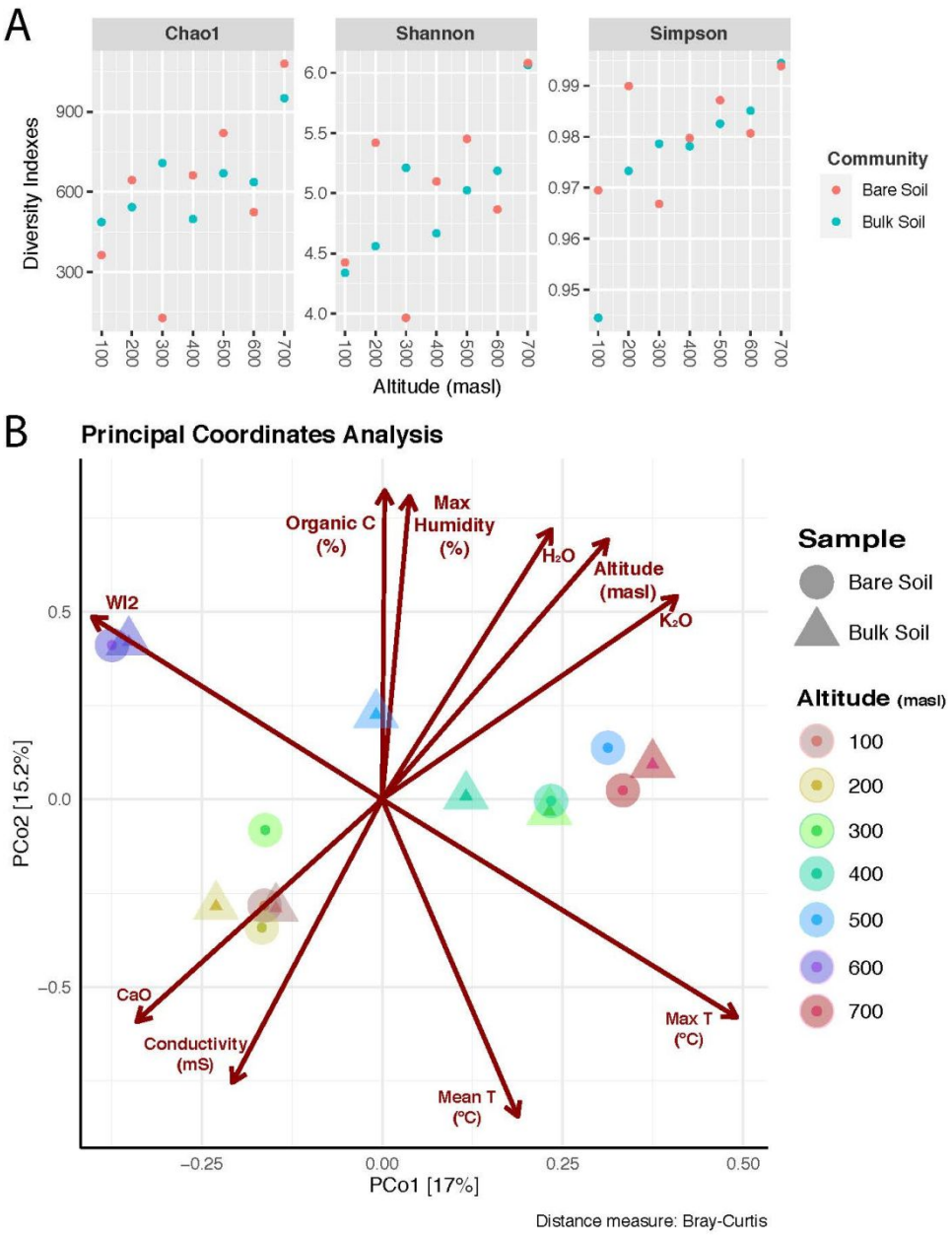

844

845 **Figure 4.** Variability of the microbial communities in the MMNP. **(A)** Alpha diversity indices for each
846 studied MMNP microbial community. Colours represent different samples. **(B)** Beta diversity based
847 on principal component analysis (PCA) on Hellinger transformed amplicon sequence variant (ASV)
848 relative abundances. The points correspond to the soil samples from different altitudes (identified by
849 the shapes and colours), and the relative distance indicates the level of similarity to all other samples.
850 The arrows indicate the explanatory power of the statistically significant environmental and soil
851 parameters regarding the observed variation in the community composition.

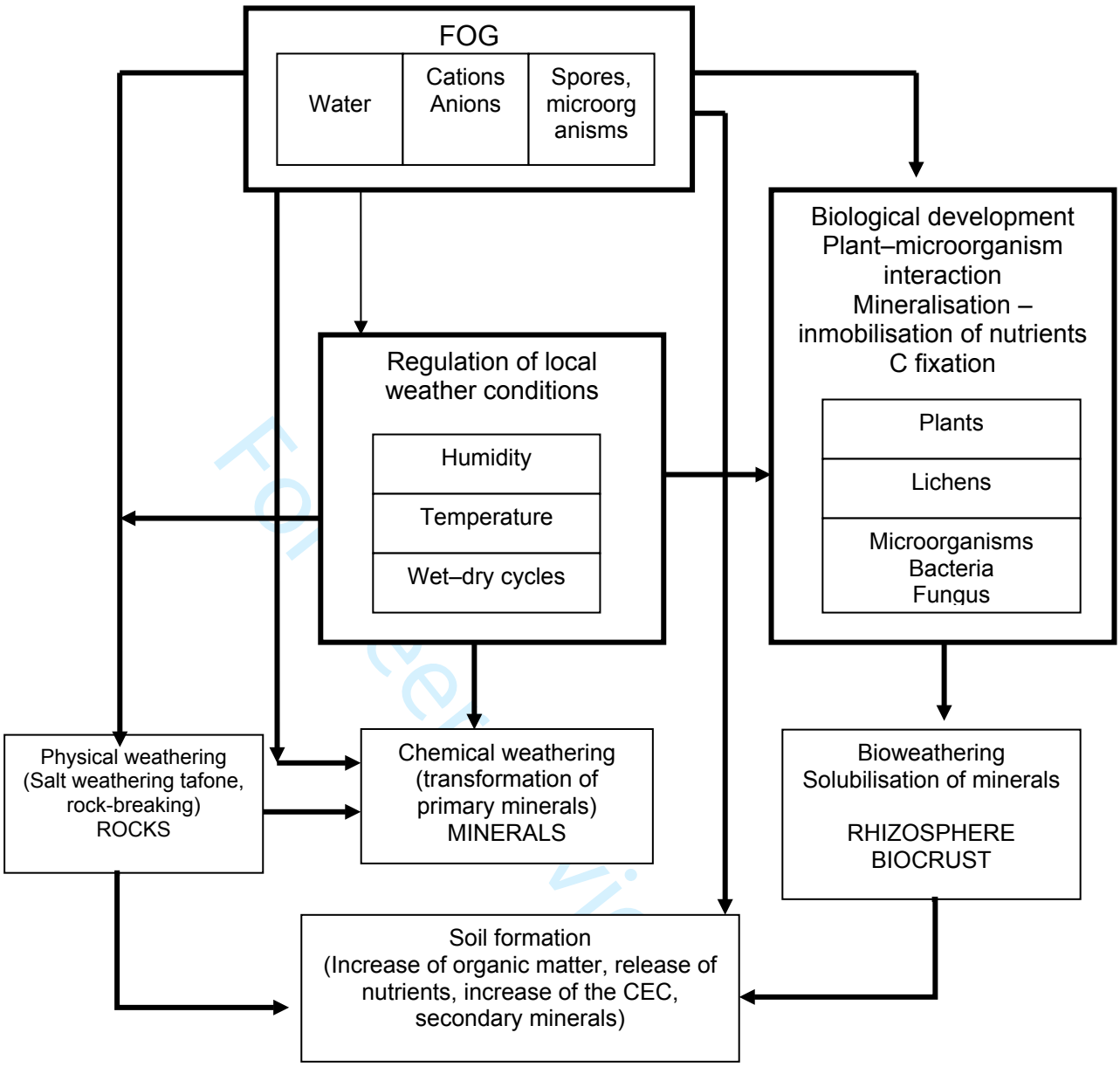

Figure 5. Diagram illustrating the effect of coastal fog on soil formation.

TABLES

Table 1. Variation of the pH, electrical conductivity (EC), organic matter (OM), Phosphorus (total P, Inorganic P and organic P) in bare and bulk soils at different altitudes in Morro Moreno National Park.

Altitude (masl)	pH		Electrical conductivity ($mScm^{-1}$)		Organic Matter (%)		Phosphorus (mg kg^{-1})					
							Pt	Pi	Po	Pt	Pi	Po
	Bare Soil	Bulk Soil	Bare Soil	Bulk Soil	Bare Soil	Bulk Soil	Bare soil			Bulk Soil		
100	8.53 ± 0.1	8.18 ± 0.3	6.86 ± 1.0	10.96 ± 1.4	0.17 ± 0.0	0.43 ± 0.1	1002 ± 140	843 ± 57	159 ± 94	806 ± 123	681 ± 171	124 ± 74
200	8.29 ± 0.5	8.69 ± 0.2	3.55 ± 0.7	2.81 ± 0.5	0.07 ± 0.0	0.41 ± 0.2	873 ± 45	753 ± 64	120 ± 33	695 ± 27	689 ± 38	6 ± 1
300	7.86 ± 0.2	8.04 ± 0.5	5.10 ± 2.6	5.50 ± 1.1	0.33 ± 0.0	1.06 ± 0.1	299 ± 30	228 ± 60	71 ± 35	260 ± 11	176 ± 20	84 ± 12
400	7.13 ± 0.6	7.44 ± 0.2	6.28 ± 1.3	4.08 ± 0.2	0.77 ± 0.1	1.40 ±0.3	705 ± 151	651 ± 101	54 ± 75	428 ± 19	306 ± 102	122 ± 99
500	7.66 ± 0.3	7.19 ± 0.3	2.92 ± 0.6	0.99 ± 0.3	0.55 ± 0.1	2.56 ± 0.6	463 ± 80	327 ± 12	137 ± 69	465 ± 56	349 ± 23	115 ± 37
600	6.42 ± 0.1	7.62 ± 0.2	2.20 ± 0.9	1.56 ± 0.4	1.61 ± 0.2	2.19 ± 0.4	342 ± 40	273 ± 21	69 ± 30	402 ± 79	203 ± 4	198± 78
700	7.43 ± 0.4	7.01 ± 0.5	2.08 ± 0.6	1.93 ± 0.8	1.32 ±0.3	1.53 ± 0.1	998 ± 253	724 ± 278	274 ± 30	973 ± 215	665 ± 131	308 ± 148

886

887 **Table 2.** Mineralogical description of soil samples collected at different altitudes in Morro Moreno National Park.

Compounds (crystalline phase)	Chemical Composition	Bare soil (masl)							Bulk soil (masl)						
		100	200	300	400	500	600	700	100	200	300	400	500	600	700
Magnesiohornblende	$Ca_2(Mg,Fe^{+2})4Al(Si_7Al)O_{22}(OH,F)_2$	59.9	51.2	74.1	82	26.1	29.6	13.1	8.8	68.2	47.2	57.5	49.5	52.3	20.3
Calcium albite	$(Na,Ca)Al(Si,Al)_3O_8$	25.8	17.9	10.8	7.3	35.3	48.8	43.3	22.3	21.6	16.6	14.8	21	29.1	29.0
Quartz	SiO_2	13.4	1	1.7	6.8	23.9	12.3	3.9	19.7	5	6	8.1	15.6	12.8	9.4
Chlorite	$(Mg,Fe)_6(Si,Al)_4O_10(OH)_8$	0,9	18.5	0.2	2	2.5	9.2	6.1	6.9	0.6	2.4	14.5	6.1	5.2	4.5
Anortite	$CaAl_2Si2O_8$	--	7.4	--	2	--	--	29.4	17.8	--	27.8	--	--	--	16.9
Pyrophyllite	$Al_2SiO_4O_{10}(OH)_2$	--	4.1	--	--	--	--	--	--	4.6	--	--	--	--	3.5
Kaolinite	$Al_2SiO_5(OH)_4$	--	--	13.2	--	4.9	--	--	7.9	--	--	--	--	--	3.8
Anhydrite	$CaSO_4$	--	--	--	--	1.3	--	--	--	--	--	--	--	--	--
Sanidine	$K(AlSi_3O_8)$	--	--	--	--	6	--	--	--	--	--	--	--	--	--
Hematite	Fe_2O_3	--	--	--	--	--	--	--	--	--	--	1.2	2	0.2	1.2
Jarosite	$(K,H_3O)Fe_3(SO_4)_2(OH)_6$	--	--	--	--	--	--	--	--	--	--	3.9	--	--	--
Orthoclase	$KAlSi_3O_8$	--	--	--	--	--	--	4.38	5.3	--	--	--	5.8	0.3	5.9
Biotite	$K(Mg,Fe^{2+})_3(Al, Fe^{+3})Si_3O_{10}(OH,F)_2$	--	--	--	--	--	--	--	11.3	--	--	--	--	--	5.5

888

889

890 **Table 3.** Major element concentrations of soil samples from different altitudes in Morro Moreno National Park obtained by X-ray fluorescence.

	Percentage (%)											
	Bare Soil											
masl	**SiO_2**	**TiO_2**	**Al_2O_3**	**Fe_2O_3**	**MnO**	**MgO**	**CaO**	**Na_2O**	**K_2O**	**P_2O_5**	**ppc**	**H_2O**
100	53.17	0.96	15.31	10.22	0.17	5.27	8.37	3.58	0.90	0.17	1.43	0.16
200	50.42	0.70	16.22	10.85	0.18	7.28	9.29	2.97	0.42	0.10	1.09	0.24
300	45.35	0.55	22.25	9.13	0.13	4.83	6.31	2.08	0.54	0.06	7.00	1.54
400	47.56	0.59	18.94	9.47	0.15	7.35	6.74	1.80	1.11	0.09	4.81	1.22
500	50.05	1.14	16.45	10.72	0.17	5.01	5.46	2.61	1.47	0.12	4.87	1.73
600	51.22	0.91	15.04	9.25	0.16	5.25	6.57	3.00	1.08	0.12	5.21	2.03
700	47.66	0.65	14.39	9.09	0.14	10.79	6.45	2.62	0.82	0.17	6.3	0.64
	Bulk Soil											
100	52.75	0.56	18.97	6.45	0.11	5.22	8.35	4.08	0.71	0.12	2.4	0.08
200	50.39	0.67	16.46	10.36	0.17	7.37	8.88	3.03	0.52	0.10	1.63	0.23
300	50.03	0.55	16.91	9.38	0.16	7.71	8.45	2.64	0.68	0.09	2.47	0.36
400	45.43	0.62	19.05	9.14	0.14	6.42	5.86	1.96	1.04	0.10	8.21	1.90
500	50.75	1.03	15.83	10.12	0.17	4.99	5.72	2.85	1.38	0.12	5.24	1.62
600	52.49	0.91	15.14	9.42	0.16	5.34	6.53	3.00	1.16	0.11	4.53	1.03

700	49.36	0.82	15.84	9.63	0.18	8.30	8.36	2.59	0.77	0.12	3.71	0.12

891

892 **Table 4.** Calculation of weathering indices: Weathering Index of Parker (WIP), Vogt's Residual Index (V), Chemical Index of Alteration (CIA), Chemical Index
893 of Weathering (CIW), Plagioclase Index of Alteration (PIA), Weathering Index 1 (WI1), Weathering Index 2 (WI2).

Weathering Index							
Bare Soil							
masl	**WIP**	**V**	**CIA**	**CIW**	**PIA**	**WI1**	**WI2**
100	76.50	0.47	40.95	42.04	38.34	5.89	13.83
200	74.68	0.41	42.18	42.69	41.00	5.28	12.37
300	53.15	0.84	58.97	59.90	57.42	3.46	13.20
400	63.45	0.60	53.57	55.45	50.17	4.26	13.35
500	64.27	0.67	50.99	53.63	46.06	5.16	12.41
600	68.04	0.54	45.45	47.12	41.92	5.78	14.72
700	77.29	0.35	45.95	44.87	43.11	5.62	13.93
Bulk Soil							
100	79.30	0.56	45.57	46.42	43.72	4.72	21.74
200	75.29	0.43	43.14	43.79	41.67	5.19	12.93
300	72.89	0.45	45.27	46.18	43.30	5.02	13.53
400	59.53	0.67	55.94	57.85	52.63	4.05	13.21
500	66.32	0.63	48.84	51.20	44.23	5.44	13.33
600	68.86	0.54	45.60	47.39	41.82	5.88	14.81
700	74.59	0.41	43.84	44.87	41.53	5.28	13.62

894

895

Effects of altitude on soil properties in coastal fog ecosystems in Morro Moreno National Park, Antofagasta, Chile

RUNNING TITLE: Altitudinal effects on coastal fog ecosystem soils

ABSTRACT

The rare Pacific coast f~~F~~og ecosystems are under threat from climate change or local factors. Although coastal fog is known to affect soil properties and microbial diversity, ~~rare environments on the Pacific coast. Coastal fog is a unique water source for the Atacama Desert coastal ecosystems, leading to high plant diversity. Few~~ few studies on the Pacific coast have examined the specific microbiomes associated with ~~to soil of~~ these ecosystems. We evaluated the effects of coastal fog on the physicochemical, mineralogical, and microbiological properties of bare and bulk ~~–~~soils from different altitudes in the Morro Moreno National Park (MMNP) in the Antofagasta region. We found that the temperature and relative humidity of the soil varied temporally (daily) and spatially (with altitude). ~~–~~We detected that ~~Our data show that the~~ soil organic matter and organic phosphorus content~~s~~ tended to increase with altitude, whereas the pH, ~~and~~ electrical conductivity and total phosphorous decreased. ~~At the same altitude, the total phosphorus content decreases. Our~~ Our results did show that coastal fog induces physical weathering below 300 masl, and chemical weathering ~~by changing the soil weathering index~~ at the intermediate altitudes of ~400–600 masl. The biodiversity of bacteria and fungi increased considerably above 400 masl. ~~Our results show that~~ Actinobacteria and Bacteroidetes dominate the bacteria in bare soil, and Bacteroidetes dominate the bulk soil communities at all altitudes. ~~Regarding the fungi in both soil types, the~~ Ascomycota and Basidiomycota dominate the fungal community in both soil types. Moreover, the conductivity and CaO content appear to be more closely associated with microbial communities from lower altitudes ~~(up to 300 masl)~~. In addition, the organic C content, humidity, and Weathering Index 2 ~~(WI2)~~ isolate some communities at 500 and 600 masl. T~~herefore, t~~he microbiological diversity reported in this work reflects the variable and different microbial niches comprising the MMNP environment. Linkages between soil property and microbial variations with altitude within this Northern Chilean coastal fog ecosystems were elucidated. This novel scientific knowledge contributes to global network strategies for fog ecosystem conservation which aim to preserve the microbial niches and diversity in such soils.~~This study creates a baseline for soil property variation with altitude and generates the first inventory of bacterial and fungal variation with altitude. Thus, it contributes to scientific knowledge and the creation of new strategies for fog ecosystem conservation.~~

Keywords: Atacama Desert, Camanchaca, Chilean coastal desert, climate change, soil microbial diversity, Pacific coast, soil physicochemical properties

1. INTRODUCTION

Globally, fog ecosystems are scarce because they require special climatic and geographic conditions. Their formation depends on unique local characteristics, including temperature, aridity index, latitude, terrain elevation, distance from the coastline, and slope angle (Moat et al. 2021). According to Weathers et al. (2020), fog is a medium, vector, and connector because it links the atmosphere, biosphere, and hydrosphere and connects atmospheric, terrestrial, and marine ecosystems. Fog also plays a key role in controlling ecosystem processes because it modulates environmental conditions such as heat, water, and radiative interactions between the atmosphere and terrestrial systems (Sotomayor and Drezner 2019; Weathers et al. 2020). It supplies and regulates the flow of water, nutrients, and light to ecosystems and determines the strength and type of coupling between the atmosphere, vegetation, and soil processes driving ecosystem functions (Weathers et al. 2020). In addition, fog ecosystems support diverse plant species dependent on fog as the only water source. However, the soil-water-plant relationships in fog ecosystems are poorly understood.

F~~However, f~~og ecosystems are vulnerable and constantly threatened by global and local factors. Global factors include climate change and a lack of understanding of these ecosystems and the biodiversity they support. At the local scale, threats include lack of protection, urban development, atmospheric contamination, industrial and mining activities, overgrazing, invasive species, and irresponsible tourism practices (Moat et al. 2021).

Fog ecosystems occur mainly in coastal areas, such as California in the US, the coast of the Atacama Desert in Chile and Perú, South Africa, and other Mediterranean areas with dry summers, which remain unclear (Torregrosa et al. 2014). The arid and hyper-arid Pacific coast, including parts of Peru and Chile (the Sechura Desert and the Atacama Desert), extends for 3,000 km and harbours localised fog ecosystems isolated from each other (Moat et al. 2021). On the Pacific coast, the atmospheric conditions are affected by a stable, subtropical anticyclone that generates a uniform coastal climate, nearly devoid of rainfall but characterised by the regular formation of thick stratus clouds below 1,000 m (Rundel et al. 1991; Cereceda et al. 1992, 2008; Garreaud et al. 2008, 2010). Fog ecosystems

vary widely with latitude, aspect, substrate, and elevation, ranging from hilltop woody plant refugia to wider expanses of vegetation and productive crusts. The vegetation patterns in the fog ecosystems of Chile and Perú have received some attention (Rundel et al. 1991; Muñoz-Schick et al. 2001; Muenchow et al. 2013). However, the soil physicochemical and mineralogical characteristics and their effects on the microbial composition in fog ecosystems have been little studied, although they are fundamental to the dynamics of these ecosystems. It remains unknown how climate change might affect coastal fog ecosystems on the southern Pacific coast in the short, medium, and long term. The occurrence of coastal fog, named 'Camanchaca', along the northern Chile coast is strongly affected by the topography. Sectors known for their coastal fogs include higher reliefs such as the Fray Jorge National Park in the Coquimbo region, Paposo and Morro Moreno National Park (MMNP) in the Antofagasta region, and Alto Patache in the Tarapacá region. These coastal cloud banks are usually less than 250 m thick and form at altitudes ranging from 400 to 800 m (Rundel et al. 1991; Cereceda et al. 1992).

Specifically, the MMNP is a fog ecosystem with great importance for Chile's natural heritage. It is located on the hyperarid coast of the Atacama Desert, where the 'Camanchaca' supports a rich fog ecosystem with high biodiversity~~. In total, 90 plant species have been reported, among which 57 are endemic to Chile, 29 are native, and 4 have been introduced; moreover, 13 species in the Antofagasta region are endemic~~ (Oltremari et al. 1987; Guerra et al. 2010; DS 5/2010). ~~The MMNP has been protected since 2012. Coastal fog in the Park is due to water-saturated air masses from the ocean pushed by prevailing southwestern winds. These humid air masses are transported to Morro Moreno, a prominent north-to-south-oriented mountain range, which is up to 950 m high and extends over ~10 km on the south side of the Mejillones Peninsula (Figure. 1). The MMNP's location and its unique relief create a fog oasis with a verdant core of around 100 km^2. Factors favouring the oasis include elevations ≤750 m; distance from the coastline ≤5 km, strong slope angle ≤ 16.5 °, slope direction SE, high fog duration > 3 months, and great isolation > 50 km (Moat et al. 2021).~~

The geographic conditions of the MMNP ~~detailed above~~, plus formal protection from the Chilean government, make the MMNP ideal for studies on the impact of elevation on vegetation variations, soil parameters, and microbial communities. Such studies could generate invaluable information about the Pacific Coast's fog ecosystems and the potential effects of global climate change upon them. To understand these unique ecosystems and design and implement appropriate conservation strategies, it is necessary to create a soil property baseline and an inventory of bacterial and fungal variations with altitude. Therefore, this study aimed to evaluate the effects of coastal fog on the physicochemical, mineralogical, and microbiological properties of soils relative to the altitude and proximity to plants. The resulting data will constitute the first inventory of variations in soil properties, bacteria, and fungi in relation to altitude in fog ecosystems.

2. MATERIALS AND METHODS

2.1. Site description and soil sampling

The study area was the MMNP (UTM coordinates (0340496; 7397723), officially declared a protected area in 2010 (DS 5/2010) by the Chilean Government. It covers 7,313 ha on the southern Mejillones Peninsula in the Antofagasta region (northern Chile; see Figure 1). Coastal fog in the MMNP is due to water-saturated air masses from the ocean pushed by prevailing southwestern winds. These humid air masses are transported to MMNP which is up to 950 m high and extends over ~10 km on the south side of the Mejillones Peninsula (Figure 1). The MMNP's location and its unique relief create a fog oasis with a verdant core of around 100 km2. Factors favouring the oasis include elevations ≤750 m; distance from the coastline ≤5 km, strong slope angle ≤ 16.5 °, slope direction SE, high fog duration > 3 months, and great isolation > 50 km (Moat et al. 2021). In MMNP a total of 90 plant species have been reported, among which 57 are endemic to Chile, 29 are native, and 4 have been introduced; moreover, 13 species in the Antofagasta region are endemic (Oltremari et al. 1987; Guerra et al. 2010; DS 5/2010).

Soil samples were collected at different altitudes (100, 200, 300, 400, 500, 600, and 700 metres above sea level, masl) along a transect on the southern, fog-exposed Morro Moreno hillslope

~~(Supplementary material Figures S1 and S2).~~ The altitudinal transect including the central sampling points and geographical coordinates are shown in Figure 1. The vegetation was visually identified by the team.

We defined a radius of 15 m around each sampling point for soil sample collection. At each altitude, topsoil samples were collected in random geographical directions at fixed distances, 5, 10, and 15 m between the individual sampling points. The samples ranged from almost unweathered materials to poorly regolitized diorites to metadiorites (mainly plagioclase, quartz, amphibole, and biotite as well as minor apatite, sphene, and opaque minerals; Cortés et al. 2007). The soil layers are thin, and bedrock outcrops are common; therefore, topsoil samples were collected from a depth ranging from 0 to 3 cm. This sampling strategy was helpful for the lowest sampling point, characterised by poorly regolitized colluvium built up by pebble–boulder clasts of diorite to metadiorite. Six samples were collected within a 15 m radius of each sampling point: including three bare soils (vegetation-free) and three bulk soils (surrounding the plant ~~proximal to roots~~~~vegetation~~). Note that plants in the MMNP have different conservation statuses based on Chilean regulations (DS 29/ 2012). Consequently, the rhizospheric soil underneath plants was inaccessible, and we did not disturb the ecosystem.

Furthermore, bare soil samples without lithic elements or vegetation cover were selected, and each sampling point was at least 1.5 m away from the nearest plant. Bulk soil samples were collected underneath the foliage, near plants, or around cacti. In both cases, sampling points for replicates were separated by at least 5 m. Approximately 200 g of soil was collected and stored in polyethylene bags. Subsamples for microbiological analysis were stored in sterile tubes.

2.2. Soil temperature and relative humidity monitoring

The soil surface temperature (T) and relative humidity (RH) at different altitudes (300, 500, 600, 700 masl) were monitored every hour daily for two months (June and July 2019, winter) using THERMO-S-KIT-H Hygrochron temperature and humidity data loggers (iButtonLink LLC, Whitewater, WI, USA). The temperature and RH measurement accuracies were ± 0.5 °C and ± 3.5%, respectively. The

loggers were installed at the central soil sampling point at each altitude. The temperature and RH data at 400 masl were calculated as the mean of the data recorded at 300 and 500 masl.

2.3. Soil physicochemical properties

The electrical conductivity (EC) and pH were measured in a soil–distilled water suspension with a solution ratio of 1:2.5 using a conductivity meter (HANNA HI98192) and pH meter (HANNA HI991001). The organic matter (OM) content was determined using dichromate oxidation. The total P (TP), inorganic P (IP), and organic P (OP) contents of the soils were determined using the extraction method proposed by Saunders and Williams (1955). The P concentration was measured with the method reported by Murphy and Riley (1962). The exchangeable bases Ca^{2+}, Mg^{2+}, Na^{+}, and K^{+} and cation exchange capacity (CEC) were calculated.

2.4. Fog water sampling and characterisation

Fog water samples were obtained with a handmade fog collector installed on a hilltop. The fog collector was constructed using a standard raschel mesh with a fog-collecting area of 1.0 m^2. Plastic pipes formed the mesh support. Fog water was collected in a glass bottle and stored until measurement. The fog water was filtered through a 0.45 µm membrane and analysed using inductively coupled plasma optical emission spectrometry (ICP-OES) with a Perkin Elmer Optima 7,000 DV.

2.5. Mineralogical characterisation

The soil sample mineralogy was determined with X-ray diffraction (XRD) analysis. The XRD analysis was carried out using a Siemens D5000 diffractometer (Cu Kα1 radiation). The X-ray generator was operated at a power of 40 kV and 30 mA. The goniometer was equipped with a graphite monochromator. Powder patterns were analysed using DiffracPlus and total pattern analysis software (TOPAS). Crystalline phases were identified using the International Centre for Diffraction Data (ICDD) database. The X-ray fluorescence (XRF; Siemens SRS-3000) was used to quantify the total oxides.

2.6. Weathering index calculations

In this study, the most frequently used weathering indices (WIs) were calculated using the total oxides, quantified by XRF, and expressed in moles. The WIs include the Weathering Index of Parker (WIP), Vogt's Residual Index (V), Chemical Index of Alteration (CIA), Chemical Index of Weathering (CIW), Plagioclase Index of Alteration (PIA), weathering index 1 (WI1), and weathering index 2 (WI2) (see the index formulation in Supplementary material Table S1; Vogt 1927; Ruxton 1968; Parker 1970; Nesbitt and Young 1982; Harnois 1988; Fedo et al. 1995; Price and Velbel 2003).

2.7. Metabarcoding and microbial community analysis

The total DNA was extracted from the bare and bulk soil samples collected at the seven different altitudes using the DNeasy PowerSoil Kit ® (Qiagen) according to the manufacturer's instructions. The bacterial 16S rRNA gene V4 region (~250 bp) amplification (515F and 806R primers: Caporaso et al. 2012), the fungal rRNA internal transcribed spacer (ITS) gene region (ITS1F and ITS2 primers: White et al. 1990; Gardes and Bruns 1993), 250 bp paired-end library construction, and sequencing on a MiSeq (Illumina) platform were performed at the Environmental Sample Preparation and Sequencing Facility at the Argonne National Laboratory (Illinois, USA). Subsequently, analyses were conducted using R v3.5.2 (R Core Team, 2018) and RStudio v1.1.463 (RStudio Team, 2016). The R package DADA2 v1.16.0 pipeline (Callahan et al., 2016) was used to infer each sample's amplicon sequence variants (ASVs). Briefly, the reads were evaluated for quality control and subsequently trimmed (Ns = 0, length ≥ 150 bp, expected errors ≤ 2), followed by dereplication, denoising, and merging of paired reads. After the ASV table was built by 97% clustering, the chimeras were removed, and the taxonomic assignment was carried out using the Silva v138 (for bacteria; Quast et al. 2012) and UNITE v8.2 (for fungi; Abarenkov et al. 2020) databases and the DADA2 Ribosomal Database Project's (RDP) naive Bayesian classifier (Wang et al. 2007). The data were normalised by variance-stabilising transformation using the R package DESeq2 v1.28.1 (Love et al. 2014). Using the R package DECIPHER v2.16.1 (Wright 2016), a multi-sequence alignment was performed to infer the phylogeny using FastTree v2.1.10 (Price et al. 2009). Furthermore, a phyloseq object (containing the ASVs, taxonomy assignation, phylogenetic tree, and meta-data) was created using the R package

Phyloseq v1.32.0 (McMurdie and Holmes 2013) and used to calculate the alpha diversity indexes (Shannon, Simpson, and Chao1). The beta diversity (Principal Coordinates Analysis PCA–Bray Curtis distance with environmental variables fit) was calculated using the R package ampvis2 v2.4.5 (Andersen et al. 2018). Finally, taxonomy composition plots were generated using the R package ggplot2 v3.3.2 (Wickham 2016).

2.8. Statistical analysis

The normal distribution of the data obtained from the bare and bulk soil analyses (pH, CE, OM, TP, IP, and OP) was tested using the Shapiro–Wilk test ($n < 50$). Because the distribution was normal, a parametric statistic was used ($\alpha = 0.05$, considered significant). The Levene test was used to verify the homogeneity of the variances ($\alpha = 0.05$). Analysis of variance (ANOVA) between groups (bare and bulk soil) and the altitude was used, and comparisons were made for each pair using Tukey's test. Differences were considered significant at $p \leq 0.05$. All statistical analyses were performed using IBM SPSS statistical software v22.

3. RESULTS AND DISCUSSION

3.1. Vegetation associated with the MMNP

Soil stores water and provides nutrients and specific niches for microbial life, supporting the fog ecosystem flora and fauna. A vegetation gradient was observed along the studied altitude transect across the MMNP. The study area's lower section (100 masl) is vegetation-free, but *Nolana* spp. is sporadically present at ~200 masl (Supplementary material, Figure S13). Oltremari et al. (1897) reported mainly *Nolana aplocaryoides, Cristaria oxyptera,* and *Philippiamra pachyphilla* for the Morro Moreno sector (150–350 masl). At 300 masl, *Tetragonia angustifolia* shrubs and *Copiapoa boliviensis* appeared (Supplementary material, Figures S14 and S5). Between 400 and 500 masl and above, lichens were observed in addition to the above-mentioned species (Supplementary material, Figure S16). Lichens have also been reported on granitoid particles in foggy ecosystems of the Pan de Azúcar National Park (Jung et al. 2020a). In the Alto Patache Chilean fog oasis, 77 lichen species

have been identified (Vargas Castillo et al. 2017). Above 600 masl, *Copiapoa boliviensis* and *Eulychnia morromorenoensis* (endemic species) were prevalent (Supplementary material, Figure S17). *Copiapoa boliviensis*, known as the 'Atacameño cactus', occurs as a solitary body or in the form of cushions, whereas *Eulychnia morromorenoensis* is a branched columnar cactus, reaching 2 to 7 m in height. In addition, *Eriosyce recondita* (common name: 'Quisquito') was also observed at this altitude (Supplementary material, Figure S18). This small cactus stands alone at ground level in the sand, and identification with the naked eye is difficult. It should be noted that *Eriosyce recondita* and *Eulychnia morromorenoensis* are classified as 'Endangered' and 'Vulnerable', respectively, in the Chilean National Species Inventory (DS 29/2012). Oltremari et al. (1987) reported *Heliotropium picnophyllum, Polyachyrus fuscus,* and *Copiapoa boliviana* at altitudes ranging from 350 and 750 masl. The authors also reported *Heliotropium chenopodiaceum*, *Lycium fragosum*, and *Eulychnia morromorenoensis* above 500 masl. Our observations are consistent with those previously described in MMNP, and several of the species have also been found in other 'Camanchaca' areas in Chile (Oltremari et al. 1987; Luebert et al. 2007; Guerra et al. 2010; Pliscoff et al. 2017). In addition, our observations of the altitude-dependent plant variation are similar to previous reports on the flora in foggy ecosystems in North Chile. For example, Oltremari et al. (1987) stated that the vegetation in the Morro Moreno sector exhibits a clearly defined altitudinal stratification including four strips: coastal desert strip (150–350 masl) in the east, middle desert strip (350–750 masl), fertile strip (750–900 masl), and desert over 900 masl. On the other hand, there is a sector with abundant coastal fog in the Antofagasta region close to Tocopilla (22°S, Chile), which is characterised by desert scrub consisting of *Nolana peruviana* on the ravines and slopes below 500 m and *Eulychnia iquiquensis* and *Ephedra breana* on slopes above 500 m (Luebert et al. 2007).

3.2. Variations in temperature and relative humidity

The daily T and RH patterns at different altitudes are shown in Figure 2. Both parameters varied temporally and spatially. A distinctive curve can be observed during the day at all studied altitudes. As expected, like Cáceres et al. (2007), we registered large daily oscillations in addition to the maximum RH values, which are reached at night. A temperature increase was recorded between

8:45 am and 6:45 pm at all altitudes (Figure 2A). The RH decreased within this time frame at all altitudes (Figure 2B). These variations are expected because T and RH are related, and temperature changes cause variations in the evaporation and humidity ratios (Figure 2). The minimal RH was observed at ~12:45 pm and 1:45 pm. The temperature maxima at altitudes of 700 and 300 masl were 29.7 and 23.5 °C, respectively. At intermediate altitudes, lower maximum temperatures of 21.0 °C (400 masl), 18.6 °C (500 masl), and 15.6 °C (600 masl) were recorded (Figure 2A). At noon, it is hotter at 700 masl than at the low altitudes. In the evening and night, the temperatures are lower at all altitudes. Lower temperatures were recorded during the night and early morning. These data demonstrate the amelioration of extreme temperature conditions by fog at intermediate altitudes of 400, 500, and 600 masl. Marzol-Jaén et al. (2011) showed the effect of fog on the microclimatic conditions on Tenerife. They observed lower temperatures and wind speeds and increased humidity during fog.

Regarding the RH, minima of 32.6% and 54.0% were detected at 700 and 300 masl, respectively (Figure 2B). At intermediate altitudes, RH minima were recorded at 59.5% (400 masl), 64.9% (500 masl), and 72.8% (600 masl). Therefore, the soil surface temperature decreased with increasing RH. On the other hand, higher temperatures and lower RH values were recorded at the extreme altitudes of 300 and 700 masl. These findings indicated that the RH from fog buffered the soil surface temperature at intermediate altitudes. As the fog decreased at noon, temperatures increased at all altitudes. Thus, the RH increase due to fog leads to a decrease in the soil surface temperature and affects the soil moisture. The tempering effect of fog is most apparent at 500–600 masl, where it creates suitable conditions for plant establishment and survival. Gultepe et al. (2009) reported a similar relationship between the T and RH. They showed that fog reduces extreme weather conditions, and at fog-affected sites, the temperature and moisture generally fluctuate less. Fog improves local conditions by reducing longwave radiation and creating fewer extreme temperatures. Together with fog, the plant canopy ameliorates high temperatures. On the other hand, in foggy ecosystems, plant species act as condensation surfaces. They are integral parts of the ecosystem, improving the storage of water, which can be used by other species (Sotomayor and Drezner 2019).

Li et al. (2018) studied the effects of potential changes in fog distribution on the soil moisture dynamics in the Namib Desert and demonstrated that fog affects the soil moisture dynamics during rainless periods, which has critical implications for the biogeochemical soil processes.

3.3. Impact of fog on soil properties

The soil pH variations along the altitudinal transect are shown in Table 1~~Figure 3A~~. The pH values of all samples (bare and bulk soils) ranged between 6.4 and 8.7. With increasing altitude, the pH decreased. The observed differences were significant ($p < 0.05$). High alkaline pH values were recorded at elevations of 100, 200, and 300 masl. However, above 400 masl, the pH values began to decrease and tended to be around 7.5 above this altitude. In addition, the pH differences between the bulk and bare soil samples at each altitude were insignificant ($p < 0.05$). In fog ecosystems, the soil is exposed to constant wetting and drying such that the soil moisture is related to the arrival rate of the fog and soil depth (Li et al. 2018). The soil pH decrease is a consequence of multiple simultaneous processes such as the release of H^+ by the weathering of the soil minerals, production of carbonic acid by atmospheric CO_2 dissolution, organic acid release by the soil microorganisms and plant roots, decomposition of organic matter, and ion uptake by biota. Water is also a source of H^+ ions, and the H^+ from fog water is absorbed by the clay complex in an exchangeable form, leading to a reduction in soil pH (Tan 1993).

Variations in the EC along the altitudinal transect are shown in Table 1~~Figure 3B~~. The EC decreased with increasing altitude, and the differences were significant ($p < 0.05$). However, the differences between the EC values of bare and bulk soils were insignificant. The highest EC values were recorded at 100 masl (6.86 and 10.96 mS cm^{-1} for bare and bulk soil, respectively). The lowest ECs were detected at 500 masl, with an average value of 1.95 ± 0.06 mS cm^{-1}.

On the other hand, the base saturation percentage of bare and bulk soils was high (>90%) along the altitudinal transect. However, the CEC was low at all sample points, with an average of 5.5 ± 0.67 meq 100 g^{-1}, consistent with the CEC of sandy soils (Tan 1993). Notably, samples collected at 400

and 500 masl exhibited slightly higher CEC values (6.5 ± 0.24 meq 100 g^{-1}) than those from other altitudes (5.1 ± 0.3 meq 100 g^{-1}). The analysed fog water from MMNP had a pH value of 5.54 ± 0.11 and a low EC of 204.66 ± 3.79 µS cm^{-1}. This acidic pH does not pose problems for soil. The main cations in the fog water are: Na^+ (20.28 ± 1.31 mg L^{-1}); Ca^{2+} (7.76 ± 0.16 mg L^{-1}); Mg^{2+} (3.94 ± 0.07 mg L^{-1}); and K^+ (1.47 ± 0.15 mg L^{-1}). The main anions are: Cl^- (99.01 ± 3.85 mg L^{-1}), SO_4^{2-} (45.80 ± 2.62 mg L^{-1}), and HCO_3^- (27.33 ± 3.06 mg L^{-1}). The Mg^{2+}, Na^+, and Cl^- ions in the fog water originate from sea salts, and SO_4^{2-}, K^+, and HCO_3^- are derived from soil dust (Schemenauera and Cerecedab 1992). Similar results were reported for fog water samples by Beiderwieden et al. (2005), with median pH and EC values of 4.58 and 23 µS cm^{-1}, respectively. Nieberding et al. (2018) reported that the pH values of fog events in a subtropical mountain cloud forest varied from acidic (pH < 5.0) to very acidic (pH < 4.0). Both Beiderwieden et al. (2005) and Nieberding et al. (2018) reported varying concentrations of ions such as Ca^{2+}, Mg^{2+}, Na^+, SO_4^{2-}, and NO_3^-. The fog deposition and continuous wetting and drying cycles contribute nutrients, salts, and contaminants to the soil. The effects of these external inputs on the soil properties should be investigated further.

The OM concentration significantly increased ($p < 0.05$) along the altitudinal transect (Table 1~~Figure 4~~). In general, we detected a higher OM content in the bulk soil than in the bare soil, and the difference was significant ($p < 0.05$). The bulk soil OM concentration ranges from 0.40% to 2.56%. Higher values were detected at 500 and 600 masl. Regarding bare soil, the OM content varied between 0.07% and 1.61%, and the highest value was detected at 600 masl. Above 400 masl, the OM concentration increased, possibly because the moisture from fog promotes vegetation growth at these altitudes. For example, in the southern Iquique coastal area (in North Chile), the vegetation cover is associated with constant coastal fog events, leading to vegetation development between 300 and 800 masl (Muñoz-Schick et al. 2001). Vegetation adds OM to the soil, as shown by the higher OM concentrations in bulk soil (associated with plants). Therefore, we infer that the highest OM content is related to the high RH generated by fog and the amelioration of the temperature.

On the other hand, Table 1~~Figure 5~~ shows the TP, IP, and OP concentrations of bare and bulk soil along the altitudinal gradient. The TP and IP concentrations of bare soil decreased with the increase in the altitude from 100 to 600 masl and significantly differed ($p < 0.05$). In two subgroups, a higher TP content was identified at altitudes of 100, 200, 400, and 700 masl. A lower TP was obtained at 300, 500, and 600 masl. In contrast, the variation in the OP content of bare soil with the altitude was insignificant ($p < 0.05$; Table 1~~Figure 5A~~). The IP content of bare soil varied between 61% and 99% along the altitudinal transect, with an average of 80%. Significantly low TP and IP values were obtained for bulk soil at 300, 400, 500, and 600 masl ($p < 0.05$). The highest TP and IP values were recorded at 100–200 and 700 masl (Table 1~~Figure 5B~~). The high OP content at 300 masl might be due to P immobilisation in the soil biomass. Therefore, the lower TP values might be due to uptake and extraction by the vegetation. In general, higher TP contents were detected in bare soil samples (average of 669 ± 306 mg kg^{-1}; n = 21) than in bulk soils (average of 576 ± 439 mg kg^{-1}; n = 21). The OP percentage was slightly higher in bulk soil, accounting for 26% of TP on average, than in bare soil (19% of TP). The TP and IP concentrations of bare and bulk soils varied with altitude (significant difference, $p < 0.05$). However, significant differences between bare soil and bulk soil were not observed.

3.4. Mineralogical characteriz~~s~~ation

The XRD analyses revealed a variety of minerals along the altitudinal gradient (Table 2~~1~~). The main minerals in the bare and bulk soils from all altitudes were magnesiohornblende, calcium albite, quartz, and chlorite. Anorthite, pyrophyllite, kaolinite, anhydrite, and sanidine mainly occurred in the bare soil samples. Hematite, jarosite, and orthoclase were detected in the bulk soil samples collected above 400 masl. Based on the Jackson–Sherman soil weathering stages, an abundance of primary minerals (inherited from parent materials, particularly igneous rocks), such as magnesiohornblende and calcium albite, indicates an early stage of weathering (Sposito 2008). In arid regions, the early weathering stage is mainly associated with low water content, low humus content, and limited leaching (Sposito 2008). Secondary minerals, such as kaolinite and haematite, produced by primary mineral weathering, were also detected (Table 2~~1~~).

The presence of chlorite is related to low-degree metamorphism deep below the surface. Feldspars weathering (e.g. albite and anorthite) generates clay minerals and releases Ca, Na, and K ions, whereas amphiboles weathering (e.g. hornblende) releases Fe and Mg into the solution (Wani et al. 2016). ~~The presence of chlorite is related to low-degree metamorphism, which occurs deep below the surface. Chemical weathering is controlled by water–rock interaction. Hydrolytic reactions cause progressive changes in the primary minerals and release various ions into the soil solution. The weathering of feldspars, such as albite and anorthite, generates clay minerals and releases Ca^{2+}, Na^{+}, and K^{+} ions. In contrast, the weathering of amphiboles, such as hornblende, releases Fe^{2+} and Mg^{2+} into the solution (Wani et al. 2016).~~ The detection of kaolinite and iron oxides originating from chemical weathering in the soil indicates hydrolysis, removal of cations and silica, and oxidation of Fe^{2+}. Muenchow et al. (2013), who studied soils from different altitudes in a Peruvian Desert fog oasis, showed that the altitude reflected the water availability and soil properties and identified a humid bromeliad vegetation belt (at ~700 masl), which harboured the largest number of species). In addition to the signs of humification and a brownish colour due to iron oxide release from primary minerals, the elevated clay, soil OM, and cation concentrations indicated advanced soil development.

The major oxide compositions of the bare and bulk soils from different altitudes were determined by XRF analysis (Table 3~~2~~). Similar values were obtained for the bare and bulk soils. The major element analyses showed that SiO_2 strongly resists weathering and ranges from 45.35% to 53.17% in both soils. Lower values ranging from 45.35% to 47.56% were detected at 300 and 400 masl in bulk soil. On the other hand, the Al_2O_3 values of bare and bulk soil ranged between 15.04% and 22.25% and 15.14% and 19.05%, respectively. The highest values were detected at 300 and 400 masl, indicating the high clay mineral content generated by weathering. The MgO and CaO contents of all samples varied between 4.83% and 7.31% and 5.46% and 9.29%, respectively. The Na_2O and K_2O concentrations ranged from 1.80% to 3.58% and 0.42% to 1.47%, respectively. Muenchow et al. (2013) reported a correlation between the soil properties and the vegetation composition of fog oases and highlighted that the low proportions of sand and high proportions of silt and clay promote vegetation growth by increasing the available soil water.

Long-term exposure of rocks to atmospheric conditions causes physical and chemical weathering, and visual signs of physical weathering occur in the MMNP. For example, the occurrence of tafone rocks below 300 masl (Supplementary Material, Figures S29 and S10) indicates salt weathering in the coastal area. Physical weathering causes rock disintegration, generating smaller grains without changing their chemical or mineralogical composition (Wani et al. 2016). For example, salt bursts occur in coastal deserts and are promoted by frequent alternating drying and wetting cycles. Dissolved substances are not eluted; instead, they accumulate in the soil and on the rocks' outer surfaces due to evaporation (Blume et al. 2016).

Weathering indices are used to approximate the degree of weathering of the rocks. Most indices are based on the molar ratio between mobile and immobile major oxides. Feldspars are the most abundant reactive (labile) minerals. Consequently, the dominant process during chemical weathering of the upper crust is the degradation of feldspars and the concomitant formation of clay minerals (Nesbitt and Young 1982). Table 43 lists the WIs calculated for the bare and bulk soils at different altitudes (WIP, V, CIA, CIW, PIA, WI1, and WI2). The WIP considers the susceptibility of Na^{+}, K^{+}, Ca^{2+}, and Mg^{2+} to be mobilised during weathering (Parker 1970). The WIP values are commonly between 0 and 100, with the least weathered rocks having the highest values. The WIP obtained in this study ranges from 53.13 to 76.50. High WIP values were determined for lower altitudes of 100 and 200 masl, indicating a lower degree of weathering than at higher altitudes. Vogt's Ratio (V) is defined by the ratio of the number of oxides of immobile cations (mainly Al) to that of mobile cations (magnesium, calcium, and sodium) based on the assumption that the potassium content remains constant during weathering (Price and Velbel 2003). The optimum Vogt's ratio (V) of fresh and weathered rocks is 0 and 1, respectively. A larger value indicates higher weathering intensity (Price and Velbel 2003). The V ratio obtained in our study varies between 0.41 and 0.47. The highest values occurred above 300 masl. The CIA index measures the weathering intensity on a scale from 1 to 100, where a higher value represents more intense chemical weathering (Fedo et al. 1995). The CIA index in this study ranged between 40.95 and 45.27. These

~~low values suggest the lack of chemical alterations and cool and/or arid climate conditions (Fedo et al. 1995).~~ The CIA index in this study ranged between 40.9 and 45.3 indicating a low weathering. Low values of CIA suggest the lack of chemical alterations and cool and/or arid climate conditions (Fedo et al. 1995). Unweathered rocks and minerals ranging from gabbro through K-feldspar have a similar CIA value of ~50 (Fedo et al. 1995).

The CIW index is similar to the CIA but eliminates K_2O from the equation. The CIW measures the weathering intensity on a scale from 1 to 100, where a higher value represents more intense chemical weathering (Fedo et al. 1995). The WIP index obtained in this study for both bare and bulk soils ranged from 42.04 to 59.90. Despite the low CIW values obtained at intermediate altitudes, higher values were detected for bare soil at 300, 400, and 500 masl. The CIW values were 59.90, 55.45, and 53.63, respectively. The CIW values of bulk soil were 57.85 and 51.20 at 400 and 500 masl, respectively.

The PIA value of non-weathered rocks is 50, and that of clay minerals, such as kaolinite, illite, and gibbsite, is close to 100 based on the CIA formula (Fedo et al. 1995). The PIA index determined in this study ranges from 38.34 to 57~~43~~.42~~30~~, which indicates a low degree of weathering. Silica-based WIs, such as WI1 and WI2, show the ratio between the mobile/immobile index (Ruxton 1968). The WI1 (also known as Ruxton Ratio R) is expressed by the SiO_2/Al_2O_3 ratio and assumes that Al_2O_3 remains immobile during weathering. Meanwhile, silica is lost from total element content (Ruxton 1968), where 0 indicates the optimum weathering value and >10 indicates the optimum fresh value. In our case, the WI1 ranges between 3.46 and 5.89, and the WI2 varies from 12.37 to 14.81 for both bare and bulk soils. The WI1 values of bare soils are lower at 300 and 400 masl (3.46 and 4.26) than those of bulk soil (5.2 and 4.05). The WI2 does not show an altitude-dependent trend. The WI values obtained for soil samples from different altitudes in the MMNP indicate the low level of soil weathering along the altitudinal transect. However, WI changes were detected at intermediate altitudes, indicating a high level of weathering, possibly related to the fog at this height. However, additional studies are required to clarify the processes.

3.5. Diversity and variability of soil microbiomes

Our results indicate that the environmental parameters (T and RH) vary significantly (Figure 2), which is reflected in the substantial variation in microbial communities and soil characteristics at different altitudes. The Atacama array of ecological niches is a microbial diversity reservoir, rich in organisms adapted to challenging conditions (Azua-Bustos et al. 2012; Bull et al. 2016) and highly niche-specific. In this context, a vastly different microbial diversity can occur in geographical and altitudinal proximity. Although research on these systems is sparse, it is known that fog affects the species diversity in coastal deserts (Rundel and Mahu 1976). Our results show the dominance of Actinobacteria and Bacteroidetes taxa in the bare soil and a clear dominance of Bacteroidetes in the bulk soil communities at all altitudes. This trend suggests different adaptations for each niche associated with the particular abiotic conditions, namely moisture and physicochemical parameters (Figure 3~~6~~).

The Proteobacteria abundance was roughly homogeneous in all communities in both soil types (Figure 3~~6~~A). However, Halobacterota, Planctomycetota, and Firmicutes phyla distribution and abundance were highly heterogeneous, and they were only detected in communities exhibiting contrasting abundances (Figure 3~~6~~A). The dominance of Actinobacteria was expected since this phylum is especially prevalent in soils and has been detected in extreme and foggy environments; while Proteobacteria, Firmicutes, Bacteroidetes, and Chloroflexi (although they are also prevalent, mainly due to their stress tolerance and metabolic versatility) were less abundant (Dueker et al. 2011; Nielson et al. 2017; Evans et al. 2019; Warren-Rhodes et al. 2019). Despite the vital roles Cyanobacteria taxa play in bio-weathering and lithomatrix transformation processes (Jung et al. 2020b), they were absent in both soil types (Figure 3~~6~~A). This may be due to a lack of the liquid water these microorganisms require. Therefore, microalgae, which are more efficient at obtaining water from fog or air humidity, may dominate these communities. Moreover, it is known that Cyanobacteria members are associated with superficial biocrusts, where they are exposed to sunlight (Samolov et al. 2020), explaining why we did not detect them. Nonetheless, it has been reported that other heterotrophic microorganisms, such as basidiomycete fungi (Kirtzel et al. 2020) and bacteria (Matlakowska et al. 2012), can carry out bio-weathering, fulfilling the role of the absent Cyanobacteria.

While evaluating the fungi in these communities, we found their abundance and composition were more stable than the bacteria in MMNP. Our results show that the Ascomycota members dominated both soil types, followed by the Basidiomycota (Figure 3~~6~~B), which is the same pattern reported for coastal Maine (USA), the Namib Desert (Namibia), and Salar Grande (Chile) (Evans et al. 2019; Gómez-Silva et al. 2019). Variations in this pattern only occur in some bare soil communities. In addition, there were not many differences between the bare and bulk soil fungal communities, despite the substantial differences in their bacterial compositions (Figure 3~~6~~). This may be due to plants' ability to select and shape the soil microbiology, a process in which fungal communities tend to remain more stable (Fonseca-García et al. 2016; Yan et al. 2017). On the other hand, it has been reported that plant-growth-promoting microorganisms increase plant organic acid exudation, degrade minerals, and intensify the weathering (Lopez-Bacillio et al. 2020), dynamics that might occur in the MMNP. Also, hypolithic microbial communities thriving on the seaward face of the coastal range can survive by using fog as their primary moisture source (Azúa-Bustos et al. 2011). However, the fog biotic input to the communities (ocean–terrestrial cells transfer) must also be considered, as the presence of aerosol microorganisms has been verified (Dueker et al. 2011; Evans et al. 2019). The results of studies in the Namib Desert showed that different wetting events and soil environmental conditions affect the microbial community structures of the desert (Evans et al. 2019).

Regarding the alpha diversity measures, the Chao1, Shannon, and Simpson indexes showed that the greatest bacterial and fungal biodiversity occurred in samples collected between 500 and 700 masl, showing that these indexes increase considerably from 400 masl (Figure 4~~7~~A). Several of the previously studied physicochemical and environmental factors can explain the increased microbial diversity of these samples. At these altitudes, the humidity (Figure 2~~1~~), the OM concentration (Table 1~~Figure 4~~), the degree of soil weathering (Table 4~~3~~), and the plant coverage/diversity (Supplementary Material, Figure~~s~~ S1~~3, S4, S5, S7, and S8~~) are all higher, suggesting that these parameters could influence diversity. However, the interplay among the variables has not been determined.

To determine this, we tested the effects of all environmental variables and soil properties on the microbial community composition and structure. We observed that many variables were significant and could affect the communities' structure, distribution, and grouping (by similitudes) (Figure 4~~7~~B). This confirms previous reports describing the considerable impact of polyextreme environments on organisms, resulting in heterogeneous taxonomic patterns (Vásquez-Dean et al. 2020). In addition, some structure or grouping by altitude was evident among communities. In most cases, bare and bulk soil communities from the same altitude were similar and distinct from those of other altitudes. Furthermore, the conductivity and CaO content seem more associated with microbial communities from lower altitudes (100, 200, and 300 masl). At the same time, the organic C content, humidity, and WI2 weathering index isolated some communities (bulk soils from the 500 masl and both soil types from the 600 masl) from the main groups, which were under different levels of pressure from other variables. This finding supports previous reports in which the soil RH and T are correlated with microbial diversity richness and diversity, and a combination of these variables with altitude and EC best explains community composition variations for several Atacama areas (Nielson et al. 2017: Warren-Rhodes et al. 2019).

Furthermore, as mentioned before, microorganisms can be transported over varying distances by air or moving animals, but efficient dispersal depends on the species resistance to unfavourable conditions during transport (Samolov et al. 2020). However, fungal and bacterial communities can adapt to long-term drought regimes (Frossard et al. 2015). A study by Evans et al. (2019) reported that local sources strongly control fog microbial communities, resulting in more marine species in fog near the coast; in addition, fog deposits show a higher microbial diversity than air. Also, Jung et al. (2020b) discovered a ground cover or biocrust named grit–crust biocenosis, dominated by lichens, fungi, and algae attached to grit-sized (~6 mm) quartz and granitic particles in fog soils on the coast of the Atacama Desert (comparable to biocenosis forming a layer on top of the soil and rock surfaces, i.e. cryptogamic ground cover). The authors stated that every fog event in the Atacama Desert led to photosynthetic activity by the soil communities. This enabled the unique biocenosis to fulfil various ecosystem services, preventing erosion, contributing to C, N, and P accumulation, and assisting soil

549 formation through bioweathering. These effects could significantly contribute to biogeochemical
550 cycles in low-OM desert environments. In accordance with these studies, our results also show a
551 correlation between water availability and high microbial diversity.
552
553 On the other hand, Lopez and Bacilio (2020) proposed that cacti could act as rock-weathering and
554 soil formation pioneers. They could fulfil this function due to their long-life cycles and association with
555 beneficial microbial communities in the rhizosphere, rhizoplane, or endosphere, which enable them
556 to participate in the early development of soil. The microbial biomass associated with cacti improves
557 growth by increasing photosynthesis and the exudation of organic acids that degrade minerals and
558 increase nutrient uptake. Together, plants and microbes intensify the weathering and cover a broader
559 spectrum of mineralisation. This is relevant because, as we previously described, the coverage by
560 cactus species in the MMNP is substantial, and the species differ along the altitude gradient. Hence,
561 the changes in vegetation correlate with the changes in microbiological composition.
562
563 Notably, our results highlight the variability of conditions in this 'small' altitudinal range, evidenced by
564 the number of environmental and physicochemical variables significantly influencing the composition
565 and structure of microbial communities. Also, the considerable microbiological diversity reported in
566 this work reflects the different niches comprising the MMNP environment.
567
568 Finally, using our study results, we constructed a diagram of the fog effect on soil formation, including
569 the essential aspects of soil weathering (Figure 5~~8~~). Single processes of biogeophysical and
570 biogeochemical weathering by bacteria (phototrophs), green algae, lichens, and fungi have been
571 reported. Such processes include the biological transformation of clay minerals, for example, by the
572 K depletion of interlayers of mica/illite and the oxidation of structural Fe (II) in less weathering-
573 resistant silicates such as biotite, as well as the dissolution of phosphate salts such as apatite. Many
574 studies have investigated the weathering of quartz, one of the commonest minerals. The atoms are
575 linked in a SiO_4 framework in quartz, making it one of the most weathering-resistant minerals. It has
576 been demonstrated that various microorganisms mediate biochemical weathering processes of rock-

forming minerals such as the excretion of pH-shifting substances that interfere with the lithomatrix (acidolysis or alkalinolysis) and the production of chelating compounds, such as siderophores, for the manipulation of the redox potential via extracellular enzymes (Jung et al. 2020b).

4. CONCLUSIONS

This is the first report showing the variations of soil properties and microbial communities with altitude on the Pacific coast. Significant ~~In this study, the effects of fog on the properties of both bare and bulk soils in Morro Moreno National Park (Antofagasta, Chile) were investigated for the first time.~~ c~~C~~hanges in the soil parameters and microbial communities (bacteria and fungi) along an altitudinal gradient (100–700 masl) were detected ~~.~~at Morro Moreno National Park (MMNP). Fog increased the relative humity ~~RH~~ and reduced the daily temperature ranges affecting the vegetation and the soil and microbial community. We also found strong weathering at intermediate altitudes. ~~The significant~~ C~~c~~hanges in soil parameters and microbial community composition were more closely related ~~more strongly~~ to altitude than to soil type (bulk or bare). B~~Notably, our results indicate that b~~acteria differed at each altitude, while fungi tend to be more stable, suggesting specialisations related to other conditions (amount and type of vegetation and the water availability). Linkages between soil property and microbial variations with altitude within these Northern Chilean coastal fog ecosystems were elucidated. This novel scientific knowledge contributes to global network strategies for fog ecosystem conservation which aim to retain microbial niches and diversity.~~, such as the amount and type of vegetation and the water availability. We provide evidence of physical and chemical soil weathering and soil weathering index changes, revealing strong weathering at intermediate altitudes, where fog is predominant.~~ The study data on the characteristics, particularly the biodiversity, of these unique environments can be used to create a baseline of soil properties and a first inventory of the microbial community in fog ecosystems on the Pacific coast. ~~In addition, the MMNP is protected by the Chilean government and can thus be considered as a natural laboratory for the study of fog ecosystems in the face of global threats such as climate change~~. This information will be invaluable for creating a global study network to evaluate fog ecosystems on the Pacific coast and elsewhere.

605

606

5. REFERENCES

1. Abarenkov, K., Zirk, A., Piirmann, T., Pöhönen, R., Ivanov, F., Nilsson, H., & Kõljalg, U. (2020). UNITE general FASTA release for Fungi. Version 04.02.2020. UNITE Community. https://doi.org/10.15156/BIO/786368".
2. Andersen, K. S., Kirkegaard, R. H., Karst, S. M., & Albertsen, M. (2018). ampvis2: an R package to analyse and visualise 16S rRNA amplicon data. *BioRxiv*, 299537. https://doi.org/10.1101/299537
3. Azúa-Bustos, A., González-Silva, C., Mancilla, R. A., Salas, L., Gómez-Silva, B., McKay, C. P., & Vicuña, R. (2011). Hypolithic cyanobacteria supported mainly by fog in the coastal range of the Atacama Desert. *Microbial Ecology, 61(3)*, 568–581. https://doi.org/10.1007/s00248-010-9784-5
4. Azua-Bustos, A., Urrejola, C., & Vicuña, R. (2012). Life at the dry edge: microorganisms of the Atacama Desert. *FEBS Letters, 586(18),* 2939–2945. https://doi.org/10.1016/j.febslet.2012.07.025
5. Beiderwieden, E., Wrzesinsky, T., & Klemm. O. (2005). Chemical characterization of fog and rainwater collected at the eastern *Andes cordillera*. *Hydrology and Earth System Sciences Discussions, 2 (3)*, 863-885. https://doi.org/10.5194/hess-9-185-2005
6. Blume, H.P., Brümmer, G. W., Fleige, H., Horn, R., Kandeler, E., & Kögel-Knabner, I. (2016). Inorganic soil components – minerals and rocks. In: Scheffer/Schachtschabel Soil Science. Sringer, Berlin Heidelberg. pp. 7–53. https://doi-org.ezproxy2.ucn.cl/10.1007/978-3-642-30942-7_2
7. Bull, A. T., Asenjo, J. A., Goodfellow, M., & Gómez-Silva, B. (2016). The Atacama Desert: technical resources and the growing importance of novel microbial diversity. *Annual Review of Microbiology, 70,* 215–234. https://doi.org/10.1146/annurev-micro-102215-095236
8. Cáceres, L., Gómez-Silva, B., Garró, X., Rodríguez, V., Monardes, V., & McKay, C. P. (2007). Relative humidity patterns and fog water precipitation in the Atacama Desert and biological implications., *Journal of Geophysical Research, 112,* G04S14., https://doi.org/10.1029/2006JG000344 doi:10.1029/2006JG000344.

9. Callahan B., McMurdie P., Rosen M., Han A., Johnson A., & Holmes S. (2016). DADA2: High-resolution sample inference from Illumina amplicon data. *Nature Methods, 13(7),* 581–583. https://doi.org/10.1038/nmeth.3869

10. Caporaso, J. G., Lauber, C.L., Walters, W. A., Berg-Lyons, D., Huntley, J., Fierer, N., Owens, S. M., Betley, J., Fraser, L., Bauer, M., & Gormley, N. (2012). Ultra-high-throughput microbial community analysis on the Illumina HiSeq and MiSeq platforms. *The ISME Journal 6(8),* 1621-1624. https://doi.org/10.1038/ismej.2012.8

11. Cereceda, P., Larrain, H., Osses. P., Farías, M., & Egaña, I. (2008). The spatial and temporal variability of fog and its relation to fog oases in the Atacama Desert, Chile. *Atmospheric Research, 87(3-4),* 312-323. https://doi.org/10.1016/j.atmosres.2007.11.012

12. Cereceda, P., Schemenauer, R. S., & Valencia, R. (1992). Posibilidades de abastecimiento de agua de niebla en la Región de Antofagasta, Chile. *Revista de Geografía Norte Grande, 19*, 3–14.

13. Cortés, J., Marquardt, C., González, G., Wilke, H.-G., Marinovic, N. (2007). Cartas Mejillones y Península de Mejillones, Región de Antofagasta. Servicio Nacional de Geología y Minería, Carta Geológica de Chile, Serie Geología Básica, Nos. 103 y 104, 58 p., 1 mapa escala 1:100.000. Santiago.

14. DS 5. (2010). Crea Parque Nacional "Morro Moreno", en la Región de Antofagasta. Ministerio de Bienes Nacionales. Chile.

15. DS 29. (2012). Aprueba reglamento para la clasificación de especies silvestres según estado de conservación. Ministerio del Medio Ambiente. Chile.

16. Dueker, M. E., O'Mullan, G. D., Weathers, K. C., Juhl, A. R., & Uriarte, M. (2011). Coupling of fog and marine microbial content in the near-shore coastal environment. *Biogeosciences Discussions, 8(5), 9609-9637*. doi:10.5194/bgd-8-9609-2011

17. Evans, S. E., Dueker, M. E., Logan, J. R., & Weathers, K. C. (2019). The biology of fog: results from coastal Maine and Namib Desert reveal common drivers of fog microbial composition. *Science of the Total Environment, 647,* 1547–1556. https://doi.org/10.1016/j.scitotenv.2018.08.045

18. Fedo, C. M., Eriksson, K. A., Krogstad, E. J. (1995). Geochemistry of shales from the Archean (~3.0 Ga) Buhwa Greenstone Belt, Zimbabwe: implications for provenance and source-area weathering. *Geochimica et Cosmochimica Acta, 60(10),* 1751–1763. https://doi.org/10.1016/0016-7037(96)00058-0

19. Fonseca-García, C., Coleman-Derr, D., Garrido, E., Visel, A., Tringe, S. G., & Partida-Martínez, L. P. (2016). The cacti microbiome: interplay between habitat-filtering and host-specificity. *Frontiers in Microbiology, 7,* 150. https://doi.org/10.3389/fmicb.2016.00150

20. Frossard, A., Ramond, J. B., Seely, M., & Cowan, D. A. (2015). Water regime history drives responses of soil Namib Desert microbial communities to wetting events. *Scientific Reports, 5,* 12263 https://doi.org/10.1038/srep12263

21. Gardes, M., & Bruns, T. D. (1993). ITS primers with enhanced specificity for basidiomycetes-application to the identification of mycorrhizae and rusts. *Molecular Ecology, 2(2),* 113–118. https://doi.org/10.1111/j.1365-294X.1993.tb00005.x

22. Garreaud, R., Barichivich, J., Christie, D. A., & Maldonado, A. (2008). Interannual variability of the coastal fog at Fray Jorge relict forests in semiarid Chile. *Journal of Geophysical Research: Biogeosciences, 113*(G04). 011, doi:10.1029/2008JG000709.https://doi.org/10.1029/2008JG000709

23. Garreaud, R. D., Molina, A. Y., & Farias, M. (2010). Andean uplift, ocean cooling and Atacama hyperaridity: A climate modeling perspective. *Earth and Planetary Science Letters, 292(1-2),* 39–50. https//doi:10.1016 /j.epsl.2010.01.017

24. Gómez-Silva, B., Vilo-Muñoz, C., Galetović, A., Dong, Q., Castelán-Sánchez, H. G., Pérez-Llano, Y., Sánchez-Carbente, M. D. R., Dávila-Ramos, S., Cortés-López, N. G., Martínez-Ávila, L., Dobson, A. D. W., & Batista-García, R. A. (2019). Metagenomics of Atacama lithobiontic extremophile life unveils highlights on fungal communities, biogeochemical cycles and carbohydrate-active enzymes. *Microorganisms, 7(12),* 619. https://doi.org/10.3390/microorganisms7120619

25. Guerra C., Guerra, C., & Silva, A. (2010). Guía de la Biodiversidad en la Península de Mejillones Morro Moreno, Parque Nacional. Gobierno de Chile, Ministerio del Medio Ambiente. Tercera edición. Gráfhika Impresores.

26. Gultepe, I., Pearson, G., Milbrandt, J., Hansen, B., Platnick, S., Taylor, P., Gordon, M., Oakley, J. P., & Cober, S. G. (2009). The fog remote sensing and modeling field project. *Bulletin of the American Meteorological Society, 90(3),* 341–359. http://www.jstor.org/stable/26220960

27. Harnois, L. (1988). The CIW index: a new chemical index of weathering. *Sedimentary Geology, 55,* 319–322. 10.1016/0037-0738(88)90137-6

28. Jung, P., Baumann, K., Emrich, D., Springer, A., Felde, V. J. M. N. L., Dultz, S., Baum, C., Frank, M., Büdel, B., & Leinweber. P. (2020a). Lichens bite the dust – A bioweathering scenario in the Atacama Desert, *iScience, 23 (11)*, 101647. https://doi.org/10.1016/j.isci.2020.101647

29. Jung, P., Baumann, K., Lehnert, L. W., Samolov, E., Achilles, S., Schermer, M., Wraase, L. M., Eckhardt, K., Bader, M. Y., Leinweber, P., Karsten, U., Bendix, J., & Büdel, B. (2020b). Desert breath—How fog promotes a novel type of soil biocenosis, forming the coastal Atacama Desert's living skin. *Geobiology. 18,* 113–124. https://doi.org/10.1111/gbi.12368

30. Kirtzel, J., Ueberschaar, N., Deckert-Gaudig, T., Krause, K., Deckert, V., Gadd, G. M., & Kothe, E. (2020). Organic acids, siderophores, enzymes and mechanical pressure for black slate bioweathering with the basidiomycete Schizophyllum commune. *Environmental Microbiology, 22(4),* 1535–1546. https://doi.org/10.1111/1462-2920.14749

31. Li, B., Wang, Li., Kaseke, K.F., Vogt, R., Li, L., & Seely, M. K. (2018). The impact of fog on soil moisture dynamics in the Namib Desert. *Advances in Water Resources, 113,* 23–29. https://doi.org/10.1016/j.advwatres.2018.01.004

32. Lopez, B.R., & Bacilio, M. (2020). Weathering and soil formation in hot, dry environments mediated by plant–microbe interactions. *Biology and Fertility of Soils, 56(4),* 447–459. https://doi.org/10.1007/s00374-020-01456-x

33. Love, M., Huber W. & Anders S. (2014). Moderated estimation of fold change and' ' dispersion for RNA-seq data with DESeq2. *Genome Biology, 15(12)*, 550. https://doi.org/10.1186/s13059-014-0550-8

34. Luebert, F., García, N., & Schulz, N. (2007). Observaciones sobre la flora y vegetación de los alrededores de tocopilla (22°S, chile). *Boletín del Museo Nacional de Historia Natural, Chile, 56*, 27–52.

35. Marzol-Jaén, M., Sànchez-Megía, J., & García-Santos, G. (2011). Effects of fog on climatic conditions at a sub-tropical montane cloud forest site in northern Tenerife (Canary Islands, Spain). In L. A. Bruijnzeel, F. N Scatena, & L. S. Hamilton (Eds.), Tropical Montane Cloud Forests: Science for Conservation and Management (International Hydrology Series, pp. 359–364). Cambridge: Cambridge University Press. doi:10.1017/CBO9780511778384.040

36. Matlakowska, R., Skłodowska, A., & Nejbert, K. (2012). Bioweathering of Kupferschiefer black shale (Fore-Sudetic Monocline, SW Poland) by indigenous bacteria: implication for dissolution and precipitation of minerals in deep underground mine. *FEMS Microbiology Ecology. 81(1),* 99–110. https://doi.org/10.1111/j.1574-6941.2012.01326.x

37. McMurdie, P. J., & Holmes, S. (2013). phyloseq: An R package for reproducible interactive analysis and graphics of microbiome census data. *PloS One, 8(4),* e61217. https://doi.org/10.1371/journal.pone.0061217

38. Moat, J., Orellana-Garcia, A., Tovar, C., Arakaki, M., Arana, C., Cano, A., Faundez, L., Gardner, M., Hechenleitner, P., Hepp, J., Lewis, G., Mamani, J.- M., Miyasiro, M., & Whaley,O. Q. (2021). Seeing through the clouds – Mapping desert fog oasis ecosystems using 20 years of MODIS imagery over Peru and Chile. *International Journal of Applied Earth Observation and Geoinformation, 103,* 102468.~~,~~ https://doi.org/10.1016/j.jag.2021.102468.

39. Muenchow, J., Hauenstein, S., Bräuning, A., Bäumler, R., Rodríguez, E. F., & von Wehrden, H. (2013). Soil texture and altitude, respectively, largely determine the floristic gradient of the most diverse fog oasis in the Peruvian Desert. *Journal of Tropical Ecology, 19(5), 427-438*~~1–12~~. ~~doi:10.1017/S0266467413000436~~https://doi.org/10.1017/S0266467413000436

40. Muñoz-Schick, M., Pinto, R., Mesa, A., & Moreira-Muñoz, A. (2001). “Oasis de neblina”, en los cerros costeros de sur de Iquique, Región de Tarapacá, Chile, durante el evento, El Niño 1997-1998~~”~~. *Revista Chilena de Historia Natural, 74(2),* 389–405. http://dx.doi.org/10.4067/S0716-078X2001000200014

41. Murphy, J., & Riley, J.P. (1962). A modified single solution method for the determination of phosphate in natural waters. *Analytica Chimica Acta, 27,* 31–36. https://doi.org/10.1016/S0003-2670(00)88444-5

42. Neilson, J. W., Califf, K., Cardona, C., Copeland, A., Van Treuren, W., Josephson, K. L., Knight, R., Gilbert, J. A., Quade, J., Caporaso, J. G., & Maier, R. M. (2017). Significant impacts of increasing aridity on the arid soil microbiome. *MSystems, 2(3),* e00195–16. https://doi.org/10.1128/mSystems.00195-16

43. Nesbitt, H. W., & Young, G. M. (1982). Early Proterozoic climates and plate motions inferred from major element chemistry of lutites. *Nature, 299(5885),* 715–717. https://doi.org/10.1038/299715a0

44. Nieberding, F., Breuer, B., Braeckevelt, E., Klemm, O., Song, Q. & Zhang, Y. (2018). Fog water chemical composition on Ailaoshan Mountain, Yunnan Province, SW China. *Aerosol Air Quality. Research. 18(1)*, 37–48. https://doi.org/10.4209/aaqr.2017.01.0060

45. Oltremari, J., Schlegel, F., & Schlatter, R. (1987). Perspectiva de Morro Moreno como área silvestre protegida. *Bosque, 8(1),* 21–30.

46. Parker, A. 1970. An index of weathering for silicate rocks. Geological Magazine 107(6): 501–504. https://doi.org/10.1017/S0016756800058581

47. Pliscoff, P., Zanetta, N., Hepp, J., & Machuca, J. (2017). Efectos sobre la flora y vegetación del evento de precipitación extremo de agosto 2015 en Alto Patache, Desierto de Atacama, Chile. *Revista de geografía Norte Grande, (68),* 91–103. https://dx.doi.org/10.4067/S0718-34022017000300091

48. Price, J., & Velbel, M. (2003). Chemical weathering indices applied to weathering profiles developed on heterogeneous felsic metamorphic parent rocks. *Chemical Geology, 202(3-4), 397–416.* ~~, 202(3-4)~~ https://doi.org/10.1016/j.chemgeo.2002.11.001

49. Price, M. N., Dehal, P. S., & Arkin, A. P. (2009). FastTree: computing large minimum evolution trees with profiles instead of a distance matrix. *Molecular Biology and Evolution, 26(7),* 1641–1650. https://doi.org/10.1093/molbev/msp077

50. Quast, C., Pruesse, E., Yilmaz, P., Gerken, J., Schweer, T., Yarza, P., Peplies, J. & Glöckner, F. O. (2012). The SILVA ribosomal RNA gene database project: improved data processing and web-based tools. *Nucleic Acids Research, 41(D1),* D590–D596. https://doi.org/10.1093/nar/gks1219

51. R Core Team. (2018). R: A language and environment for statistical computing. R Foundation for Statistical Computing, Vienna, Austria. URL https://www.R-project.org/.

52. RStudio Team. (2016). RStudio: Integrated development for R. Boston, MA: RStudio Inc. Retrieved from http://www.rstudio.com/

53. Rundel, P. W., & Mahu, M. (1976). Community structure and diversity in a coastal fog desert in northern Chile. *Flora, 165(6),* 493–505. https://doi.org/10.1016/S0367-2530(17)31888-1

54. Rundel, P. W., Dillon, M. O., Palma, B., Mooney, H.A., Gulmon, S. L., & Ehleringer, J. R. (1991). The phytogeography and ecology of the coastal Atacama and Periuvan Deserts. *Aliso: A Journal of Systematic and Evolutionary Botany, 13(1),* 1–49. DOI 10.5642/aliso.19911301.02

55. Ruxton, B. (1968). Measures of the degree of chemical weathering of rocks. *The Journal of Geology, 76(5),* 518-527. ~~http://www.jstor.org/stable/30066179~~https://doi.org/10.1086/627357

56. Samolov, E., Baumann, K., Büdel, B., Jung, P., Leinweber, P., Mikhailyuk, T., Karsten, U., & Glaser, K. (2020). Biodiversity of algae and cyanobacteria in biological soil crusts collected along a climatic gradient in chile using an integrative approach. *Microorganisms, 8(7),* 1047. https://doi.org/10.3390/microorganisms8071047

57. Saunders, W. M. H., & Williams, E. G. (1955). Observations on the determination of total organic phosphorus in soil. *European Journal of Soil Science, 6(2),* 254–267. https://doi.org/10.1111/j.1365-2389.1955.tb00849.x

58. Schemenauer, R., & Cereceda, P. (1992). The quality of fog water collected for domestic and agricultural use in Chile. *Journal of Applied Meteorology and Climatology, 31(3),* 275-290. https://doi.org/10.1175/1520-0450(1992)031<0275:TQOFWC>2.0.CO;2

59. Sotomayor, D-. A., & Drezner, T. D. (2019). Dominant plants alter the microclimate along a fog gradient in the Atacama Desert. *Plant Ecology, 220(4),* 417–432. https://doi.org/10.1007/s11258-019-00924-1

60. Sposito, G. 2008. The chemistry of soils. Second Edition. Ed. Oxford University Press
61. Tan, K. H. (1993). Principles of soil chemistry. Second edition. Ed. Dekker Inc., USA.
62. Torregrosa, A., O'Brien, T., & Faloona, I. (2014). Coastal fog, climate change, and the environment. *Eos, Transactions American Geophysical UnionOS, 95(50),* 473–474. https://doi.org/10.1002/2014EO500001
63. Vargas Castillo, R., Stanton, D., & Nelson, P. R. (2017). Aportes al conocimiento de la biota liquénica del oasis de neblina de Alto Patache, Desierto de Atacama. *Revista de geografía Norte Grande, (68),* 49–64. https://dx.doi.org/10.4067/S0718-34022017000300049
64. Vásquez-Dean, J., Maza, F., Morel, I., Pulgar, R., & González, M. 2020. Microbial communities from arid environments on a global scale. A systematic review. *Biological Research, 53(1),* 1–12. https://doi.org/10.1186/s40659-020-00296-1
65. Vogt, T. 1927. Sulitjelmafeltets geologi og petrografi. *Norges Geologiske Undersokelse, 121,* 1–560 (in Norwegian, with English abstract).
66. Wang, Q., Garrity, G. M., Tiedje, J. M., & Cole, J. R. (2007). Naive Bayesian classifier for rapid assignment of rRNA sequences into the new bacterial taxonomy. *Applied and Environmental Microbiology, 73(16),* 5261–5267. https://doi.org/10.1128/AEM.00062-07
67. Wani S. A., Najar G. R., Wani J. A. A., Ramzan M., & Hakeem K. R. (2016). Weathering and approaches to evaluation of weathering indices for soil profile studies – An Overview. In: K. Hakeem, J. Akhtar, M. Sabir (Eds.), Soil Science: Agricultural and Environmental Prospectives. Springer, Cham DOI https://doi-org.ezproxy2.ucn.cl/10.1007/978-3-319-34451-5_8
68. Warren-Rhodes, K. A., Lee, K. C., Archer, S. D., Cabrol, N., Ng-Boyle, L., Wettergreen, D., Zacny, K., Pointing, S. B., & the NASA Life in the Atacama Project Team (2019). Subsurface microbial habitats in an extreme desert Mars-analog environment. *Frontiers in Microbiology, 10,* 69. https://doi.org/10.3389/fmicb.2019.00069
69. Weathers, K. C., Ponette-González, A. G., & Dawson, T. E. (2020). Medium, vector, and connector: Fog and the maintenance of ecosystems. *Ecosystems, 23(1),* 217–229. https://doi.org/10.1007/s10021-019-00388-4

828 70. White, T. J., Bruns, T., Lee, S. J. W. T., & Taylor, J. (1990). Amplification and direct sequencing
829 of fungal ribosomal RNA genes for phylogenetics. *PCR Protocols: A Guide to Methods and*
830 *Applications, 18(1),* 315–322.
831 71. Wickham, H. (2016). ggplot2: elegant graphics for data analysis. Springer.
832 72. Wright, E. S. (2016). Using DECIPHER v2. 0 to analyse big biological sequence data in R. *R*
833 *Journal, 8(1).*
834 73. Yan, Y., Kuramae, E. E., de Hollander, M., Klinkhamer, P. G., & van Veen, J. A. (2017).
835 Functional traits dominate the diversity-related selection of bacterial communities in the
836 rhizosphere. *The ISME Journal, 11(1),* 56–66. https://doi.org/10.1038/ismej.2016.108

FIGURES

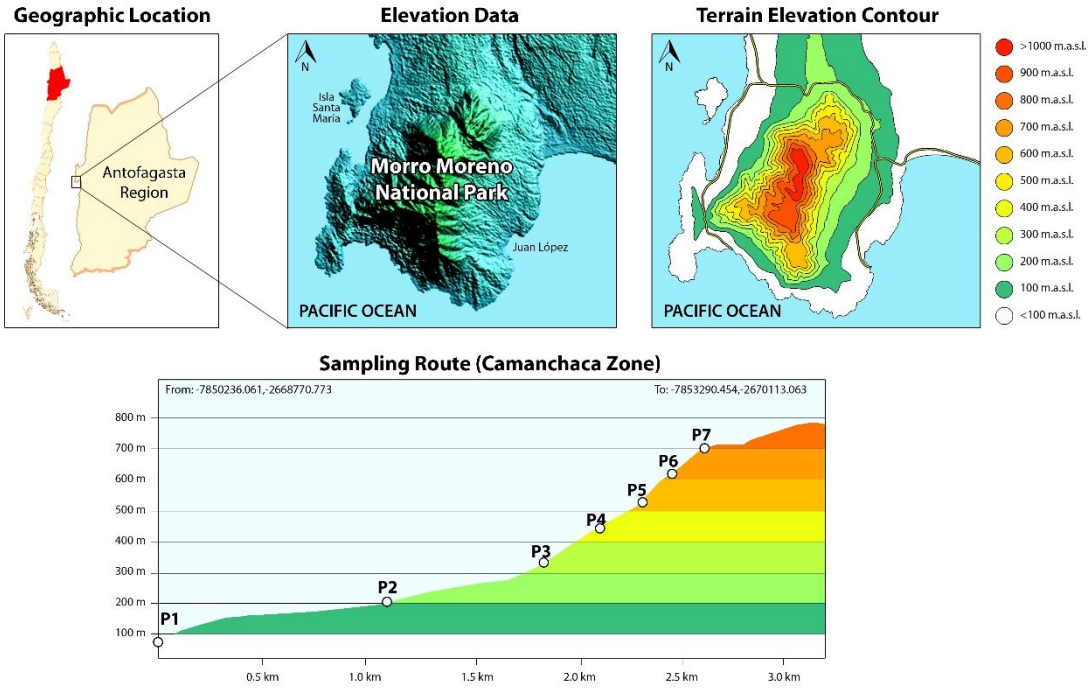
Geographic Location
Elevation Data
Terrain Elevation Contour
Antofagasta Region
Isla Santa María
Morro Moreno National Park
Juan López
PACIFIC OCEAN
>1000 m.a.s.l.
900 m.a.s.l.
800 m.a.s.l.
700 m.a.s.l.
600 m.a.s.l.
500 m.a.s.l.
400 m.a.s.l.
300 m.a.s.l.
200 m.a.s.l.
100 m.a.s.l.
<100 m.a.s.l.
Sampling Route (Camanchaca Zone)
From: -7850236.061,-2668770.773
To: -7853290.454,-2670113.063
800 m
700 m
600 m
500 m
400 m
300 m
200 m
100 m
P1
P2
P3
P4
P5
P6
P7
0.5 km
1.0 km
1.5 km
2.0 km
2.5 km
3.0 km

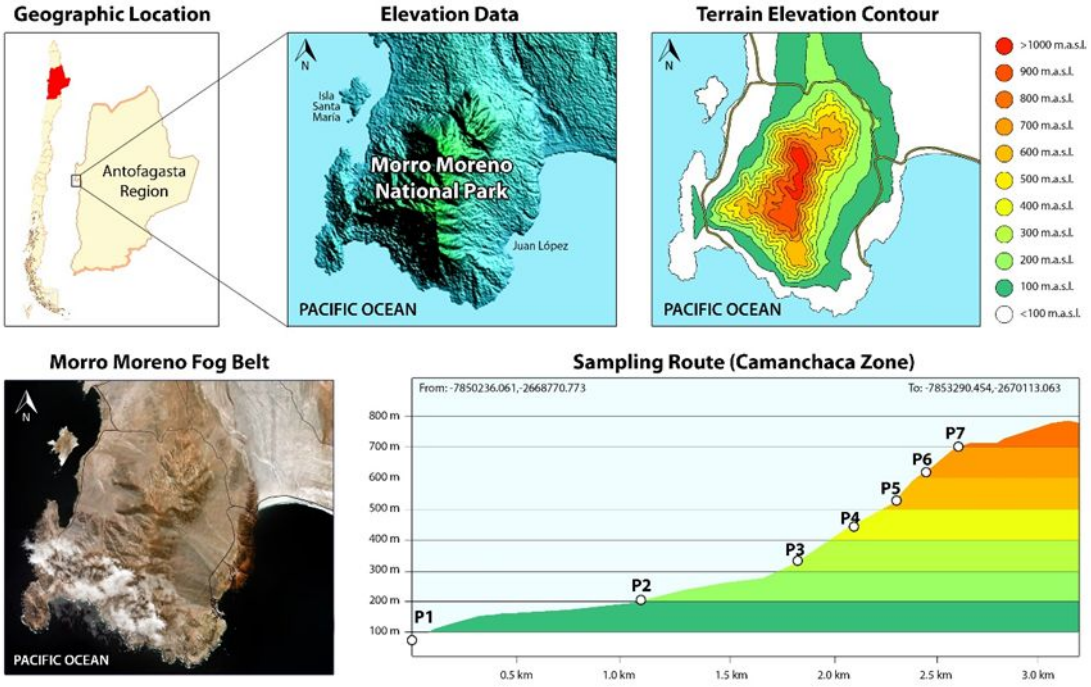
Geographic Location
Elevation Data
Terrain Elevation Contour
Antofagasta Region
Isla Santa María
Morro Moreno National Park
Juan López
PACIFIC OCEAN
>1000 m.a.s.l.
900 m.a.s.l.
800 m.a.s.l.
700 m.a.s.l.
600 m.a.s.l.
500 m.a.s.l.
400 m.a.s.l.
300 m.a.s.l.
200 m.a.s.l.
100 m.a.s.l.
<100 m.a.s.l.
Morro Moreno Fog Belt
PACIFIC OCEAN
Sampling Route (Camanchaca Zone)
From: -7850236.061,-2668770.773
To: -7853290.454,-2670113.063
800 m
700 m
600 m
500 m
400 m
300 m
200 m
100 m
P1
P2
P3
P4
P5
P6
P7
0.5 km
1.0 km
1.5 km
2.0 km
2.5 km
3.0 km

841 **Figure 1**. Location of Morro Moreno National Park and sampling points at different altitudes.
842 Geographical Universal Transverse Mercator UTM coordinates: 100 masl (0340496; 7397723), 200
843 masl (0340338; 7398100), 300 masl (0340519; 7398122), 400 masl (0340507; 739828), 500 masl
844 (0340478; 7398482), 600 masl (0340523; 7398628), and 700 masl (0340542; 7398713).

845

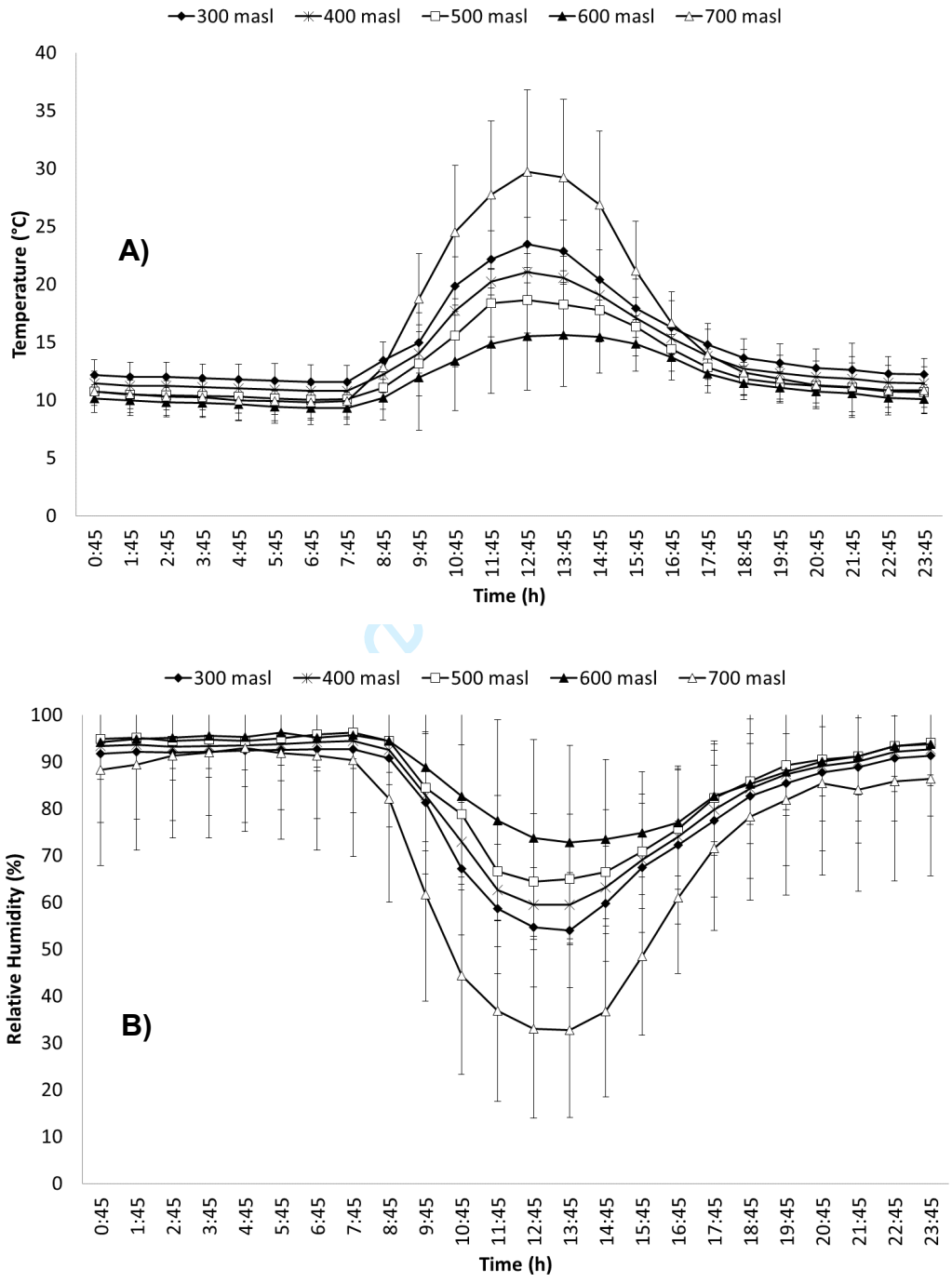

846

847

848 **Figure 2.** Temperature (A) and relative humidity (B) at different altitudes in the Morro Moreno National
849 Park. The data in both graphs represent averages of 69 measures. The vertical bar indicates the
850 standard deviation.

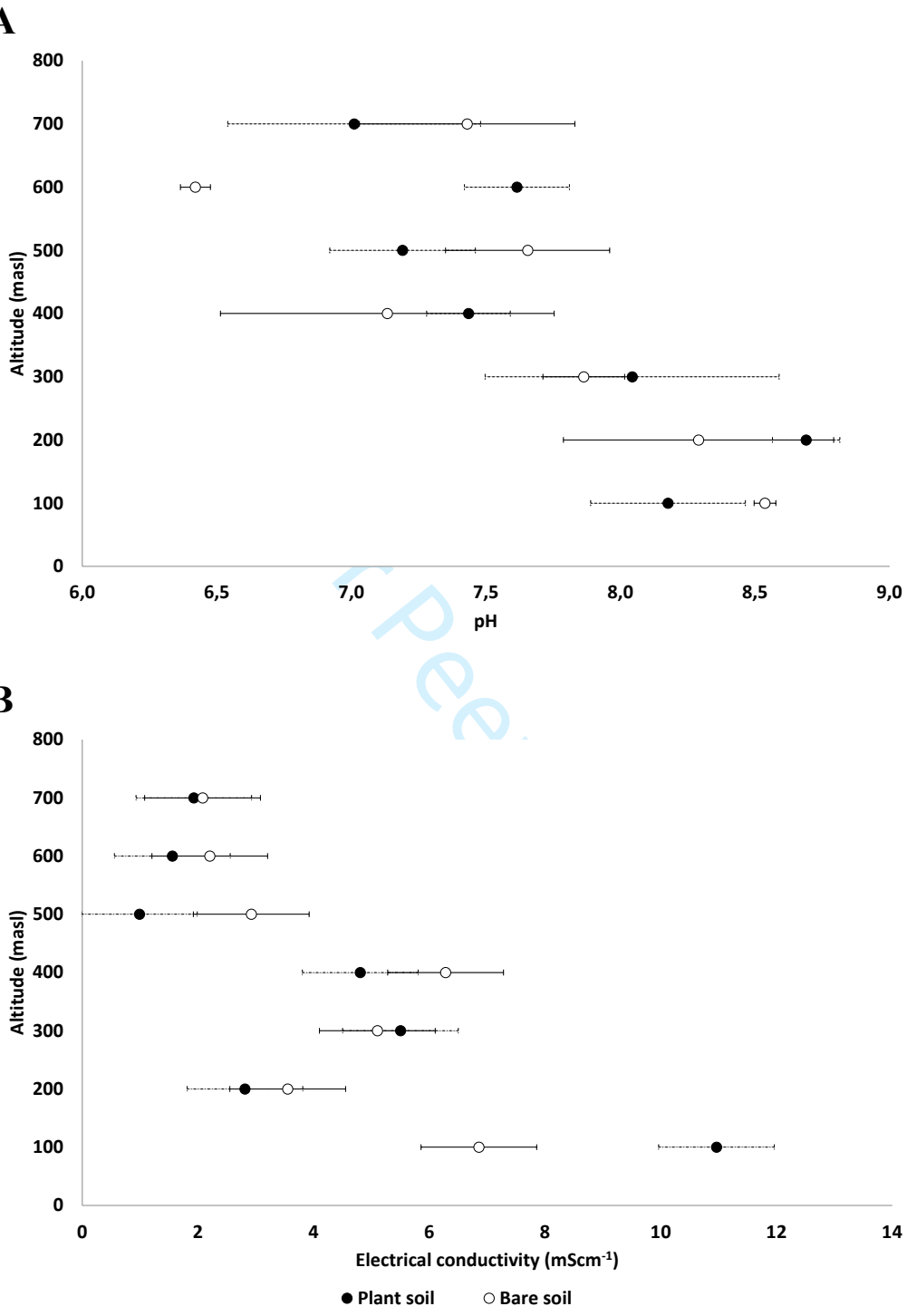

Figure 3. Variation of the pH (A) and electrical conductivity (EC) (B) in bare and bulk soils at different altitudes in Morro Moreno National Park.

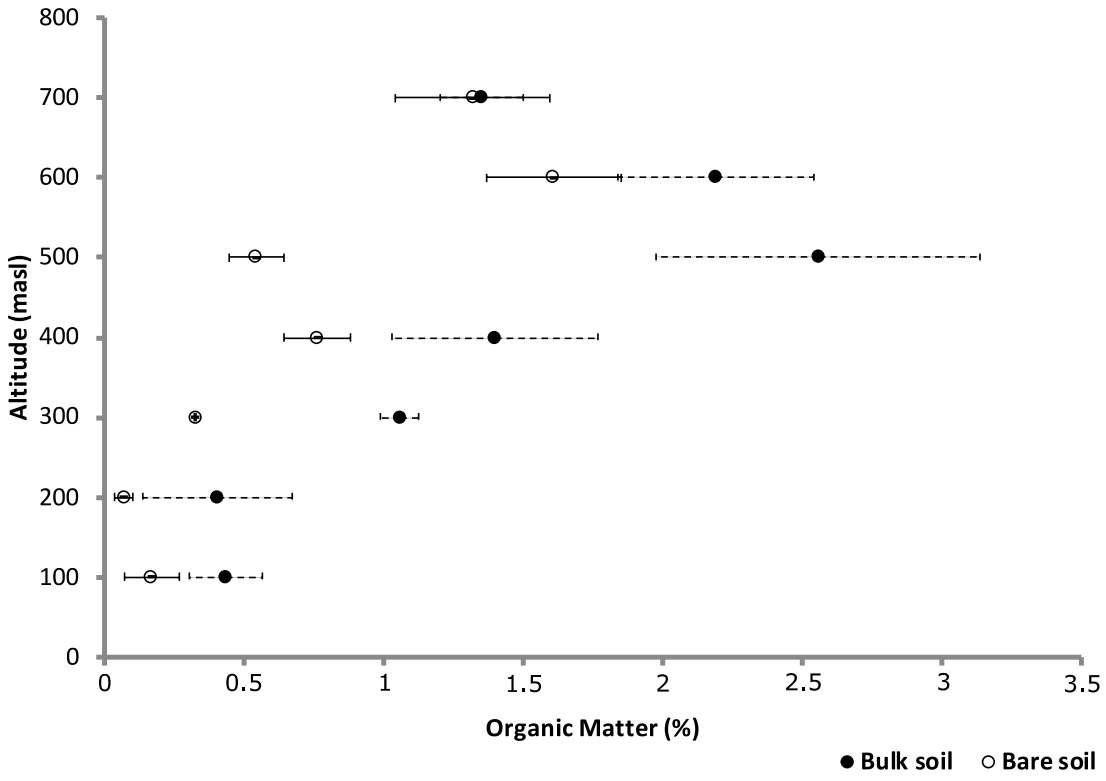

Figure 4. Variations in organic matter (%) in bare and bulk soil with altitude in Morro Moreno National Park.

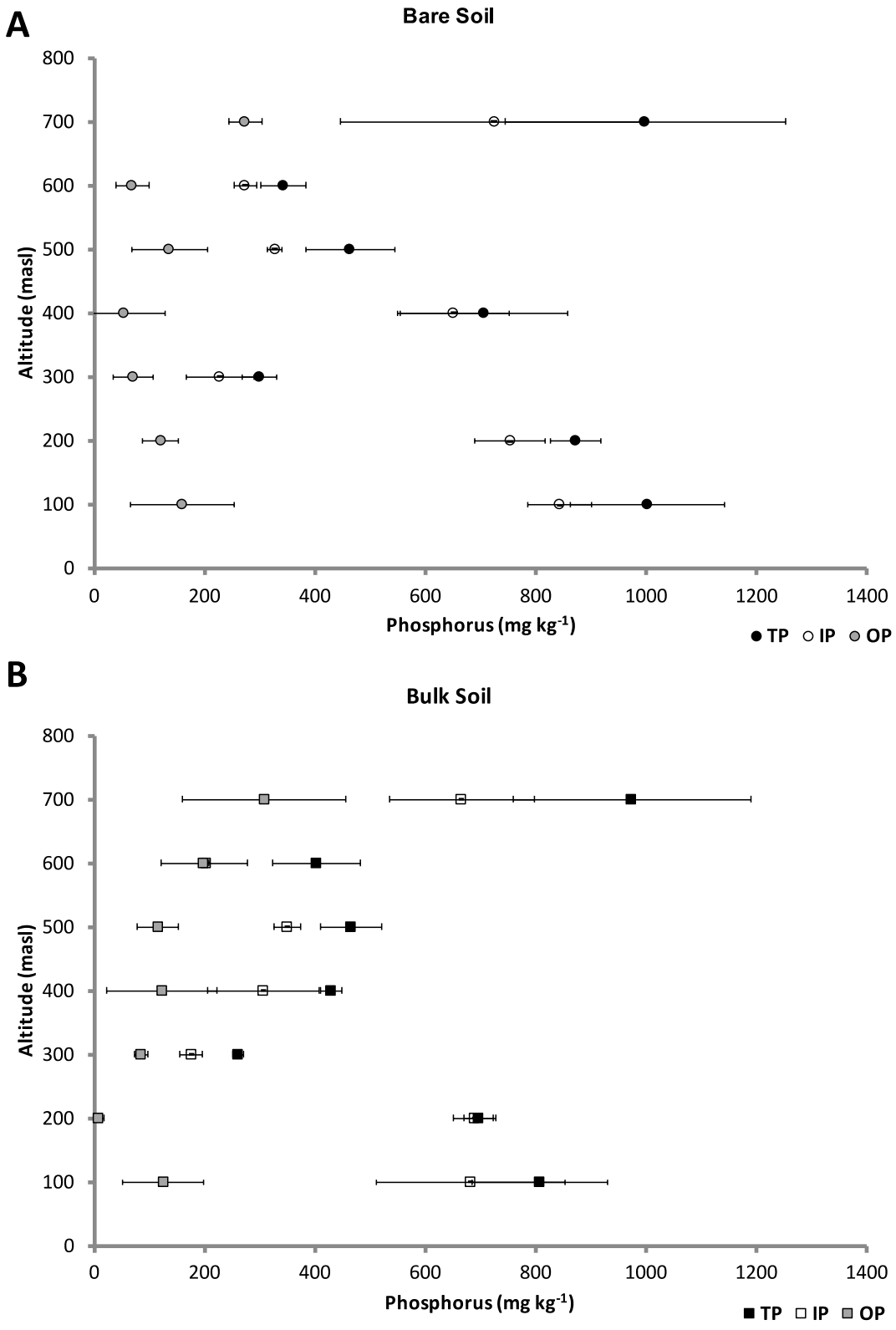

Figure 5. Variations in phosphorus in bare **(A)** and bulk **(B)** soils depending on altitude in Morro Moreno National Park (TP: total P, IP: inorganic P, and OP: organic P).

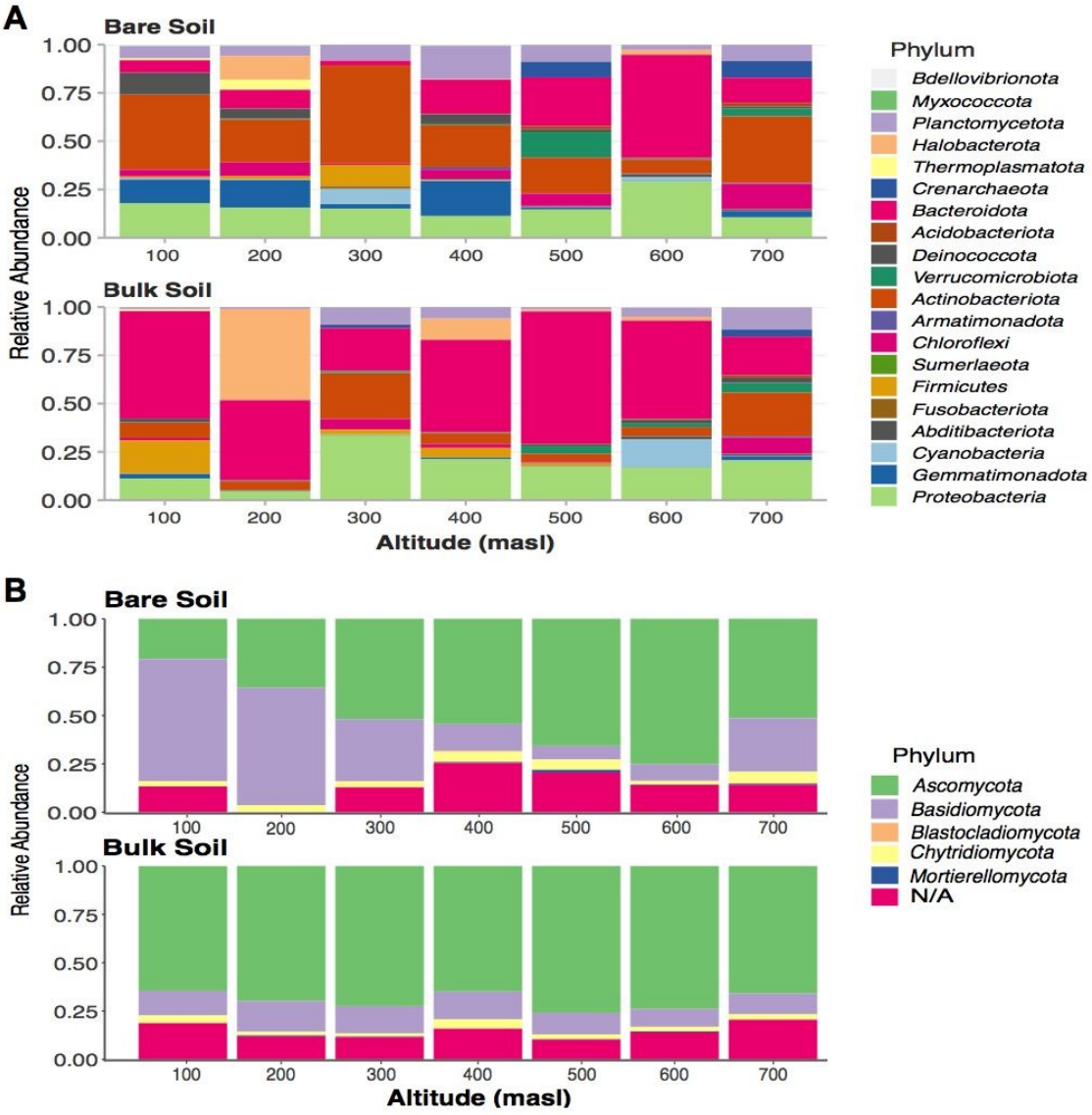

Figure 36. Taxonomic composition and relative abundance of microbial communities in bare and bulk soil samples from different altitudes in the MMNP. Stacked bars show **(A)** the top 20 most abundant bacteria and the **(B)** identified fungi at the phylum taxonomic level.

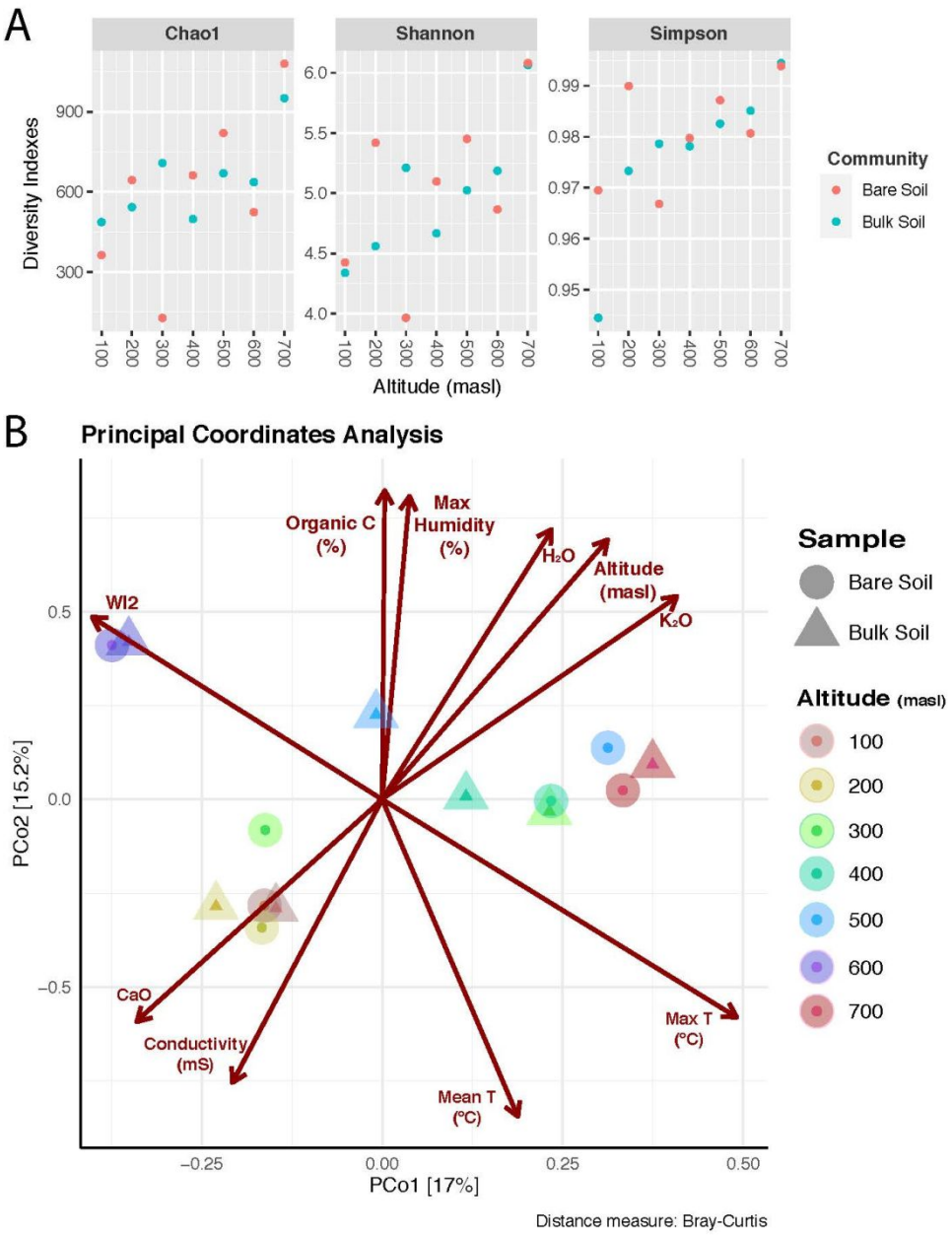

Figure 47. Variability of the microbial communities in the MMNP. **(A)** Alpha diversity indices for each studied MMNP microbial community. Colours represent different samples. **(B)** Beta diversity based on principal component analysis (PCA) on Hellinger transformed amplicon sequence variant (ASV) relative abundances. The points correspond to the soil samples from different altitudes (identified by the shapes and colours), and the relative distance indicates the level of similarity to all other samples. The arrows indicate the explanatory power of the statistically significant environmental and soil parameters regarding the observed variation in the community composition.

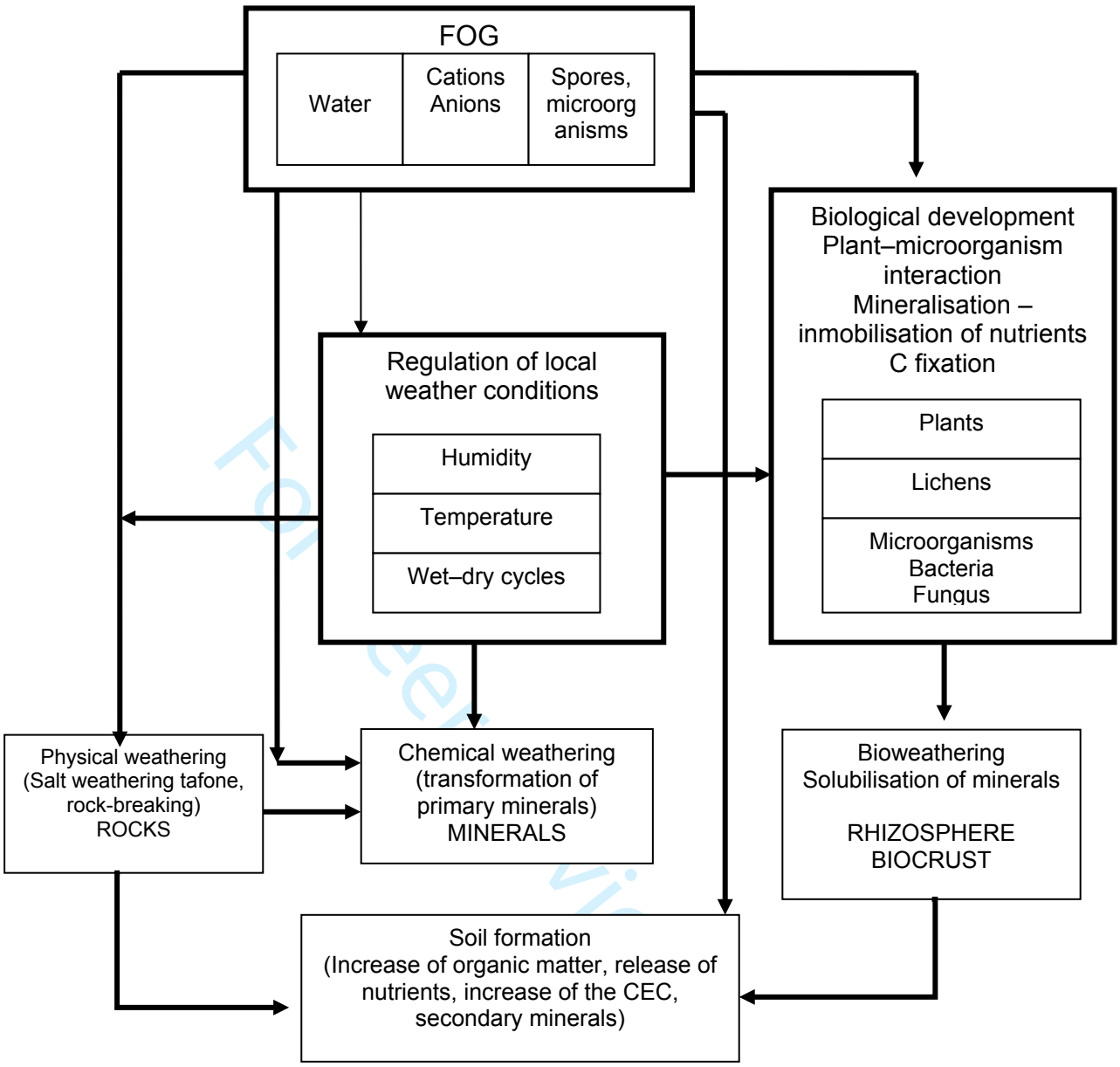

Figure 58. Diagram illustrating the effect of coastal fog on soil formation.

TABLES

Table 1. Variation of the pH, electrical conductivity (EC), organic matter (OM), Phosphorus (total P, Inorganic P and organic P) in bare and bulk soils at different altitudes in Morro Moreno National Park

Altitude (masl)	pH		Electrical conductivity ($mScm^{-1}$)		Organic Matter (%)		Phosphorus ($mg\ kg^{-1}$)					
							Pt	Pi	Po	Pt	Pi	Po
	Bare Soil	Bulk Soil	Bare Soil	Bulk Soil	Bare Soil	Bulk Soil	Bare soil			Bulk Soil		
100	8.53 ± 0.1	8.18 ± 0.3	6.86 ± 1.0	10.96 ± 1.4	0.17 ± 0.0	0.43 ± 0.1	1002 ± 140	843 ± 57	159 ± 94	806 ± 123	681 ± 171	124 ± 74
200	8.29 ± 0.5	8.69 ± 0.2	3.55 ± 0.7	2.81 ± 0.5	0.07 ± 0.0	0.41 ± 0.2	873 ± 45	753 ± 64	120 ± 33	695 ± 27	689 ± 38	6 ± 1
300	7.86 ± 0.2	8.04 ± 0.5	5.10 ± 2.6	5.50 ± 1.1	0.33 ± 0.0	1.06 ± 0.1	299 ± 30	228 ± 60	71 ± 35	260 ± 11	176 ± 20	84 ± 12
400	7.13 ± 0.6	7.44 ± 0.2	6.28 ± 1.3	4.08 ± 0.2	0.77 ± 0.1	1.40 ±0.3	705 ± 151	651 ± 101	54 ± 75	428 ± 19	306 ± 102	122 ± 99
500	7.66 ± 0.3	7.19 ± 0.3	2.92 ± 0.6	0.99 ± 0.3	0.55 ± 0.1	2.56 ± 0.6	463 ± 80	327 ± 12	137 ± 69	465 ± 56	349 ± 23	115 ± 37
600	6.42 ± 0.1	7.62 ± 0.2	2.20 ± 0.9	1.56 ± 0.4	1.61 ± 0.2	2.19 ± 0.4	342 ± 40	273 ± 21	69 ± 30	402 ± 79	203 ± 4	198± 78
700	7.43 ± 0.4	7.01 ± 0.5	2.08 ± 0.6	1.93 ± 0.8	1.32 ±0.3	1.53 ± 0.1	998 ± 253	724 ± 278	274 ± 30	973 ± 215	665 ± 131	308 ± 148

911

912 **Table 21.** Mineralogical description of soil samples collected at different altitudes in Morro Moreno National Park.

Compounds (crystalline phase)	Chemical Composition	Bare soil (masl)							Bulk soil (masl)						
		100	200	300	400	500	600	700	100	200	300	400	500	600	700
Magnesiohornblende	$Ca_2(Mg,Fe^{+2})4Al(Si_7Al)O_{22}(OH,F)_2$	59.9	51.2	74.1	82	26.1	29.6	13.1	8.8	68.2	47.2	57.5	49.5	52.3	20.3
Calcium albite	$(Na,Ca)Al(Si,Al)_3O_8$	25.8	17.9	10.8	7.3	35.3	48.8	43.3	22.3	21.6	16.6	14.8	21	29.1	29.0
Quartz	SiO_2	13.4	1	1.7	6.8	23.9	12.3	3.9	19.7	5	6	8.1	15.6	12.8	9.4
Chlorite	$(Mg,Fe)_6(Si,Al)_4O_10(OH)_8$	0,9	18.5	0.2	2	2.5	9.2	6.1	6.9	0.6	2.4	14.5	6.1	5.2	4.5
Anortite	$CaAl_2Si2O_8$	--	7.4	--	2	--	--	29.4	17.8	--	27.8	--	--	--	16.9
Pyrophyllite	$Al_2SiO_4O_{10}(OH)_2$	--	4.1	--	--	--	--	--	--	4.6	--	--	--	--	3.5
Kaolinite	$Al_2SiO_5(OH)_4$	--	--	13.2	--	4.9	--	--	7.9	--	--	--	--	--	3.8
Anhydrite	$CaSO_4$	--	--	--	--	1.3	--	--	--	--	--	--	--	--	--
Sanidine	$K(AlSi_3O_8)$	--	--	--	--	6	--	--	--	--	--	--	--	--	--
Hematite	Fe_2O_3	--	--	--	--	--	--	--	--	--	--	1.2	2	0.2	1.2
Jarosite	$(K,H_3O)Fe_3(SO_4)_2(OH)_6$	--	--	--	--	--	--	--	--	--	--	3.9	--	--	--
Orthoclase	$KAlSi_3O_8$	--	--	--	--	--	--	4.38	5.3	--	--	--	5.8	0.3	5.9
Biotite	$K(Mg,Fe^{2+})_3(Al, Fe^{+3})Si_3O_{10}(OH,F)_2$	--	--	--	--	--	--	--	11.3	--	--	--	--	--	5.5

913

914

915 **Table 32.** Major element concentrations of soil samples from different altitudes in Morro Moreno National Park obtained by X-ray fluorescence.

	Percentage (%)											
	Bare Soil											
masl	**SiO_2**	**TiO_2**	**Al_2O_3**	**Fe_2O_3**	**MnO**	**MgO**	**CaO**	**Na_2O**	**K_2O**	**P_2O_5**	**ppc**	**H_2O**
100	53.17	0.96	15.31	10.22	0.17	5.27	8.37	3.58	0.90	0.17	1.43	0.16
200	50.42	0.70	16.22	10.85	0.18	7.28	9.29	2.97	0.42	0.10	1.09	0.24
300	45.35	0.55	22.25	9.13	0.13	4.83	6.31	2.08	0.54	0.06	7.00	1.54
400	47.56	0.59	18.94	9.47	0.15	7.35	6.74	1.80	1.11	0.09	4.81	1.22
500	50.05	1.14	16.45	10.72	0.17	5.01	5.46	2.61	1.47	0.12	4.87	1.73
600	51.22	0.91	15.04	9.25	0.16	5.25	6.57	3.00	1.08	0.12	5.21	2.03
700	47.66	0.65	14.39	9.09	0.14	10.79	6.45	2.62	0.82	0.17	6.3	0.64
	Bulk Soil											
100	52.75	0.56	18.97	6.45	0.11	5.22	8.35	4.08	0.71	0.12	2.4	0.08
200	50.39	0.67	16.46	10.36	0.17	7.37	8.88	3.03	0.52	0.10	1.63	0.23
300	50.03	0.55	16.91	9.38	0.16	7.71	8.45	2.64	0.68	0.09	2.47	0.36
400	45.43	0.62	19.05	9.14	0.14	6.42	5.86	1.96	1.04	0.10	8.21	1.90
500	50.75	1.03	15.83	10.12	0.17	4.99	5.72	2.85	1.38	0.12	5.24	1.62
600	52.49	0.91	15.14	9.42	0.16	5.34	6.53	3.00	1.16	0.11	4.53	1.03

700	49.36	0.82	15.84	9.63	0.18	8.30	8.36	2.59	0.77	0.12	3.71	0.12

916

Table 43. Calculation of weathering indices: Weathering Index of Parker (WIP), Vogt's Residual Index (V), Chemical Index of Alteration (CIA), Chemical Index of Weathering (CIW), Plagioclase Index of Alteration (PIA), Weathering Index 1 (WI1), Weathering Index 2 (WI2).

Weathering Index							
Bare Soil							
masl	**WIP**	**V**	**CIA**	**CIW**	**PIA**	**WI1**	**WI2**
100	76.50	0.47	40.95	42.04	38.34	5.89	13.83
200	74.68	0.41	42.18	42.69	41.00	5.28	12.37
300	53.15	0.84	58.97	59.90	57.42	3.46	13.20
400	63.45	0.60	53.57	55.45	50.17	4.26	13.35
500	64.27	0.67	50.99	53.63	46.06	5.16	12.41
600	68.04	0.54	45.45	47.12	41.92	5.78	14.72
700	77.29	0.35	45.95	44.87	43.11	5.62	13.93
Bulk Soil							
100	79.30	0.56	45.57	46.42	43.72	4.72	21.74
200	75.29	0.43	43.14	43.79	41.67	5.19	12.93
300	72.89	0.45	45.27	46.18	43.30	5.02	13.53
400	59.53	0.67	55.94	57.85	52.63	4.05	13.21
500	66.32	0.63	48.84	51.20	44.23	5.44	13.33
600	68.86	0.54	45.60	47.39	41.82	5.88	14.81
700	74.59	0.41	43.84	44.87	41.53	5.28	13.62

920

SUPPLEMENTARY MATERIAL

Effect of the altitude on the properties of soil in the coastal fog ecosystem in Morro Moreno National Park, Antofagasta-Chile

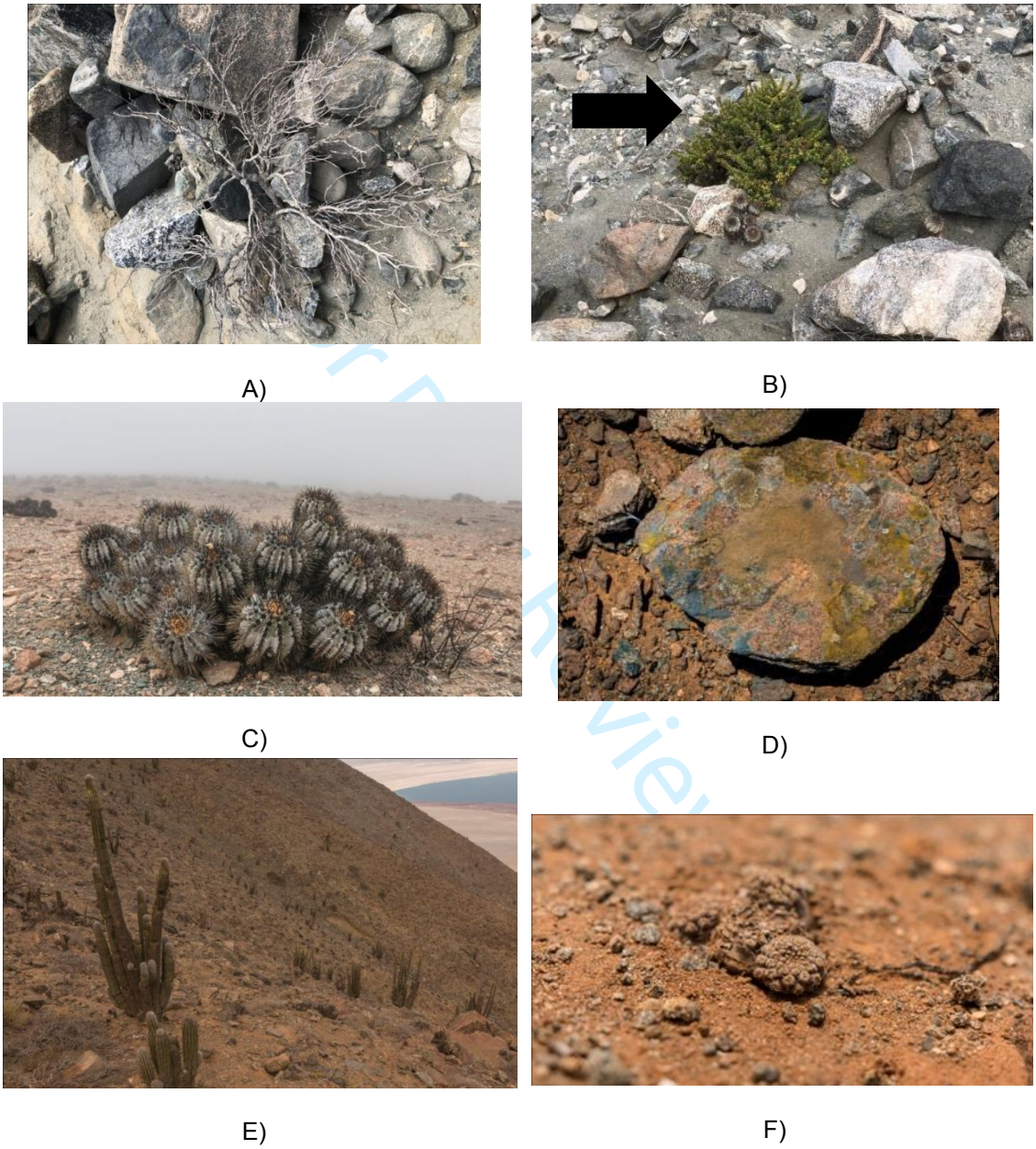

Figure S1. Vegetation and liquen species in Morro Moreno National Park (MMNP) in the Antofagasta Region, Chile. A) *Nolana spp*. vegetal specie found around 200 masl; B) *Tetragonia angustifolia* vegetal specie found from 300 masl; C) *Copiapoa boliviensis* vegetal specie found from 300 masl, D) Lichens observed from 500 masl, E) *Eulychnia Morromorenoensis*, F) *Eriosyce recondite*.

Figure S2. Tafoni rock formations observed in Morro Moreno National Park (MMNP) in the Antofagasta Region, Chile.

1 **Table S1.** Weathering Indices (WI).

Index	Formula	Description	Reference
Weathering Index of Parker (WIP)	$WIP = \left[\frac{Na_2O}{0.35} + \frac{MgO}{0.9} + \frac{2K_2O}{0.25} + \frac{CaO}{0.7}\right] x100$	Weathering Index of Parker (WIP), based on the proportions of the alkali and alkaline earth metals present. These are considered to be the most mobile of the major elements. WIP measures both the degree to which a rock has already been weathered with respect to the parent material, and also its susceptibility to further weathering. WIP its useful for reflecting changes in the amount of Na^+, K^+, Ca^{2+} and Mg^{2+} cations, if the alteration of feldspars into clay minerals is the major chemical weathering process, and there are similar mobilities between the major cations.	Parker (1970) see also Price and Velbel (2003)
'Vogt's Residual Index (V)	$V = \frac{Al_2O_3 + K_2O}{MgO + CaO + Na_2O}$	Vogt's Residual Index (V) is defined by the ratio of the amount of oxides of immobile cations (mainly Al) to mobile cations (magnesium, calcium and sodium) with the assumption that the potassium content remains constant during the weathering process.	Vogt (1927) see also Price and Velbel (2003)
Chemical Index of Alteration (CIA)	$CIA = \frac{Al_2O_3}{Al_2O_3 + CaO + Na_2O + K_2O} x\ 100$	Chemical Index of Alternation (CIA), represents a ratio of predominantly immobile Al_2O_3 to the mobile cations Na+, K+ and Ca^{2+} given as oxides. The CIA is interpreted as a measure of the extent of feldspars (which dominate the upper crust of laterite) conversion to clays such as kaolinite. CIA monitors the progressive alteration of plagioclase and potassium feldspars to clay minerals.	Nesbitt and Young (1982) Fedo et al. (1995)
Chemical Index of weathering (CIW)	$CIW = \frac{Al_2O_3}{Al_2O_3 + CaO + Na_2O} x\ 100$	The chemical index of weathering (CIW), which is identical to the CIA except that it eliminates K_2O from the equation.	Harnois (1988) Fedo et al. (1995)
Plagioclase index of Alteration (PIA)	$PIA = \frac{Al_2O_3 - K_2O}{Al_2O_3 + CaO + Na_2O - K_2O} x\ 100$	PIA index is an alternative to the CIW. Because plagioclase is abundant in silicate rocks and dissolves relatively rapidly.	Fedo et al. (1995) Price and Velbel (2003)

Weathering index (WI1) or Ruxton Ratio (R)	$WI1 = \frac{SiO_2}{Al_2O_3}$	Ruxton ratio (R) is simply a SiO_2 to Al_2O_3 ratio, relates silica loss to total-element loss and considers alumina (and other sesquioxides) to be immobile during weathering. In humid regions, the silica-to-alumina ratios have been found to provide an easy way to quantify the degree of rock weathering. Ruxton Ratio is best suited for weathering profiles developed on uniform acid to intermediate bedrock, with constant sesquioxide content during weathering, and which produces kaolin and/or allophane weathering products.	Ruxton (1968) Price and Velbel (2003)
Weathering index (WI2)	$WI2 = \frac{SiO_2}{Fe_2O_3}$		

The optimum values for the indices in the fresh and weathered rocks are: WIP (0, 100), V (0, 1), CIA (50, 100), CIW (50, 100), PIA (50, 100), R (0, 10).

REFERENCES

1. Fedo, C. M., Nesbitt, H. W., & Young, G. M. (1995). Unraveling the effects of potassium metasomatism in sedimentary rocks and paleosols, with implications for paleoweathering conditions and provenance. *Geology*, *23(10)*, 921–924. https://doi.org/10.1130/0091-7613(1995)023<0921:UTEOPM>2.3.CO;2

2. Harnois, L. (1988). The CIW index: A new chemical index of weathering. *Sedimentary Geology, 55(3)*, 319-322. doi:10.1016/0037-0738(88)90137-6

3. Nesbitt, H., & Young, G. (1982). Early Proterozoic climates and plate motions inferred from major element chemistry of lutites. *Nature, 299 (5885)*, 715–717. https://doi.org/10.1038/299715a0

4. Parker, A. (1970). An Index of Weathering for Silicate Rocks. *Geological Magazine, 107(6)*, 501-504. https://doi.org/10.1017/S0016756800058581

5. Price, J., & Velbel, M. (2003). Chemical weathering indices applied to weathering profiles developed on heterogeneous felsic metamorphic parent rocks. *Chemical Geology, 202(3-4)*, 397-416. https://doi.org/10.1016/j.chemgeo.2002.11.001

6. Ruxton, B. (1968). Measures of the Degree of Chemical Weathering of Rocks. *The Journal of Geology, 76(5)*, 518-527. https://doi.org/10.1086/627357

7. Vogt, T. (1927) Sulitjelmafeltets geologi og petrografi. Norges Geologiske Undersokelse, 121, 1-560. (In Norwegian, with English Abstract).

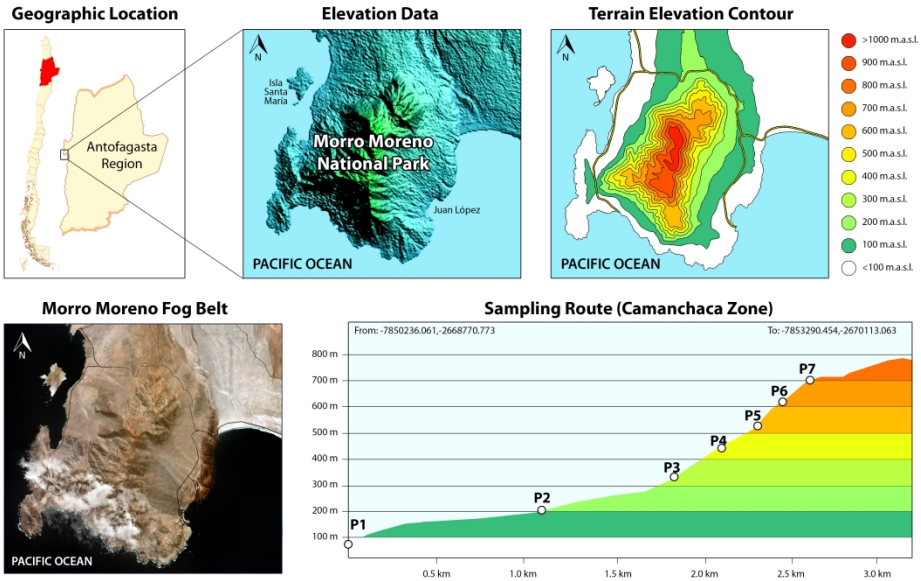

Figure 1. Location of Morro Moreno National Park and sampling points at different altitudes. Geographical Universal Transverse Mercator UTM coordinates: 100 masl (0340496; 7397723), 200 masl (0340338; 7398100), 300 masl (0340519; 7398122), 400 masl (0340507; 739828), 500 masl (0340478; 7398482), 600 masl (0340523; 7398628), and 700 masl (0340542; 7398713).

352x229mm (300 x 300 DPI)

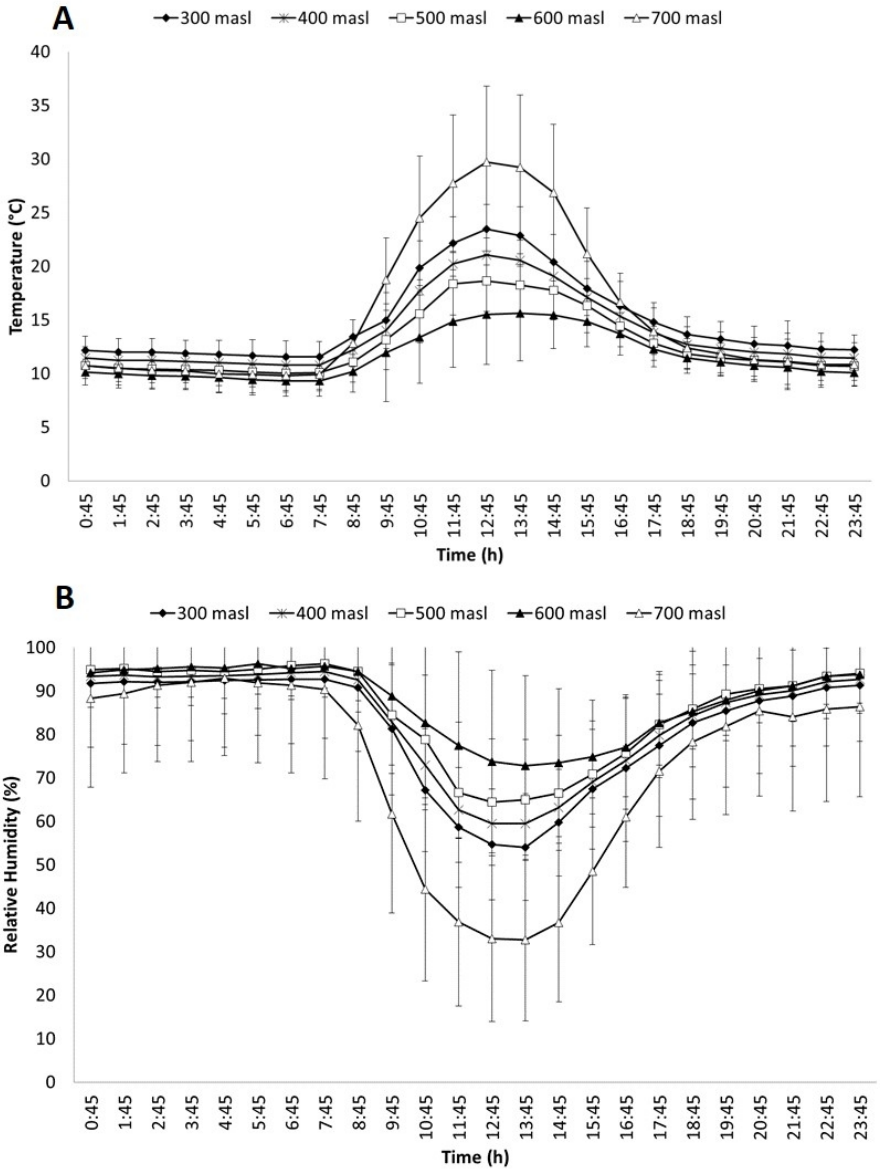

Figure 2. Temperature (A) and relative humidity (B) at different altitudes in the Morro Moreno National Park. The data in both graphs represent averages of 69 measures. The vertical bar indicates the standard deviation.

139x183mm (150 x 150 DPI)

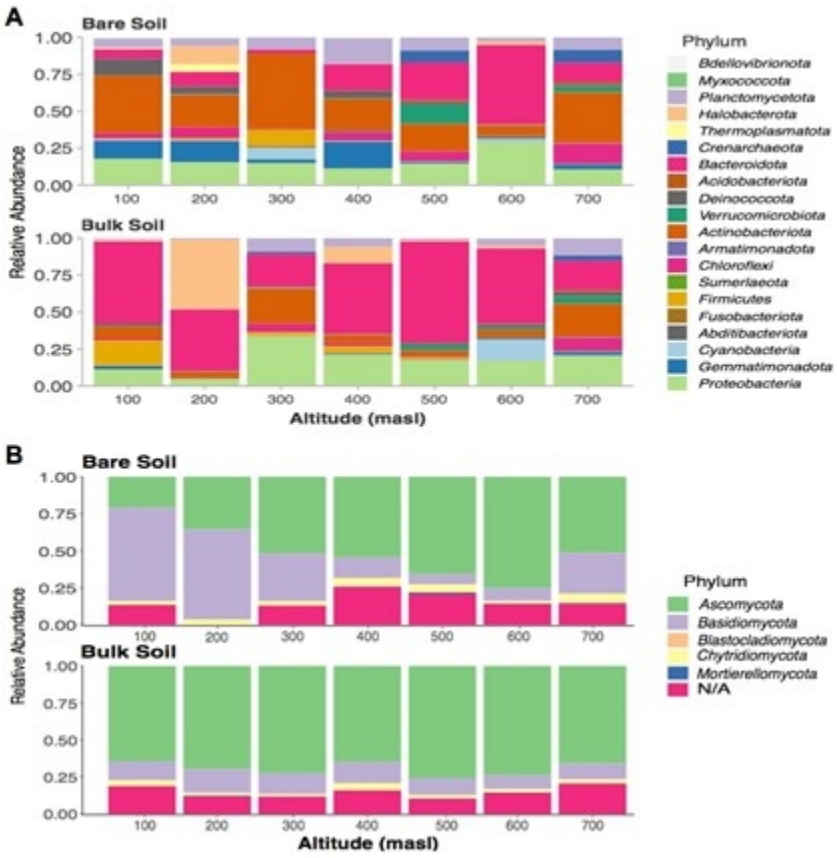

Figure 3. Taxonomic composition and relative abundance of microbial communities in bare and bulk soil samples from different altitudes in the MMNP. Stacked bars show (A) the top 20 most abundant bacteria and the (B) identified fungi at the phylum taxonomic level.

149x150mm (72 x 72 DPI)

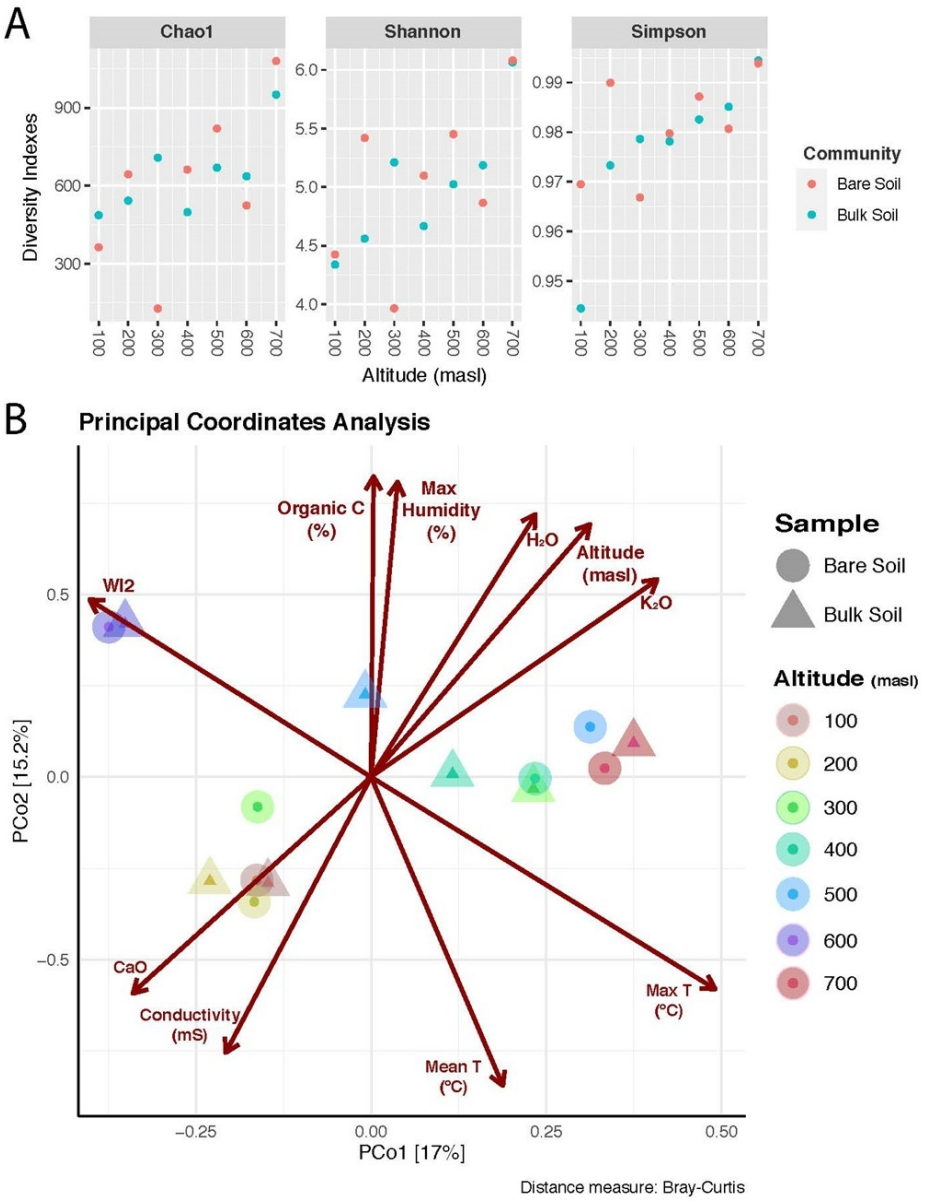

Figure 4. Variability of the microbial communities in the MMNP. (A) Alpha diversity indices for each studied MMNP microbial community. Colours represent different samples. (B) Beta diversity based on principal component analysis (PCA) on Hellinger transformed amplicon sequence variant (ASV) relative abundances. The points correspond to the soil samples from different altitudes (identified by the shapes and colours), and the relative distance indicates the level of similarity to all other samples. The arrows indicate the explanatory power of the statistically significant environmental and soil parameters regarding the observed variation in the community composition.

127x165mm (200 x 200 DPI)

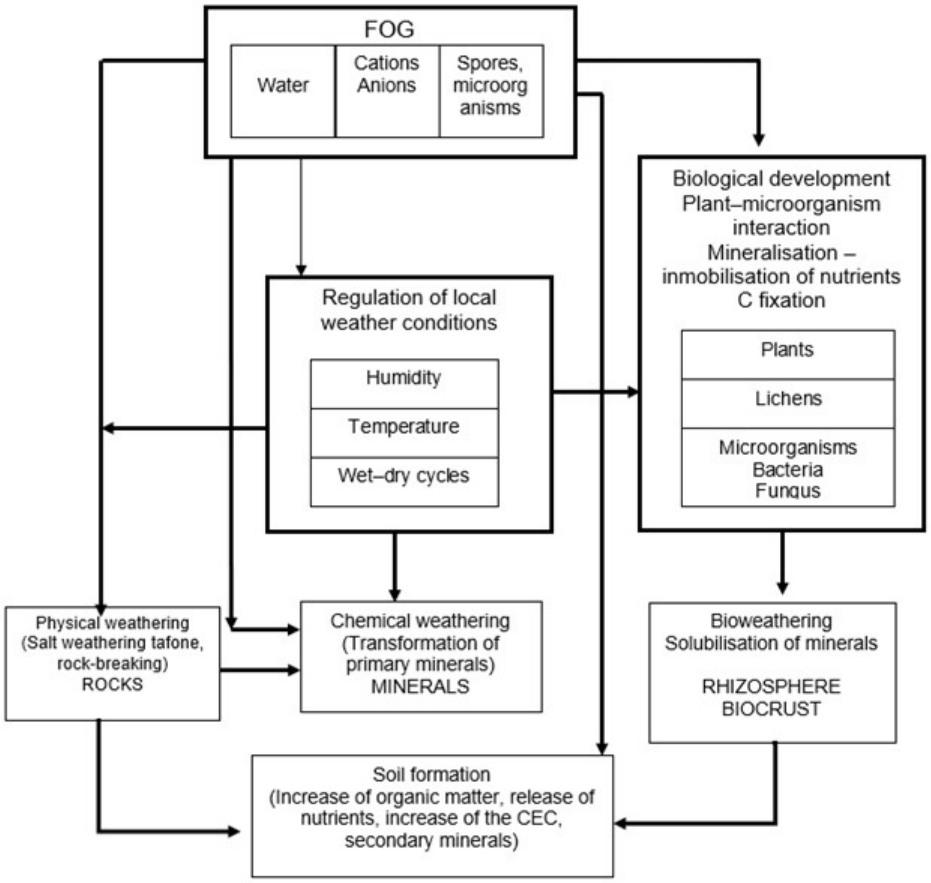

Figure 5. Diagram illustrating the effect of coastal fog on soil formation.

176x173mm (96 x 96 DPI)